



Cite this: DOI: 10.1039/d6lf00005c

# Emerging one-dimensional metal hydroxide nanostructures for high-performance supercapacitors: recent progress and future prospects

Swapna Rout,<sup>a</sup> Vinay Soni,<sup>a</sup> Sejal Tiwari,<sup>a</sup> Suraj R. Sankapal,<sup>b</sup> Ji Man Kim,<sup>c</sup> Ravindra N. Bulakhe<sup>d</sup> and Babasaheb R. Sankapal<sup>id</sup>\*<sup>a</sup>

Supercapacitive energy storage devices are attractive due to the high-power density and long cycle life; however, their broader application is limited by relatively low energy density. The primary objective of this review article is to identify one-dimensional (1D) nanostructured metal hydroxides as effective electrode materials for supercapacitors. Electrodes with 1D nanostructures have attracted significant attention owing to their unique structural features, which provide a high surface area, efficient directional ion transport pathways, enhanced utilization of electroactive materials, and diverse topologies that facilitate rapid electron and ion diffusion to active sites. This article comprehensively explores recent advances in metal hydroxide-based one-dimensional nanoforms, with particular emphasis on their design, synthesis strategies, and structural and chemical modifications for electrochemical supercapacitor applications. Furthermore, recent trends, existing challenges, and future prospects are critically discussed, highlighting their potential role in the development of flexible energy storage devices for the modern technological era.

Received 8th January 2026,  
Accepted 5th March 2026

DOI: 10.1039/d6lf00005c

rsc.li/RSCApplInter

## 1. Introduction

Rapid depletion of non-renewable energy resources, including fossil fuels such as coal, petroleum, and natural gas, results from their extensive use in fulfilling world energy needs. Thermal, mechanical, chemical, and electrochemical energy are among the different sources of energy that can be stored (Fig. 1). Amongst these, electrochemical energy storage has emerged as a reliable solution for sustainable energy management and environmental protection. Numerous systems, such as flywheel energy storage (FES) and compressed air energy storage (CAES), flow batteries, capacitors, supercapacitors and fuel cells, are widely used in many different industries.<sup>1</sup> Batteries are widely used due of their large storage capacity and high energy density (ED). However, numerous difficulties arise due to low power density and thermal

instability that limits the usage of batteries.<sup>2,3</sup> The risk of short circuits in batteries has increased issues like flammability, dendritic development, volatility, loss of liquid electrolytes, and limited lifespan.<sup>4</sup> The limited life span also reduces their applications so a steady power source is needed for prolonged periods.<sup>5</sup> Numerous creative solutions have resulted from advancements in capacitor technology, with supercapacitors being one of the most noteworthy contemporary advances.<sup>6</sup> An effective Ragone plot can be used to show the basic link between energy density (ED) and power density (PD), as well as how energy storage devices fit into the system (Fig. 2). Supercapacitors have a longer lifespan, a wider operating temperature range, and stable electrical characteristics. Supercapacitor performs similarly to an electrochemical cell but has quicker response times and better cycle performance.<sup>7</sup> Table 1 describes the comparison of all the feature parameters between batteries, supercapacitors, and capacitors.<sup>8</sup>

Necessity for better energy storage technology is highlighted by the world's growing energy consumption and shift to renewable energy sources.<sup>9</sup> Defect engineering plays an important role in one-dimensional metal hydroxides by optimizing the electrochemical performance by increasing active surface sites and enhancing electrical conductivity to provide better structural stability that further increases the electrochemical performance.<sup>10</sup> Various defect engineering

<sup>a</sup> Nano Materials and Device Laboratory, Department of Physics, Visvesvaraya National Institute of Technology, South Ambazari Road, Nagpur – 440010, M.S., India. E-mail: brsankapal@gmail.com, brsankapal@phy.vnit.ac.in

<sup>b</sup> Centre for Interdisciplinary Research, D. Y. Patil Education Society, Kolhapur 416003, India

<sup>c</sup> Department of Chemistry, Sungkyunkwan University, Suwon, 16419, Republic of Korea

<sup>d</sup> Symbiosis Centre for Nanoscience and Nanotechnology, Symbiosis International (Deemed University), Pune 412115, India



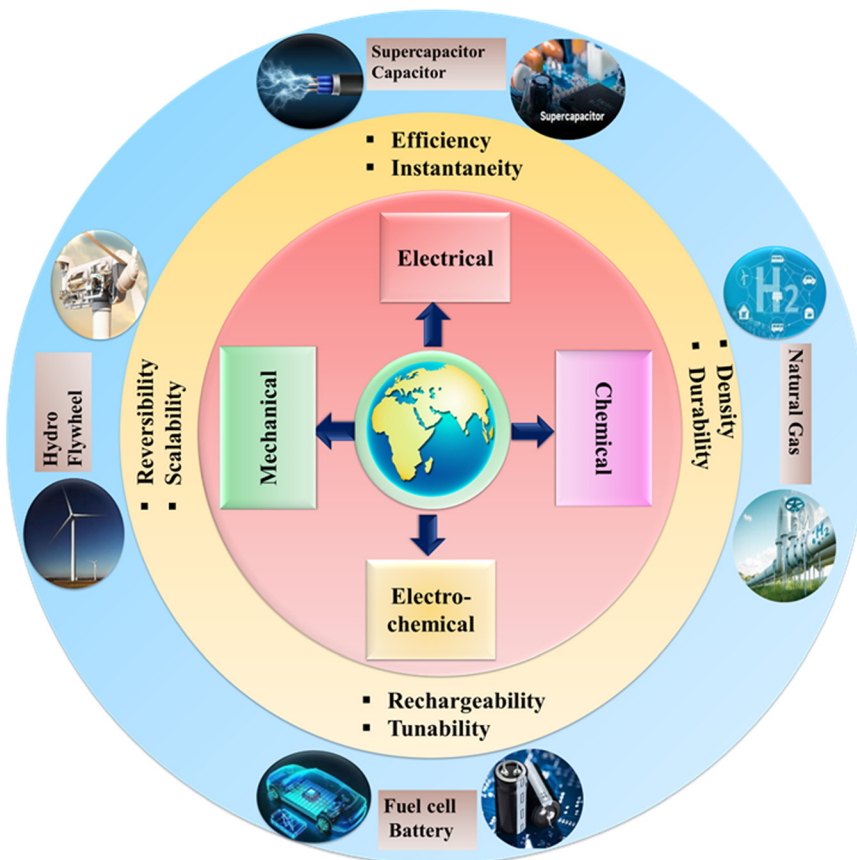


Fig. 1 Various energy storage technologies for sustainable applications.

technologies like vacancy defect engineering, doping heteroatom substitution, lattice distortion, surface defect engineering, morphological defect engineering and phase defect engineering. The lattice structure creates vacancies that enable active surface sites, which provide enhanced charge carrier transport pathways. The effect of annealing temperature or synthesis of materials through chemical methods enables these types of defect mechanisms.<sup>11,12</sup> By forming composites with other metal oxides and polymers, charge carrier flow

easily. Due to the formation of surface dislocations and unsaturated coordination sites, electrochemical active surface sites can be increased. There are several studies on composite structures that combine carbon with pseudocapacitive phases, such as conducting polymers,<sup>13</sup> metal phosphates,<sup>14</sup> MXene,<sup>15</sup> and materials derived from metal organic frameworks that create percolated electron and ion channels and lessen mechanical deterioration.<sup>16</sup> Several reports are found on carbon-based electrodes for supercapacitor application by altering the structure by doping and composite variation through defect assisted engineering strategies.<sup>17-19</sup> Some reports are found on biomass derived carbon materials that explore their synthesis, functionalization, and structural engineering.<sup>20,21</sup> Nowadays, many researchers utilize lithium-ion batteries, but the scarcity of lithium (Li) resources has led to price increased, which limits the development of greener energy sources.<sup>22</sup> Two-dimensional metal borides have unique surface terminations with elemental composition that make them an ideal choice for supercapacitor application.<sup>23</sup> Nickel manganese sulfide has been reported by Faisal *et al.*<sup>24</sup> resembles the surface architecture of a battery, which boosts the power density component for supercapacitor application. Fig. 3 describes the key aspects for metal hydroxides towards supercapacitor application. Generally various studies are reported on specific classes of metal hydroxides rather than specific comparison depending on dimensional dependent

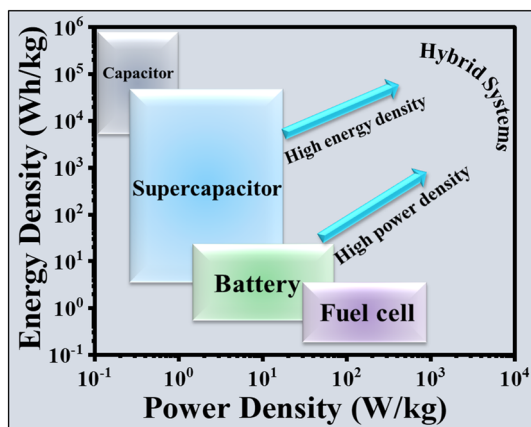
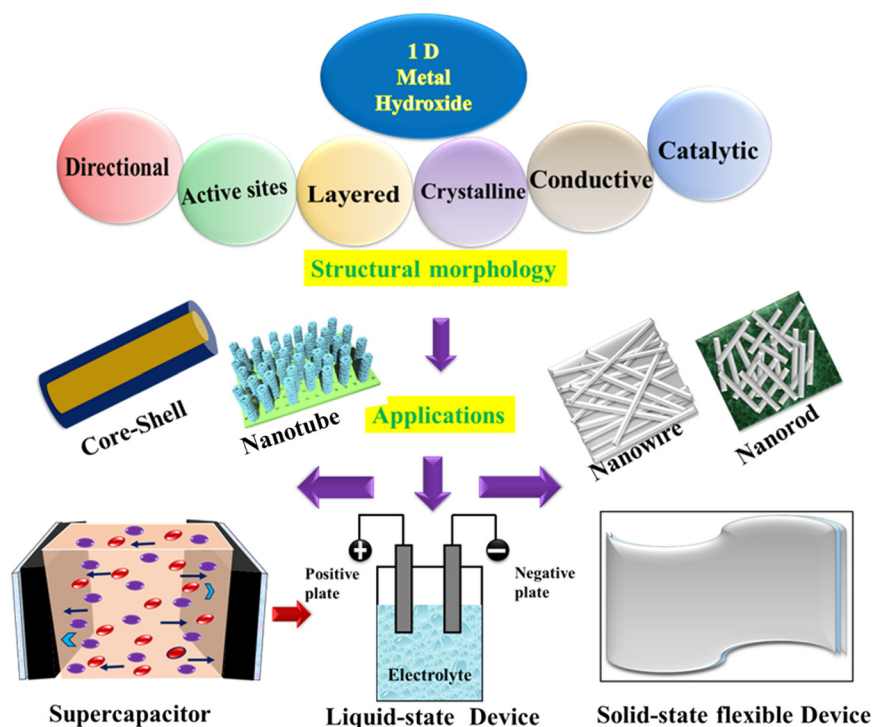


Fig. 2 Ragone plot.



**Table 1** Distinctive characteristics of potential electrochemical energy storage devices<sup>27,148</sup>

Parameters	Capacitor	Supercapacitor	Battery
Energy storage mechanism	Electrostatically using electric double layer	Faradaic redox reaction and non-faradaic process	Surface chemical reaction
Energy density (Wh kg <sup>-1</sup> )	Less than 0.1	Less than 100	150–200
Power density (W kg <sup>-1</sup> )	>10 000	~200k	<1000
Charging/discharging time (s)	Picoseconds to milliseconds	Milliseconds to seconds	1–10 h
Dimensions	Small to large	Small	Large
Weight	1 g–10 kg	1–2 g	>10 kg
Cycle life	Infinite	>500k	~1k
Temperature (°C)	–20–100	–40–85	–20–65
Coulombic efficiency	= 100%	85–98%	70–85%
Application	Pulsed power weapons	Power grid and stabilization	Prolonged energy supply

**Fig. 3** Key aspects of 1D metal hydroxides towards supercapacitor application.<sup>107</sup>

morphology. Pei *et al.*<sup>25</sup> comprehensively discussed two-dimensional transition metal oxide/hydroxide hierarchical structures for supercapacitors, but metal hydroxides are treated together with oxides and within the restricted context of 2D architectures, without a systematic comparison across different hydroxide chemistries and nanostructures. One review reported medium-entropy and high-entropy hydroxide-based hybrid supercapacitors emphasizing the entropy-engineered compositions and device design rather than conventional binary/ternary hydroxides with their electrochemical aspects.<sup>26</sup> The report on a cobalt hydroxide-based electrode has been only element-specific and did not cover other first-row transition metal hydroxides or heterostructure/hybrid configurations in a unified framework.<sup>27</sup> Recently, various reviews have focused on metal oxides<sup>28</sup> and chalcogenides<sup>29,30</sup>

for supercapacitor application and only briefly touched on metal hydroxides as a subset of pseudocapacitors.

The present review emphasizes a unique approach on one-dimensional (1D) metal hydroxide nanostructures for electrochemical energy storage. Furthermore, the current review specifically concentrates on metal hydroxides with a general view on layered double hydroxides and MOF hydroxides with an efficient dimensional nanostructure idea; it also provides insight into core-shell composites with metal hydroxides, doping in metal hydroxides, metal hydroxide nanowires – conductive polymer nanocomposites, and 1D nanoform composites. Previous reports frequently highlight high specific capacitance values obtained from three-electrode topologies, with little focus on full-device (two-electrode) performance, long-term cycling stability, degradation mechanisms, and scalability issues. These



important gaps are well focused from synthesis, characterization and application perspectives as (i) developing design guidelines for one-dimensional (1D) metal hydroxide nanostructures, (ii) critically assessing electrochemical data with focus on three-electrode and two electrode configurations, and (iii) modifying the structure and metal atom doping by creating core-shell composites, and combining them with polymers to make the hydroxide valuable for use in supercapacitors.

## 2. Basics of the supercapacitors

Together with cutting-edge and effective energy storage technologies, supercapacitors have created new prospects for an energy storage revolution. They have remarkable durability, long cycle life, higher power density, and outstanding reversibility.<sup>31</sup> Supercapacitors are essential for uninterrupted power supplies in a variety of devices, including wearable electronics, laptops, cell phones, video cameras, and hybrid electric vehicles. Supercapacitors are rapidly emerging as a crucial technological advancement to serve as a connection between traditional capacitors and batteries because of their speedy charge and discharge rates.<sup>32</sup> Supercapacitors have exceptional cycle performance and require less maintenance. An efficiency of approximately 95% is achieved because even at power rates greater than  $1 \text{ kW kg}^{-1}$ , the energy loss is quite less and can be readily controlled using simple heat control techniques. This method for energy storage is more eco-friendly than other electronic storage systems.<sup>33</sup>

### 2.1 Structural features of supercapacitors

Typically, the supercapacitor is composed of two electrodes, an electrolyte, and a porous separator that lets ions flow through, as illustrated in Fig. 4. It can perform similarly to conventional capacitors and electrochemical batteries because of its particular architecture. For effective ionic charge transfer, the separator material must be resistive to electricity and have excellent ionic conductivity. The capacity of super-

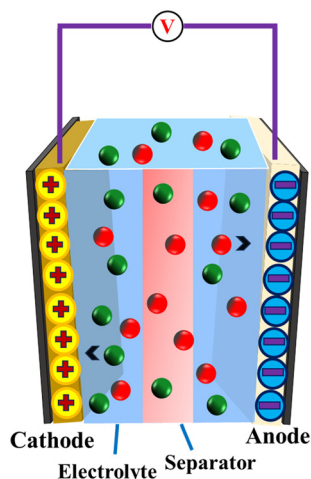


Fig. 4 Internal design of a supercapacitor.

capacitors to store energy depends on the choice of electrode and electrolyte material. The use of conductive and porous electrodes enables improved energy storage capacity.

### 2.2 Attributes of an efficient supercapacitor

An effective supercapacitor has enormous energy storage capacity and can be charged and discharged quickly. Excellent capacitance retention, dependable operating safety, and good functioning at different temperatures without performance loss are of prime importance, hence the supercapacitor's material is also electrically and thermally stable and has adequate conductivity. To attain desired characteristics, such as high-power density (PD) and energy density (ED) with exceptional cycle strength, several researchers are working to enhance supercapacitors' performance. The choice of electrodes and electrolytes has a significant impact on supercapacitors' performance. Essential elements known as electrolytes perform a major role in the transport and equilibrium of charges between the electrodes.<sup>34</sup>

## 3. Types of supercapacitors

The categorization of supercapacitors is based on faradaic and non-faradaic processes. They are electrochemical double-layer capacitors (EDLCs), pseudocapacitors and hybrid supercapacitors.<sup>35</sup> A basic comparison with respect to the working mechanism is explained in Fig. 5.

### 3.1 Electric double-layer capacitors (EDLCs)

In an EDLC, ion absorption through the electrode active layer is the main cause of capacitance (Fig. 5(a)). Here, the storage of charge carriers that occur in the electrical double layer capacitors is through a non-faradaic mechanism.<sup>36</sup> In an EDLC gravimetric and volumetric capacitance are boosted by the structural surface of active electrode materials. Graphene, carbon nanotubes (CNTs), and activated carbons are used as electrodes in these devices to increase their capacity to store charge.

### 3.2 Pseudocapacitors

Chemical adsorption, desorption, oxidation, and reduction are highly reversible processes that cause the change in capacitance response to the electrode's charge potential (Fig. 5(b)). Beyond simple electrostatic charge storage, pseudocapacitive electrodes use the intercalation and de-intercalation of ions inside the electrode materials as well as the transfer of electrical charges *via* redox processes.<sup>37</sup> Transition metal oxides (TMOs), sulphides, hydroxides, carbides and conducting polymers are said to be ideal electrode materials for pseudocapacitors. There are three different mechanisms that lead to pseudocapacitance: intercalation pseudocapacitance, redox pseudocapacitance, and underpotential deposition (Fig. 6). For underpotential deposition, the metal atom has a higher positive potential so that it would easily deposit onto the substrate surface.<sup>38</sup> Generally, faradaic charge transfer leads to a redox type pseudocapacitor mechanism. The pseudocapacitive behavior of hydrated



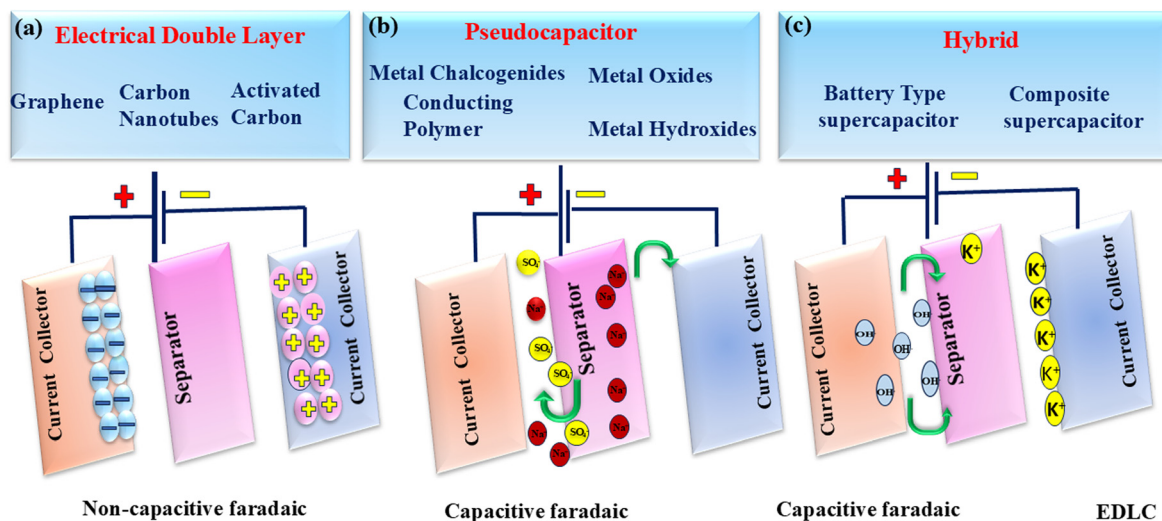


Fig. 5 Types of supercapacitors.

ruthenium oxide was discovered to facilitate redox reactions by collecting protons from the electrolyte. Intercalation leads to the process where ions immerse into the layer of the redox-active material.<sup>39</sup> The pseudocapacitive behavior can generate high PD to partially offset the battery's restricted ED and achieve high charge capacity at a high charge rate without facing the limitations of solid-state diffusion. The degree of ion diffusion across the electrode material limits insertion.<sup>40</sup> Both the  $C_s$  and the PD of the pseudocapacitor are high. The pseudocapacitors' high-PD makes them useful for energy storage in consumer electronics, automotive applications and electrical vehicles.

### 3.3 Hybrid supercapacitors

Greater specific capacitance ( $C_s$ ) is offered by the hybrid supercapacitor by combining both conventional EDLCs and pseudocapacitors. By storing electrical charges using both faradaic and non-faradaic methods (Fig. 5(c)), hybrid capacitors provide high  $C_s$ , ED, and PD as well as long-lasting per-

formance. Energy storage in an EDLC depends on the atomic charges' partitioning and intrinsic surface area.<sup>41</sup> However, quick and reversible redox processes occur in pseudocapacitors. These two principles are combined in the hybrid supercapacitor, where one half operates as a pseudocapacitor and the other as an EDLC.<sup>42</sup> Hybrid supercapacitors can be categorized as either symmetric or asymmetric depending on the types of electrodes used, whether two distinct electrodes or identical electrodes with differing mass loading. This idea was created to increase ED, with a goal range of 20–30 W h kg<sup>-1</sup>.<sup>43</sup> By mixing different redox and EDLC materials, including conducting polymers, TMOs, graphene or graphite, and activated carbon, hybrid supercapacitors are gaining popularity.<sup>44,45</sup> The capacitance values of hybrid supercapacitors are greatly increased by their asymmetric nature.<sup>46</sup> This creative method is a potential first step toward the increase of effective energy storage technologies. Supercapacitors of this kind can be further separated into battery-type supercapacitors and composite supercapacitors.

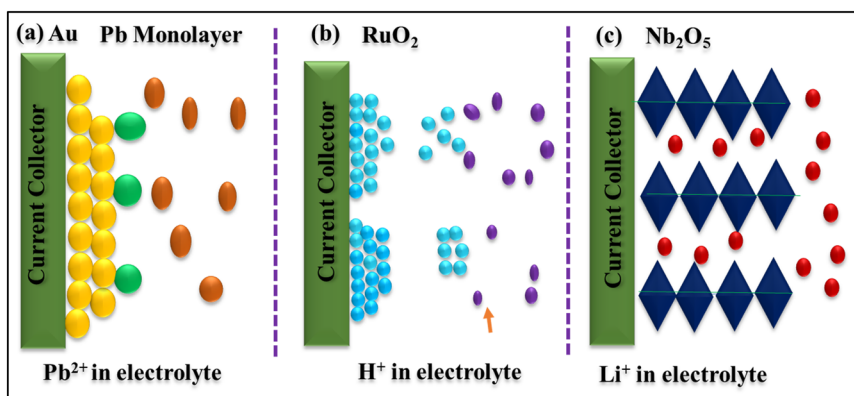


Fig. 6 Various reversible redox mechanisms contribute to pseudocapacitance, including: (a) underpotential deposition, (b) redox pseudocapacitance, and (c) intercalation pseudocapacitance.



## 4. Evaluation of performance and characterization

The three basic characterizations required to measure supercapacitor performance are cyclic voltammetry (CV), galvanostatic charge discharge (GCD), and electrochemical impedance analysis (EIS). To understand how the electrode reacts to the electrolyte and to obtain knowledge about the charge between the components of the supercapacitor, CV analysis is a helpful way to assess the electrode's specific capacitance ( $C_s$ ). Two and three electrode systems are typically used to determine the electrode and device performance of supercapacitors. In the three electrode system, the active material serves as the working electrode (WE), whereas Ag/AgCl as the reference electrode (RE) and platinum as the counter electrode (CE). By applying a consistent scan rate and a specific voltage difference between the WE and RE, CV is used to quantify the voltage difference. The GCD is used to determine the WE potential with variation in time at a constant current density. Additionally, GCD data gives information on Coulombic efficiency, PD, and ED. The charge transfer resistance, solution resistance and phase angle of the working electrodes and devices can be determined with the use of electrochemical impedance analysis. The combination of all these techniques enhances the overall performance of supercapacitor.

Specific capacitance for the three-electrode system:

The specific capacitance ( $C_s$ ) was obtained in three electrode configurations from the CV curve using the following formula,<sup>47</sup>

$$C_s = \int_{V_1}^{V_2} \frac{I(V)dV}{mv(V_2 - V_1)} \quad (1)$$

where  $m$  is the mass of the working electrode,  $v$  is the scan rate and  $V_2 - V_1$  is the voltage difference.

The specific capacitance ( $C_s$ ) from GCD analysis is calculated using the formula below for the three electrode system,<sup>48</sup>

$$C_s = \frac{I \int V(t) dt}{m(V_2 - V_1)^2} \quad (2)$$

Specific capacitance with device parameters for the two-electrode system:

The  $C_s$  for the two electrode system is measured from GCD as follows,<sup>49</sup>

$$C_s = \frac{2I \int V(t) dt}{M(V_2 - V_1)^2} \quad (3)$$

where  $M$  = mass of anode + mass of cathode.

The ED and PD were formulated as follows:<sup>50</sup>

$$ED = \frac{(C_s \times \Delta V^2)}{7.2} \quad (4)$$

$$PD = \frac{E_d \times 3600}{\Delta t} \quad (5)$$

The coulombic efficiency ( $\eta$ )<sup>51</sup> is calculated using discharge and charging times ( $t_d$  and  $t_c$ ).

$$\eta = \frac{t_d}{t_c} \times 100 \quad (6)$$

The peak value of current related to the scan rate is written below in eqn (7)<sup>52</sup>

$$i = av^b \quad (7)$$

In this case,  $i$  indicates the current,  $v$  is the scan rate,  $a$  is the constant parameter, and  $b$  is the variable parameter that falls between 0.5 and 1 in order to determine the charge storage behavior. The ideal capacitive behaviour is defined to be a  $b$  value of 1 while a  $b$  value corresponding to 0.5 indicates a diffusion-controlled mechanism.

## 5. Different nanoforms used in supercapacitive electrodes

Coming from the latest review on literature data, a significant amount of research has been done to create new electrode materials that will enhance supercapacitors' electrochemical performance along with redox-active metal compounds. These compounds can specifically be hydroxides and oxides that store charge through redox reactions with electrolyte ions which result in reversible valence changes. In recent years, there have been notable developments in aqueous supercapacitors based on metal oxides and hydroxides. Supercapacitors are beneficial, but their low ED prevents them from fulfilling the ever-growing demand of energy storage applications. A regulated porosity, higher conductivity of electrons, sufficient electroactive sites, and outstanding stability are all necessary features of ideal electrode materials for supercapacitors. It requires creative innovations to full fill these demands, such as using most advanced electrode materials with precisely engineered nanostructures. When developing sophisticated supercapacitor devices, nanostructured electrode materials provide a number of advantages over other dimension materials. Faster electron transport at high charge-discharge rates results from their tiny size, which shortens ion route lengths, along with, higher ion flow is made possible by a better interaction between the electrolyte and electrode material. 0D-nanoparticles, 1D-nanofibers, nanotubes, nanorods, nanowires, 2D-nanosheets and three dimensionally nanostructures have been greatly focussed. A schematic representation of supercapacitor electrodes is given in Fig. 7.

### 5.1 Dimension-based criteria for supercapacitor electrodes

**5.1.1 Zero-dimension.** These particles, which have all three dimensions at the nanometre scale, are known as zero-dimensions. According to this dimension, electrode materials are primarily found as core-shell and hollow nanoparticles. Activated carbon, graphene quantum dots, carbon nanoparticles, and quantum dots are all types of electrode materials



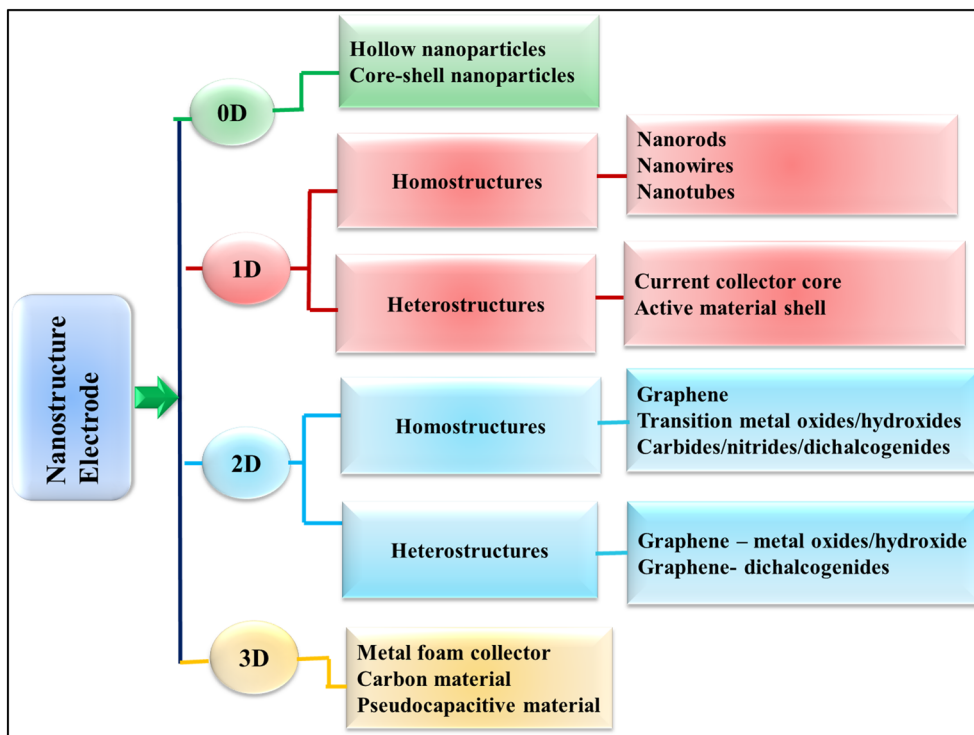


Fig. 7 The key aspects of electrode materials based on dimension (0D–3D).

used in EDLCs. Their large surface area improves the capacitance value by providing the quantum confinement effect. The supercapacitor also uses an electrode of the pseudocapacitor type with zero-dimensional nanoforms. The surface area of zero-dimensional metal hydroxide and oxide nanoparticles is larger than that of other low-dimensional nanoparticles. These dimensional nanoparticles have a high surface to volume ratio that provides quantum confinement of charge carriers thus increasing the electrochemical performance and also have better structure stability. However, it provides a limited active surface area for electrochemical reactions thus decreasing the significant value.

**5.1.2 One-dimensional.** In one direction, these nanostructures exhibit favorable electrical features that cannot be observed at the nanometre scale. They primarily focus on one dimension in the forms of heterostructures such as core-shell type and homostructures such as nanowires, nanorods, and nanotubes. Electrodes of the EDLC type include carbon nanotubes and carbon nanofibers. A good and porous active surface area for charge transportation is also provided by the homo and hetero type surface design of transition metal oxides (TMOs) and transition metal hydroxides (TMHs). In addition, it provides easy diffusion of charge carriers to the active sites of the electrode thus providing a rapid electron transport mechanism.

**5.1.3 Two-dimensional.** These nanoforms have a high aspect ratio of surface to volume and are found in thin-layer morphology. Since it offers a surface analogous to a nanosheet, its characteristics drastically diverge from those of other properties. TMOs, hydroxides, nitrides, and chalcogen-

ides are treated as supercapacitor electrodes because of their unique nanosheet-like homostructure. A heterostructure nanosheet is created by mixing graphene with either metal dichalcogenide or metal oxide/hydroxide. Due to the presence of planar structure, it provides a high surface area with excellent electronic conductivity which is helpful in electrochemical application but the synthesis procedure is quite challenging due to the presence of surface defects and impurities.

**5.1.4 Three-dimensional.** These usually have enhanced nanostructures featuring an overall increase in the electrode's surface to volume gradient. Here, all three dimensions aren't restricted to the nanometre scale. The majority of these include bulk nanopowder and nanoflower. The electrode material has a porous structure that provides easy carrier movement which also provides better mechanical stability; but due to some mechanical stress some degradation mechanism is observed. A distinctive comparison of one dimension nanostructures with 0D, 2D and 3D is explained in Table 2.

## 5.2 Importance of nanoforms towards supercapacitors

When materials are reduced to the nanoscale, their inherent properties, such as wettability, electrical conductivity and catalytic activity, give rise to new and distinctive features. The precise control of size and shape is made possible by the quantum effects associated with nanoscale dimensions. This allows for modifications in chemical potential, carrier transport and diffusion kinetics, and the band gap to be tuned.



**Table 2** Comparison of dimensional morphologies with their properties

Morphology	Crucial parameters	Surface area	Electrical conductivity	Ion diffusion routes	Structural stability	Application
0D (nanoparticles)	More active sites	High	Low-medium	Short with scattered path	Unstable	Mainly used in catalysts
1D (nanowires, nanotubes, nanorods)	Directional transport of ions	Moderate high	High	Very short	Highly stable	Supercapacitor and battery technology
2D (nanosheets)	Large surface area	Very high	High	Short with restacking issue	Moderately stable	Flexible electronics
3D (nanoparticles)	High pore volume	Extremely high	Medium	Long	High	Bulk devices

For supercapacitors, nanostructuring electrode materials is a practical way to greatly increase their surface area, allow the electrolytes to flow through the entire electrode matrix, avoid agglomeration and transfer electrons with ease. The  $C_s$  and rate capabilities are determined by both ionic and electronic conductivity. The most common zero-dimensional nanostructures are spherical nanoparticles which are also easier to produce than nanomaterials with different structural patterns. Agarwal *et al.*<sup>53</sup> synthesized zero-dimensional Mn nanoparticles at room temperature by the electroless synthesis route. The characteristics of 1D nanorods and nanowires composed of TMOs, hydroxides, and chalcogenides which are usually produced by a hydrothermal process include efficient one-dimensional electron transport and reduced external distortion during ion intercalation.<sup>54</sup> For instance, Xue *et al.* synthesized FeOOH nanorods with distinct surfaces and sizes by adjusting the concentration of  $Fe^{3+}$ . The emergence of two-dimensional (2D) nanomaterials has attracted significant research interest in the field of supercapacitor application with impressive electrochemical and mechanical properties.<sup>55</sup> Similar to 1D, 2D nanostructures, nanosheets and nanoflakes provide benefits such lower ion diffusion distances, more surface area, and improved structural stability. For example, 2D vanadium disulfide ( $VS_2$ ), a newly emerging metallic transition metal dichalcogenide (TMD) has been shown to create in-plane application in supercapacitors.<sup>56</sup> Also, 3D structures offer a flexible approach for storing and transporting ions. Three dimensionally ultrafine  $SnO_2$  nanoparticles have been produced using an economical photochemical technique.<sup>57</sup> The intricate interplay of these dimensions enhances important electrochemical properties, including capacitance and cycling stability.<sup>58</sup>

### 5.3 Importance of 1D nanostructures

A material is said to have a one-dimensional nanostructure if one or two of its dimensions fall inside the nano meter range, while the other dimension is bigger. The structure is called a nanowire when the aspect ratio is high, and a nanorod when it is low. It is referred to as a nanotube if the cross-section is spherical and hollow.<sup>59</sup> One-dimensional (1D) carbon nanotubes have gained more attention because of their remarkable chemical and physical properties that can be used in nanotechnology.<sup>60</sup> In contrast to one-dimensional solid materials, innovative one-dimensional

nanostructure materials have garnered interest recently because of their inherent higher ratio of surface-to-volume, direct current pathway, and reduced ion diffusion distance. In contrast, one-dimensional porous nanowires have shown encouraging potential applications in water treatment, fuel cells, lithium-ion batteries, sensors, catalysis, and photocatalysis as they offer good flexibility to be employed as electrodes with high electrochemical efficiency due their fibrous nature.

### 5.4 Advantage of 1D towards supercapacitor application

For energy storage devices, one-dimensional (1D) nanomaterials have high electrochemical response as compared to 2D and 3D materials. Their capacity to handle the electrochemical strain, promote quicker charge transport, and offer more effective conducting routes is primarily responsible for this increase.<sup>61</sup> Furthermore, one-dimensional nanostructures can improve accessibility to electrochemical reaction sites, especially at high current densities, and decrease the resistance provided by the electrolyte during the diffusion process. Additionally, the ability of nanowires to create porous structures further improves their performance. At the same time, scientists have been investigating novel structural designs to get high specific surface areas and distinctive morphologies. The following explains some important aspects of the influence of nano structuring (Fig. 8).

**5.4.1 Large surface area.** Due to their small dimension, one-dimensional structures have high aspect ratios of surface to volume, which leads to higher surface area-dependent material properties. The reactivity rate of the oxidation–reduction kinetics in the supercapacitor increases as the surface area rises due to the large number of surface atoms.

**5.4.2 Short ionic diffusion path.** From the perspective of supercapacitor applications, if the material is nanometer-scale in one dimension, it allows for ions to have a short diffusion path length, which results in greater capacitive behavior instead of a diffusion-like process.

**5.4.3 More active sites.** One-dimensional nanostructures offer more active sites, which also contributes to enhanced mass transfer kinetics. A good catalytic reaction is provided by its distinct molecular structure at a one-dimensional nanometre scale.

**5.4.4 Enabling nanoconfinement.** The method of nanoconfinement involves containing all of the ions and electrons



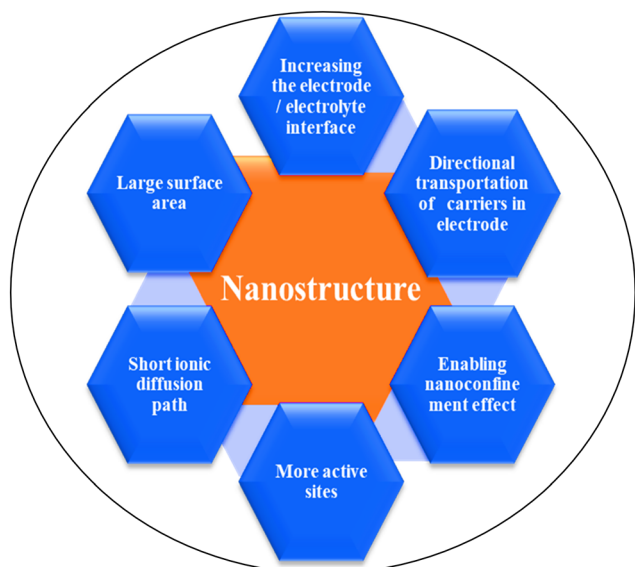


Fig. 8 Advantages of the nanostructure in supercapacitor application.

in a single area. Heterogeneous electron transfer occurs at the electrode surface because one-dimensional nanostructures are porous and offer a spatial environment for confining reactant molecules that would intensify the electrochemical process.

**5.4.5 Directional transport of carrier.** An increase in the material's electrical conductivity due to the one-dimensional pathway, which determines how quickly an electron may pass through the active electrode surface, results from the transfer of charge carriers.

**5.4.6 Increasing the electrode/electrolyte interface.** Ion adsorption and reaction rate on the electrode surface are accelerated by expanding the electrode–electrolyte contact. Additionally, it facilitates easy interaction between ions and the electrode material, thereby accelerating the chemical reaction.

## 6. General properties of one-dimensional metal hydroxides

### 6.1 Physical properties

The macroscopic aggregation state, that places the one-dimensional nanomaterial at the desired location, affects the performance of nanomaterials along their dimensions. A distinctive characteristic of metal hydroxides is the presence of a large amount of hydroxyl groups on their surface layer. Additionally, it has a lower value enthalpy change than metal oxide because it facilitates ion exchange more readily. Exploring metal hydroxides in a range of usage, such as catalysts, is made easier by this capability. Controlling the macroscopic orientation and aggregation of these materials yields a high aspect ratio for different applications (Fig. 9(a)).<sup>62</sup> A functional interface with good adhesion qualities is provided by the hydroxyl group present in the layer base (Fig. 9(b)). Research work was done on mechanically stable metal hydroxides, such as  $\text{Mg}(\text{OH})_2$  and  $\text{Ca}(\text{OH})_2$ , which showed interlayer binding energies and shear moduli less than higher dimension materials.<sup>63</sup>

### 6.2 Electrical properties

As nanotubes have a smaller dimension than higher dimension particles, electrons are confined in two-dimensional space and free only in one dimension like nanowires, nanotubes or nanorods. As with well-defined quantized shape, the electron wave mode contribution is quite smaller than the different dimension material. In carbon nanotubes, only one electron wave is responsible for electrical conductivity; and hence, due to confinement of electrons, the energy band gaps are discrete in nature.

### 6.3 Mechanical properties

Elastic modulus, hardness, toughness and Young's modulus are the different types of mechanical properties. While going from a higher dimension to the nano scale, there is a change

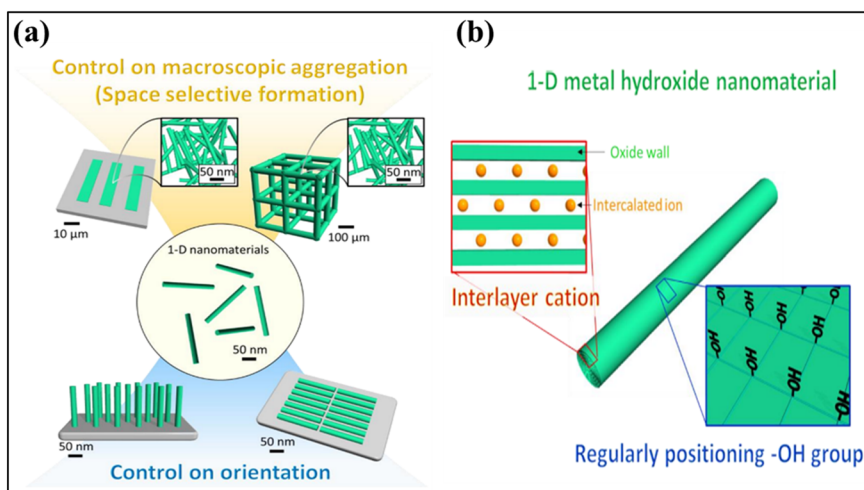


Fig. 9 (a) Orientation control and macroscopic aggregation of one-dimensional materials; (b) metal hydroxide showing the hydroxyl group.<sup>63</sup>



in mechanical properties. By decreasing the size to one dimension like nanotube and nanowire hardness, toughness is increased. Material ductility and plasticity are increased in the nano dimension.

#### 6.4 Thermal properties

The melting point of any material depends on the bond strength which depends on the surface to volume ratio. As the surface to volume ratio of one dimension nanomaterials is very high, so decreasing the particle size decreases the melting point.

#### 6.5 Chemical properties

As one-dimensional nanomaterials have a high surface area that increases the number of atoms accessible on the surface, the catalytic reaction and thus electrochemical performance also increase. Also, due to the presence of OH<sup>-</sup> groups in the metal hydroxide, it functions as a nucleophile, ligand, catalyst, and base. So, they exhibit good reactive sites that attack electrophilic sites in a chemical reaction. The presence of different crystalline structures of metal hydroxide provides open tunnels for ion insertion and extraction during redox reactions in the active surface sites. Different metal atoms have different oxidation states. Due to the well-designed structure, it provides a small diameter, good crystallinity and reduces the path length of electrolyte to pass through the electrode thus increasing the specific capacitance ( $C_s$ ) and power density (PD) value.

#### 6.6 Optical properties

Due to nano dimension the electronic confinement increases, leading to an increase in the value of energy band gap. Fig. 10(a and b) represents the material's energy band gap and electrical conductivity that fluctuate in response to changes in its dimension due to the higher electronic energy state caused by the quantum size effect.<sup>64</sup>

### 7. Properties of one-dimensional metal hydroxides towards super-capacitor applications

#### 7.1 One-dimensional conducting path

Due to nano surface architecture with one dimension, charge transport kinetics are more favorable which facilitate the overall supercapacitive electrochemical performance.

#### 7.2 Mechanical flexibility

Ions' intercalation and deintercalation in the electrode material's surface area is highly dimension dependent; therefore, 1D metal hydroxides with an O-H interlayer group permit ion movement through the material's layer, increasing electrical conductivity with little volume expansion and giving the prepared device robust mechanical flexibility for energy storage applications.

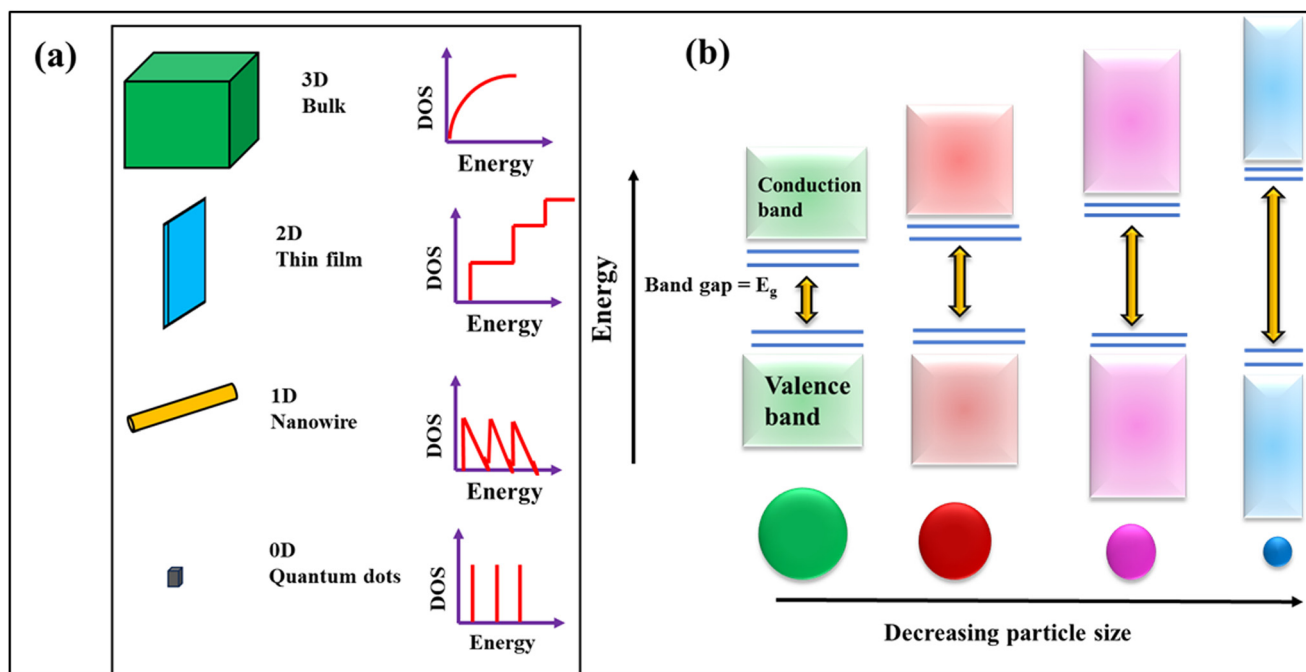


Fig. 10 (a) Density of state vs. energy, (b) energy band gap relative to decrease in particle size.<sup>64</sup> “Reprinted with permission from B. R. Sankapal, A. Agarwal, Simple Chemical Methods for Thin Film Deposition”, 1st edn, Springer Nature Singapore, Singapore, 2023, copyright © 2023 The Editors and the Authors.



### 7.3 Tunable nanostructured morphology

The widespread morphology of 1D metal hydroxides, such as nanotubes, nanowires, and nanorods, and the core-shell surface architecture facilitate easy penetration of electrolyte ions through the electrode's porous region, increasing charge carrier interaction, and ultimately enhances the specific capacitance.

### 7.4 Quick redox activity

Due to the 1D of metal hydroxides, the high surface area of transition metal provides a distinct oxidation state, causing pseudocapacitor type oxidation-reduction reactions, which causes the specific capacitance value to rise quickly.

### 7.5 Anisotropic growth

The specific capacitance value is increased as hydroxide materials are strongly bound in plane and growth preferentially occurs in one direction, resulting in an elongated structure with continuous electron route transfer that is preferred at edge locations.

### 7.6 Short ion diffusion path

As the electrical confinement occurs primarily in one direction, the resulting nanorod or nanowire morphology has an incredibly small diameter. This diameter aids in decreasing the ions' diffusion distance over the electrode's surface.

## 8. Limitations of one dimensional metal hydroxides towards supercapacitor application

Although one-dimensional metal hydroxide nanostructures offer several benefits, they also present significant challenges for supercapacitor performance. These are listed below.

### 8.1 Poor electrical conductivity

Due to the semiconducting and insulating nature of metal hydroxide, it suffers from high internal resistance with low-rate capability thus decreasing the electrical conductivity.

### 8.2 Low cyclic stability

During redox cycling, the hydroxide material undergoes phase transformation and rapid dissolution due to the presence of water content that leads to a decrease in specific capacitance value.

### 8.3 Low mechanical strength

Sometimes, due to aggregation and detachment from the surface, one-dimension metal hydroxides have lower mechanical strength.

### 8.4 Limited packing density

One-dimensional nano-structures are highly porous in nature, but have poor volumetric energy density.

### 8.5 Slow ion diffusion

Due to slow ion diffusion, the electrochemical accessibility decreases and as a result, the supercapacitor rate performance decreases.

### 8.6 Stability in electrolytes

Mainly, hydroxides are dissolved in electrolyte solution causing volume expansion due to repeated redox reactions, which causes structural breakdown of the one-dimensional nanostructure.

### 8.7 Scalability and reproducibility issues

It is very difficult to produce one-dimensional nanostructures on a large scale as their formation requires precise control over nucleation and growth conditions.

To overcome these limitations in metal hydroxide, the hybridization should be done with conducting materials like carbon, graphene or conducting polymers. Also formation of heterostructures like core-shell surface architecture provides good electrical conductivity.

## 9. Choice of electrolyte towards the stability performance of one-dimensional hydroxides

The stability mechanism of one-dimensional hydroxides was strongly affected by the choice of electrolyte. The role of the electrolyte is to alter the surface to volume ratio that amplifies the interfacial reaction between electrode-electrolyte. While water-in-salt electrolytes restrict water activity and expand the electrochemical window, improving cycling stability but posing ion-transport constraints and financial concerns, traditional alkaline electrolytes offer quick redox kinetics but speed up dissolution, surface reconstruction, and gas evolution.

### 9.1 Alkaline electrolyte

It provides strong  $\text{OH}^-$  ion availability with high ionic conductivity that provides fast faradaic reaction contribution. But sometimes, the hydroxide-based electrode material undergoes phase change with structural dissolution that leads to radial volume change or cracking. But the metal hydroxides still perform best in alkaline electrolyte as it provides a short diffusion distance with faster redox kinetics that increases the electrochemical performance.<sup>65</sup>

### 9.2 Water in salt electrolyte

It suppressed dissolution by reducing the water activity that stabilizes the morphological structure.<sup>66</sup> Also, these electrolytes provide a wide voltage window and prevent structural



collapse during cycling. Sometimes they exhibit certain limitations like high viscosity and cost issues.

## 10. Layered metal hydroxides: general view

Layered double hydroxides (LDHs) have emerged as highly promising electrode materials for supercapacitors compared to their individual counterparts like metal hydroxides or oxides due to the presence of unique 2D layered structure, consisting of positively charged metal hydroxide layers with intercalated anions and water molecules.<sup>67</sup> In general, these are typically multi-metal clay substances made up of hydroxyl-encircled brucite layers of metal cations that form  $M^{2+}(\text{OH})_6/M^{3+/4+}(\text{OH})_6$  octahedra.<sup>68</sup> They have garnered significant attention due to their easy synthesis, affordability, high catalytic efficiency, biocompatibility, and large surface area. Their unique properties stem from their two-dimensional internal framework, and high porosity. The interlayer placing of LDHs also allows the electrolyte ions to easily pass through the active surface area of the electrode. Also, bimetallic or trimetallic LDHs with significant oxidation states provide better assessment of charge carrier transportation rather than single metal oxides or metal chalcogenides. Also composites made using LDHs with other materials have provided better results during interlayer division through ion extraction and interaction effects. Additionally, modifying LDHs typically leads to structures, excellent ion exchange capacity, suitable interlayer spacing, highly tunable formation of hetero-interfaces and interconnected pathways, which reduce the diffusion distance for electron–electrolyte interactions and movement (Fig. 11).<sup>69</sup> Recently, LDHs have been used as active electrodes because they have a greater number of efficient active sites available on their exposed surfaces and also have outstanding redox properties. It has been shown that LDHs are only formed within specific compositional ranges and crystallize in a hexagonal layered structure. The NiAl-LDH pseudocapacitor electrode showed a  $C_s$  of  $1.04 \text{ C cm}^{-2}$

at  $1.68 \text{ mA cm}^{-2}$ .<sup>70</sup> Ni-Co LDH has been synthesized by a two-phase solvothermal method which gave an improved  $C_s$  of  $2682 \text{ F g}^{-1}$  at  $3 \text{ A g}^{-1}$  and an ED of  $77.3 \text{ Wh kg}^{-1}$  at a PD of  $623 \text{ W kg}^{-1}$ .<sup>71</sup> Additionally, optimizing the electrical nature of LDHs is essential, as high resistivity can result in slow charge carrier transfer and delayed redox processes. As a result, various strategies have been explored like core-shell metal hydroxides or composite based metal hydroxides to enhance the conductivity and ensure electrochemical stability.

## 11. MOF-derived hydroxides

Due to structural turnability, the hierarchical morphology of metal organic framework-based supercapacitors has achieved increasing importance. The organic ligands and secondary building units (SBUs) can be precisely controlled because of the special and movable architectures of MOFs.<sup>72</sup> Researchers are able to customize the pores' size, shape, and characteristics to match the performance requirements for a given application. However, MOF materials containing a single metallic element consistently perform poorly for inactivated sites and have an undesired structure. MOF-derived hydroxide/oxide structures are the most promising options for supercapacitor electrode materials because of their layered architectures and affordability. Compared with directly synthesized metal hydroxides, MOF derived hydroxides have a very high surface area. MOFs have excellent porosity as compared to traditional metal hydroxides which allow ions to pass easily through the electrode surface.<sup>73</sup> But majority of these investigations have synthesized MOF materials using solvothermal and hydrothermal techniques. However, these approaches frequently use expensive methodologies or multi-step, resource-intensive processes, which results in poor reproducibility. Therefore, one dimensional metal hydroxide have gained significant attention due to their simple chemical synthesis.

## 12. One-dimensional metal hydroxides

One-dimensional (1D) nanostructures offer distinctive attributes that significantly enhance their suitability for electrochemical energy systems. Beyond their well-known structural advantages, their elongated geometry ensures efficient electron transport along a direct axial pathway, minimizing resistance and enabling rapid charge transfer. This property is particularly valuable for high-power and fast-charging applications. In addition to facilitating electron transport, the structural resilience of 1D materials allows them to better accommodate mechanical strain during repeated cycling, thereby preserving integrity and improving long-term durability. The incorporation of porosity further strengthens their performance, as porous nanowires and nanotubes create interconnected channels that enhance electrolyte accessibility and mass transport. These features not only improve the utilization of the active material but also contribute to stable operation under demanding conditions. Collectively, the unique

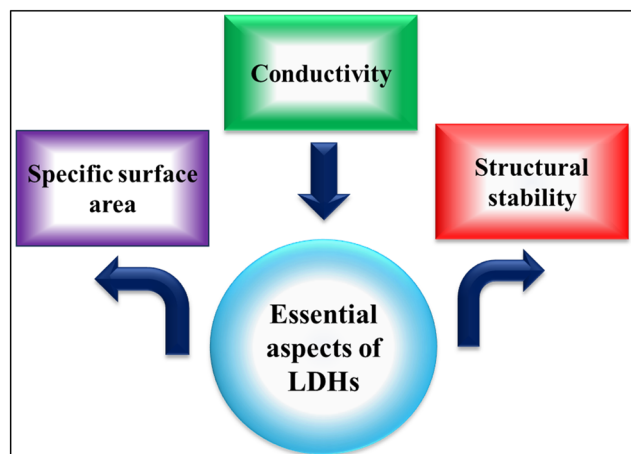


Fig. 11 Key properties of layer-based hydroxides (LDHs).<sup>69</sup>



combination of efficient charge transport, mechanical robustness, and porous design establishes 1D nanostructures as highly promising materials for next-generation supercapacitors, batteries, and other advanced electrochemical devices. In recent years, various technological advancements have been made in the fundamental and applied research for the development of electrochemical capacitors (ECs). Therefore, a promising approach to achieving high ED is to create hybrid systems utilizing various MOs/MHOs as the electrode materials for supercapacitor.<sup>74</sup> The various acid/base and redox chemistries of these materials, along with their extensive industrial use, have attracted study interest.<sup>75</sup> Pseudocapacitor type electrode materials that feature multiple oxidation states enable rapid reversible faradaic reactions, resulting in exceptionally high  $C_s$ . Metal hydroxides exhibit both high electrical conductivity and remarkable long-term stability. Oxides and hydroxides are generally viable candidates for improving the electrochemical efficiency of supercapacitors as they facilitate charge storage through redox chemical reactions with electrolyte ions. Various well-known research studies were carried out on metal hydroxides in energy storage application due to their enhanced conductivity. Currently various metals like Ni, Co, Fe, Ti, V, Mo, and Nb, are becoming notable candidates for electrode materials in hybrid supercapacitors. Mule *et al.*<sup>76</sup> synthesized mixed metallic Co–Fe–Ni–Mn hydroxide towards supercapacitor application. These findings will inspire researchers to develop next-generation energy storage devices with exceptional electrochemical qualities through the assembly and hypergrowth of TMOs and TMHs.

## 13. Deposition techniques for 1D-metal hydroxides

The benefits of using various chemical precursors and complexing agents to carry out the reaction process at specific temperatures are discussed for each strategy. There are essentially two approaches for creating nanostructures: top-down and bottom-up. The appropriate nanostructure can be formed by crushing and grinding the bulk material, but this is exceedingly challenging because of the uneven surface and considerable crystallographic loss. Different synthesis methods have been put forward for nanomaterials with individual merits and demerits. Therefore, it is more crucial to generate nanoforms utilizing the bottom-up strategy. Different synthesis techniques vary in their choice of precursors and conditions like temperature, pressure, and pH levels. A detailed explanation of metal hydroxide nanomaterials for supercapacitor electrodes is summarized as follows.

### 13.1 Hydrothermal synthesis

It is one of the best techniques for achieving good control over the morphology of the nanomaterial, a low-cost synthesis procedure and environmentally friendly nature. However, it suffers from the agglomeration of nanoparticles during re-

action time. This technique utilizes water as a solvent in a closed Teflon-lined reactor, generally at temperatures in between 100–200 °C and pressures greater than 1 bar.<sup>77</sup> This approach allows for the creation of materials that cannot be produced by traditional methods, enabling distinctive crystallization and growth processes. The elevated temperature and pressure help dissolve precursors and promote the formation of new phases, making this method essential in fields like materials science, ceramics, and nanotechnology. Interestingly, the  $\text{Co}(\text{OH})_2$  nanotube was synthesized through the hydrothermal method using the precursor salt of  $\text{CoCl}_2 \cdot 6\text{H}_2\text{O}$  with urea solution at temperature around 120 °C for 12 hours in a Teflon lined autoclave by using a three step hydrothermal method followed by ion exchange and electrochemical activation approach (Fig. 12). This method provides a uniform besom-like nanowire morphology with a high active surface area. This structure changed to nanotube morphology due to the presence of the Kirkendall effect that provides a flexible kind of cobalt hydroxide electrode with a huge specific capacitance value for supercapacitor application.

### 13.2 Chemical bath deposition (CBD)

The chemical bath deposition method helps to produce samples in thin film and powder form with good homogeneity and growth rate using a very low-cost precursor salt. The main demerits arise due to poor film adhesion with lack of uniformity. Chemical bath deposition (CBD) is simple, cost effective and applicable for large area deposition as the reaction kinetics works on spontaneous film formation with stoichiometrically accurate crystalline phases.<sup>78–80</sup> It is an appealing method for producing films of elemental, binary, and ternary compounds.<sup>81</sup> This method is straightforward and convenient for synthesis of 0D, 1D, 2D and 3D materials. Used nanowires can have many applications like in solar cells and LPG sensors.<sup>82–84</sup> Fig. 13 represents the synthesis of cobalt hydroxide on graphitic carbon foam (GCF) using CBD. First, styrene and divinylbenzene polymerized in high internal phase emulsion (HIPE) were carbonized to form GCF. Next, cobalt hydroxide was synthesized on GCF using chemical bath solution containing 50 ml of deionized water, which included  $\text{Co}(\text{NO}_3)_2 \cdot 6\text{H}_2\text{O}$  and urea as chemical reagents. The mixture was continuously agitated for ten minutes. In order to deposit  $\text{Co}(\text{OH})_2$ , GCF was then permitted to remain in the bath in a vertical position.<sup>85</sup>

### 13.3 Electrodeposition

It is a purely electrochemical method with a high chance of getting the material. It is a unique synthesis method with growth of the nanomaterial on a conducting substrate with a certain voltage window to get desired thickness of the thin film. But this synthesis method is only possible with conducting substrates not for insulating ones, and also major issues arise during mechanical adhesion with non-uniform large area coating. Electrodeposition is a process that involves the creation of a



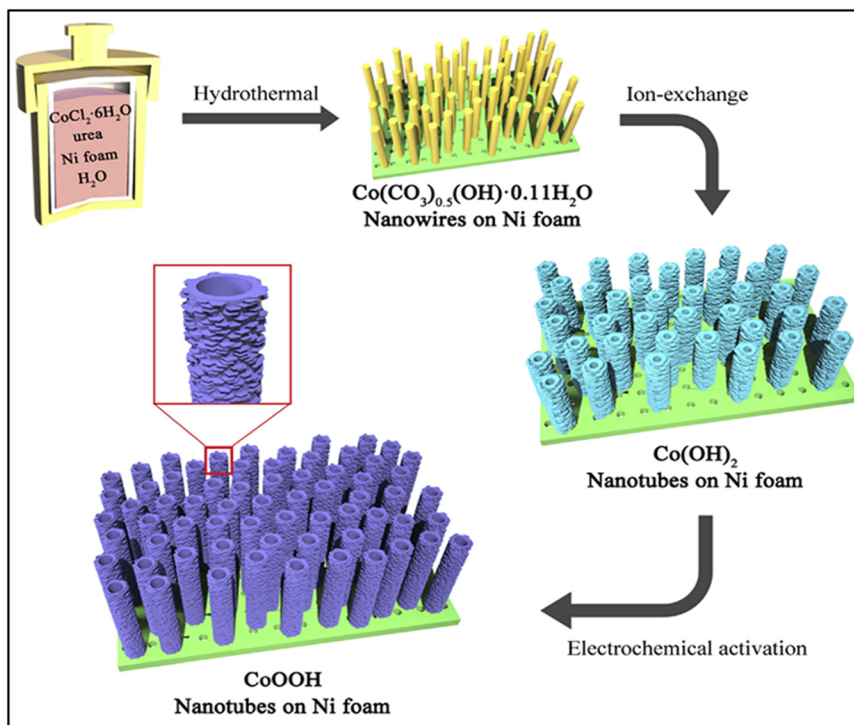


Fig. 12 Hydrothermal deposition of  $\text{Co}(\text{OH})_2$  on Ni foam. "Reprinted with permission from L. Peng, L. Lv, H. Wan, Y. Ruan, X. Ji, J. Liu, L. Miao, C. Wang, J. Jiang, Understanding the electrochemical activation behavior of  $\text{Co}(\text{OH})_2$  nanotubes during the ion-exchange process", *Mater. Today Energy* copyright © 2017 *Mater. Today Energy*.<sup>107</sup>

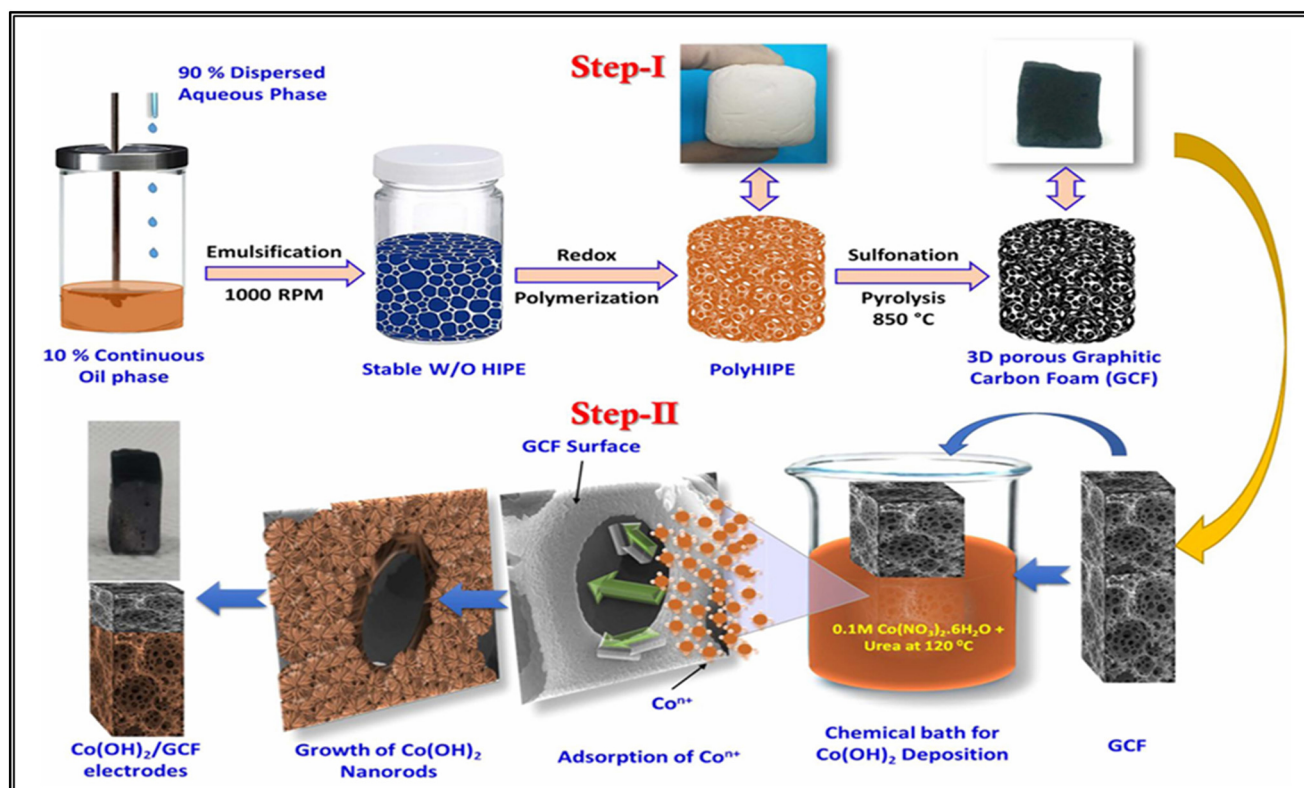
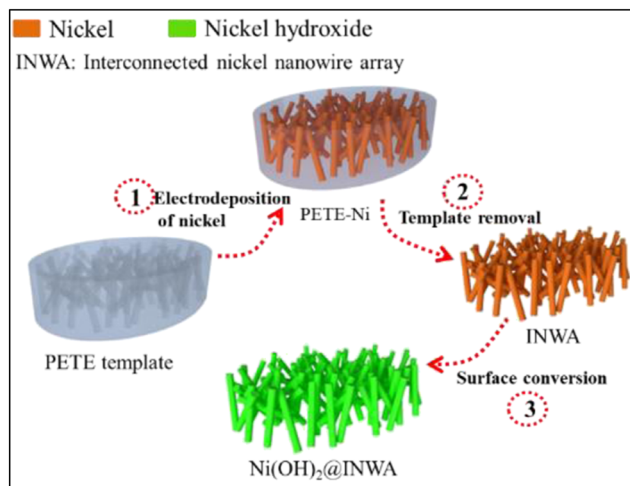


Fig. 13 Chemical bath deposition of  $\text{Co}(\text{OH})_2$  on graphitic carbon foam (GCF).<sup>85</sup> "Reprinted from U. M. Patil, R. V. Ghorpade, M. S. Nam, A. C. Nalawade, S. Lee, H. Han, S. C. Jun, PolyHIPE Derived Freestanding 3D Carbon Foam for Cobalt Hydroxide Nanorods Based High Performance Supercapacitor", via Creative Commons CC BY 4.0 licence.





**Fig. 14** Electrodeposition method of Ni(OH)<sub>2</sub>@interconnected nickel nanowire arrays (INWA). “Reprinted with permission from Ge, Wei, *et al.* Construction of amorphous Ni(OH)<sub>2</sub>@nickel nanowire with interconnected structure as advanced core-shell electrodes for asymmetric supercapacitors”, copyright © 2020 J. Energy storage.<sup>86</sup>

metallic layer on a substrate through the electrochemical reduction of metal ions. The synthesis of Ni(OH)<sub>2</sub>@interconnected nickel nanowire arrays (INWA) with a well-designed core-shell structure was accomplished *via* electrodeposition. First, porous polyester (PETE) was utilized as a template for the electrodeposition process of Ni(OH)<sub>2</sub>@INWA, as given in Fig. 14. The PETE was then coated with Ga-In eutectic on one side to provide an electrically conductive surface. A steady state voltage of 1.3 V was applied for 30 minutes to the nickel wire with NiSO<sub>4</sub>, NiCl<sub>2</sub> as the precursor, and H<sub>3</sub>BO<sub>3</sub> as the electrolyte. The template was then oxidized to produce Ni(OH)<sub>2</sub> after being dissolved to generate INWA using hexafluoroisopropanol.<sup>86</sup>

### 13.4 Coprecipitation

This method is cost-effective with a high chance of yielding the powder sample. There is requirement of post annealing temperature during the fabrication process with limited pore size controller that might get chance to addition of impurity material during synthesis procedure. This method requires low temperature to precipitate solid particles and has great uniformity control. After dissolving the metal precursor in the solution and adding a base to regulate the pH level, the resulting powder is typically cleaned and kept for drying. Reduced graphene oxide was first prepared by the modified Hummers' method. Then the composites of reduced graphene oxide/nickel hydroxide with different morphologies were grown by the co-precipitation method. The rGO/Ni(OH)<sub>2</sub> was described along with its different morphologies.<sup>87</sup>

### 13.5 Microwave

It is an efficient method having the potential to heat the material hence, it is widely used in industry and academia to synthesize porous, organic, inorganic and crystalline materials for energy storage application. Controlled micro struc-

ture, energy saving and production yield are several key factors of this method. Using an electromagnetic field for molecular interaction, energy is transferred to the surface molecule to carry out the reaction. Due to microwave assisted reaction kinetics, the nucleation and growth can be controlled; therefore it has attracted significant attention for oxide-based materials. The major disadvantages of this method are high equipment cost and pressure related safety issues. Several oxides like manganese oxide, ruthenium oxide, nickel oxide nickel hydroxide, cobalt oxide, cobalt hydroxide and iron oxides are produced using microwave assisted techniques.<sup>88</sup> Mondal *et al.*<sup>89</sup> effectively synthesized β-Ni(OH)<sub>2</sub> using a single step microwave assisted synthesis technique. Similarly, a composite was made with expanded graphite and Ni(OH)<sub>2</sub>. In accordance with HR-TEM pictures, the FESEM analysis shows that the edge planes are wrinkled and thin, and there is a substantial deposit of Ni(OH)<sub>2</sub> nanoparticles on the surface and between interlayers.<sup>90</sup> Zhou *et al.*<sup>91</sup> used a simple and economical microwave-assisted technique to synthesize flower-like α-Co(OH)<sub>2</sub> on the activated carbon surface of activated carbon substrates for supercapacitor application.

### 13.6 Electrospinning

It is a voltage-driven procedure that yields fibre with dimensions ranging from nanometres to micrometres utilising polymeric materials. Electrospinning has gained an important role in contrast to other synthesis procedures since it offers direct fabrication of a self-supported membrane with an enormous surface area and high permeability nature.<sup>92</sup> Due to its rapid production rate and regulated dimensions, it is an efficient method for creating one-dimensional polymeric hybrid nanofibers. Several core-shell, hollow, and multichannel nanofibers have been investigated using these methods.<sup>93,94</sup> The field of supercapacitors involves a variety of metal oxides, metal chalcogenides, and conducting polymer composites. However, a number of metal hydroxides in one dimension are also being investigated. The electrospun deposited Ni-Ni(OH)<sub>2</sub>/carbon nanofiber yields an excellent stability value along with a good C<sub>s</sub> value.<sup>95</sup> Additionally, a hierarchical architecture of Ni(OH)<sub>2</sub> was created using a chemically precipitated nickel hydroxide composite and electrospun carbon nanofibers, both of which exhibit excellent electrochemical performance.<sup>96</sup> Cobalt hydroxide and carbon nanofiber were combined to create a flexible, free-standing composite using electrospinning and chemical precipitation which was utilized as an effective electrode for a supercapacitor.<sup>97</sup>

## 14. Widespread 1D nanostructures for supercapacitor applications

Nanowires, nanorods and nanotubes, and nanobelts are different kinds of one-dimensional (1D) nanostructures. In contrast, 1D heterostructures consist of fiber structures, hollow nanostructures, branched nanowires, array topologies, and core-shell nanostructures. Electrode materials for



supercapacitors with a nanowire structure are attracting more and more attention from researchers worldwide. Nanowires provide more advantages than other structural morphologies when it comes to controlling electrodes. Few evaluations of oxide, hydroxide, and metal chalcogenide-based 1D materials for supercapacitor applications have been discussed earlier. But only a few reports have been published that particularly discuss nanowire materials for supercapacitor electrodes: one focusing on PEDOT-CuO nanowire arrays,<sup>98</sup> Ni<sub>3</sub>Se<sub>2</sub> nano-sheets integrated with 3D NiSe nanowire arrays and nanowire materials for supercapacitor electrodes.<sup>99</sup> However, several materials including metals, MO, MH, metal sulphides, metal nitrides, selenides and tellurides, have been developed in nanowire form. Several TMOs like manganese oxide (MnO<sub>2</sub>) nanowire were successfully synthesized by Hwang *et al.*<sup>100</sup> using the laser induced hydrothermal growth method which gives a high areal capacitance of 227 mF cm<sup>-2</sup>. Guo *et al.*<sup>101</sup> prepared TiO<sub>2</sub> nanowires on a titanium substrate which were used as a novel asymmetric supercapacitor electrode that provides a good value of ED. The hydrothermal method was used to synthesize Ti@MnO<sub>2</sub>, which provides high C<sub>s</sub>, excellent rate performance, and the requisite cycling stability for supercapacitor application.<sup>102</sup> Like metal oxides, there are various reports published on one-dimensional nanostructure-based metal sulphides. A simple and versatile chemical method was used to form nested CdS@HgS core-shell heterostructure nanowires on a stainless-steel current collector, resulting in a large surface area and demonstrating an impressive supercapacitance value.<sup>103</sup> Also, Ag<sub>2</sub>S nanowires with CdS/Ag<sub>2</sub>S core-shell heterostructures were successfully synthesized by Nair *et al.*<sup>104</sup> Several tellurides like cobalt telluride nanostructured materials with an asymmetrically designed device achieved high-PD and ED.<sup>105</sup> Manganese telluride (MnTe) and silver-doped MnTe were produced using an affordable hydrothermal synthesis technique.<sup>106</sup>

#### 14.1 Bare metal hydroxide electrodes

Literature reviewed metal hydroxides are listed in Table 3. In alkaline electrolytes, Co(OH)<sub>2</sub> is a useful material for charge storage because it has a high specific capacity, quick response time, and extended life cycle. However, the basic underlying fundamental properties that contribute to its excellent charge storage performance remain poorly understood. The nanotube morphology of cobalt hydroxide was synthesized on nickel foam using an ion-exchange method which was driven by the electrochemical method (Fig. 15(a)). A single-step method was carried out to produce a pseudocapacitor electrode of cobalt hydroxide on flexible carbon cloth Co(OH)<sub>2</sub>/CC with a well-defined nanowire morphology (Fig. 15(b)). The C<sub>s</sub> of 1108 mF cm<sup>-2</sup> achieved within a voltage range of -0.1–0.5 V (Fig. 15(c)) was sustained over 150 cycles.<sup>107</sup> As shown in Fig. 15(d), GCD performance was measured for 1000 cycles at a current density of 5 mA cm<sup>-2</sup> in the potential range of 0.1 to 0.55 V. Using the hydrothermal method formation of hydrophilic groups on the carbon cloth was possible which aids the nucleation and growth mechanism

of Co(OH)<sub>2</sub>. The supercapacitive study indicated that the Co(OH)<sub>2</sub>/CC electrode achieved an areal capacitance of 1.13 F cm<sup>-2</sup>. Additionally, it demonstrated exceptional cycling strength, retaining about 100% of the capacitance after 4000 cycles.<sup>108</sup> The Cd(OH)<sub>2</sub> electrode tested in various electrolytes shows that the nanowires exhibit supercapacitive behavior, particularly in high concentrations of OH<sup>-</sup> ions. In 6 mol dm<sup>-3</sup> KOH, a C<sub>s</sub> of up to 1164.8 F g<sup>-1</sup> at 1 A g<sup>-1</sup> and 257.6 F g<sup>-1</sup> at 10 A g<sup>-1</sup> were achieved.<sup>109</sup> At room temperature, CBD was used to grow Cd(OH)<sub>2</sub> nanowires in thin film form, and the prepared electrode achieved a notable C<sub>s</sub> of 356 F g<sup>-1</sup> at 1 A g<sup>-1</sup>, retaining 74% of its initial capacitance over 5000 cycles.<sup>110</sup> Similarly, the CBD method was employed to grow cadmium hydroxide nanowires on a stainless-steel (SS) substrate, achieving a C<sub>s</sub> of 267 F g<sup>-1</sup> at 5 mV s<sup>-1</sup>, while maintaining 86% of its capacitance after 1000 cycles.<sup>111</sup> Cobalt hydroxide nanorods with excellent pseudo capacitance by Ming-Jay Deng *et al.*<sup>112</sup> displayed a C<sub>s</sub> of 2500 F g<sup>-1</sup> within a voltage range of 0.65 V at a current density of 1 A g<sup>-1</sup> in a three-electrode cell. The hydrothermally synthesized Co(OH)<sub>2</sub> nanowire electrode exhibits a C<sub>s</sub> of 358 F g<sup>-1</sup> at a current density of 0.5 A g<sup>-1</sup> and the C<sub>s</sub> retention is measured at 86.3% over 5000 cycles.<sup>113</sup> A simple, single-step method was created for the synthesis of γ-MnOOH nanotubes. At a scan rate of 5 mV s<sup>-1</sup>, the C<sub>s</sub> of γ-MnOOH nanotubes was measured to be 147.4 F g<sup>-1</sup>.<sup>114</sup> Alpha-nickel hydroxide nanowires with a diameter of 60 nm were synthesized using a reverse migration technique. A maximum C<sub>s</sub> of 833 F g<sup>-1</sup> was achieved at a constant current of 5 mA.<sup>115</sup> A nanowire-like array of Cu(OH)<sub>2</sub> was directly synthesized through straightforward and economical reaction of liquid-solid interaction. The C<sub>s</sub> value of Cu(OH)<sub>2</sub> was measured at 511.5 F g<sup>-1</sup> with a current density of 5 mA cm<sup>-2</sup>.<sup>116</sup> Iron oxyhydroxide (FeOOH) exhibits a pseudocapacitive behavior predominantly in the negative potential region within aqueous electrolytes, and it is currently being investigated as a negative electrode material in asymmetric supercapacitors. Nonetheless, similar to other hydroxides, the exact mechanism behind charge storage in FeOOH remains unclear and many aspects are still not fully understood. FeOOH nanorods hydrothermally synthesized by Chen *et al.*<sup>55</sup> exhibit the highest C<sub>s</sub> of 714.8 F g<sup>-1</sup>. Patil *et al.* synthesized Co(OH)<sub>2</sub> nanorods chemically anchored on 3D graphitic carbon foam (GCF) through the CBD method (Fig. 16). The nanorod morphology was seen in FESEM analysis. The designed electrode shows a C<sub>s</sub> of 1235 F g<sup>-1</sup> at 1 A g<sup>-1</sup> in 1 M KOH (Fig. 16(a–d)).<sup>85</sup>

#### 14.2 Core-shell composites with metal hydroxides

To achieving a broad surface area with superior conductivity, core-shell materials can play an important role where the surface architecture expedites charge transfer and offers additional locations for faradaic reactions that ultimately improve the electrocapacitive performance of supercapacitors (C<sub>s</sub>). The core-shell structure typically consists of a central core surrounded by a shell with different characteristics such as one having high electrical conductivity and the other having strong electrochemical activity. Various assembly techniques



Table 3 Literature reports on one-dimensional metal hydroxides

Material	Method	ST	Morphology	Electrolyte	Configuration	Voltage window (V)	Specific capacitance	Energy density (Wh kg <sup>-1</sup> )	Power density (W kg <sup>-1</sup> )	Retention@cycles	Ref.
Co(OH) <sub>2</sub>	HT-IER-ED	Nickel foam	NT	6 M KOH	Three electrodes	-0.1–0.5	1108 mF cm <sup>-2</sup>				107
Co(OH) <sub>2</sub>	CBD	3D carbon foam	NR	1 M KOH	Three electrodes	-0.2–0.8	1235 F g <sup>-1</sup>				85
Co(OH) <sub>2</sub>	HT	Carbon cloth	NW	KOH	Three electrodes		1.13 F cm <sup>-2</sup>			100%@4000	108
Cd(OH) <sub>2</sub>	TFG	Ni foam	NW	KOH	Three electrodes	0–0.45	1164.8 F g <sup>-1</sup>				109
Cd(OH) <sub>2</sub>	CBD	Stainless steel	NW	NaOH	Three electrodes		356 F g <sup>-1</sup>			74%@5000	110
Cd(OH) <sub>2</sub>	CBD	Stainless steel	NW	NaOH	Three electrodes	-0.5–1.2	267 F g <sup>-1</sup>	23.61 Wh kg <sup>-1</sup>	3.30 kW kg <sup>-1</sup>	86%@1000	111
Cd(OH) <sub>2</sub> /Cd(OH) <sub>2</sub>	CBD	Stainless steel			Two electrodes	0–2	46.15 F g <sup>-1</sup>	18.53 Wh kg <sup>-1</sup>	1307.69 W kg <sup>-1</sup>	117%@1000	
Co(OH) <sub>2</sub>	HT	Platinum mesh	NW	10 mM KOH	Two electrodes	1.6	358 F g <sup>-1</sup>	13.6 Wh kg <sup>-1</sup>	153 W kg <sup>-1</sup>	86.3%@5000	113
Co(OH) <sub>2</sub> /NTAC							38.9 F g <sup>-1</sup>				
γ-MnOOH	OSF	Nickel foam	NT	0.5 mol L <sup>-1</sup> Na <sub>2</sub> SO <sub>4</sub>	Three electrodes	1.1–0.1	147.4 F g <sup>-1</sup>				114
α Ni(OH) <sub>2</sub>	TAP	Nickel foam	NW	6 M KOH	Three electrodes	0.1–0.6	833 F g <sup>-1</sup>				115
Cu(OH) <sub>2</sub>	LSR	Copper foil	NW	6 mol dm <sup>-3</sup> KOH	Three electrodes	0–0.5	511.5 F g <sup>-1</sup>	18.3 Wh kg <sup>-1</sup>	326 W kg <sup>-1</sup>	83%@5000	116
Cu(OH) <sub>2</sub> /Cu-foil										80%@5000	
FeOOH	HT		NR	2 M KOH	Three electrodes	-1.2–0.45	714.8 F g <sup>-1</sup>				55
Co(OH) <sub>2</sub>	HT	Pyrolytic graphite	NW	2 M KOH	Three electrodes	-0.3–0.6	642.5 F g <sup>-1</sup>				149
Co(OH) <sub>2</sub>	EC	3D nickel foam	NR	KOH	Three electrodes	0.6	2500 F g <sup>-1</sup>	220 Wh kg <sup>-1</sup>	0.3 kW kg <sup>-1</sup>	95%@10 000	112
Co(OH) <sub>2</sub> /Co(OH) <sub>2</sub>										87%@10 000	
Ni(OH) <sub>2</sub>	HT	Graphite foam	NW	6 mol L <sup>-1</sup> KOH	Three electrodes	0–0.5	2144 F g <sup>-1</sup>	59 Wh kg <sup>-1</sup>	2.1 kW kg <sup>-1</sup>	96%@2000	150
Ni(OH) <sub>2</sub> /graphite foam										97%@3000	
Ni(OH) <sub>2</sub> fibre electrode	HT	CF	NW	PVA–KOH–H <sub>2</sub> O	Three electrodes	-0.4–0.6	76.7 F g <sup>-1</sup>			70%@10 000	151
Ni(OH) <sub>2</sub> micro supercapacitor											
Str(OH) <sub>2</sub>	SILAR	SS	Tuberosse fibre	1 M NaOH	Three electrodes	0–0.8	413 C g <sup>-1</sup>	45.95 Wh kg <sup>-1</sup>	2.6 kW kg <sup>-1</sup>	35%@5000	152

Note: ST – substrate, IER – ion exchange reaction, HT – hydrothermal, TFG – two step facile growth, CBD – chemical bath deposition, ECM – electrochemical, OSF – one step facile, TAP – two step anodization process, LSR – liquid–solid reaction, NW – nanowire, NT – nanotubes, NR – nanorod, SILAR – successive ionic layer adsorption and reaction.



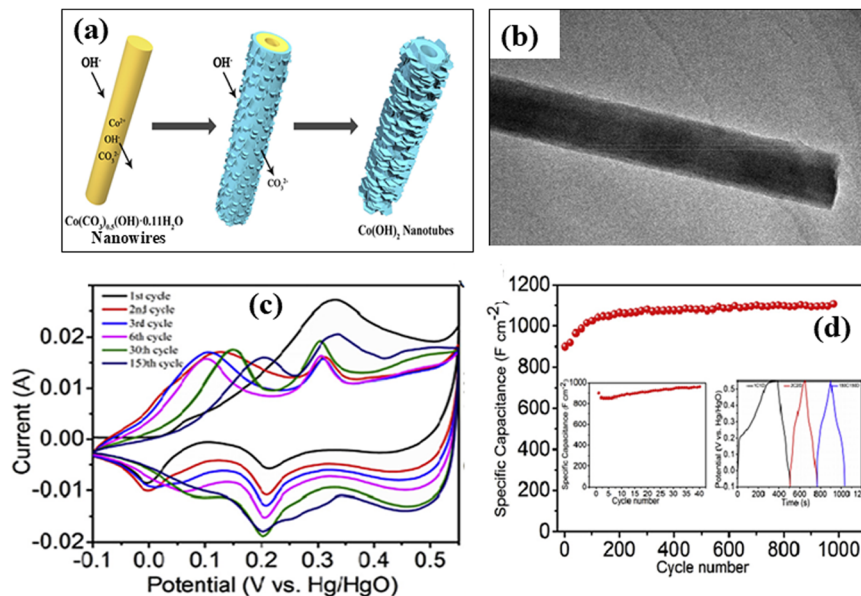


Fig. 15 (a) A diagrammatic representation of the synthesis method of Co(OH)<sub>2</sub> nanotube arrays, (b) FESEM image of the prepared sample, (c) current vs. voltage of the prepared electrode using CV, and (d) capacitance retention (inset: GCD variation). "Reprinted with permission from L. Peng, L. Lv, H. Wan, Y. Ruan, X. Ji, J. Liu, L. Miao, C. Wang, J. Jiang, Understanding the electrochemical activation behavior of Co(OH)<sub>2</sub> nanotubes during the ion-exchange process", *Mater. Today Energy* copyright © 2017 *Mater. Today Energy*.<sup>107</sup>

are possible, including applying a thin film shell over a core that facilitates rapid charge transfer or growing vertical nanosheet arrays on a core of nanorods, nanotubes, or nanoparticles.<sup>117</sup> This core-shell design enhances energy storage compared to a single material as it can mitigate the limitations of one material by combining it with another that has complementary attributes. Among the many benefits of the core-shell technique, it is also able to blend several materials with advantageous qualities and suitable morphologies that are explained in Table 4. The core-shell material for supercapacitors was made up of multi-wall carbon nanotubes (MWCNTs) and polyaniline (PANI) and achieved a  $C_s$  of 322 F g<sup>-1</sup>.<sup>118</sup> Amorphous Ni(OH)<sub>2</sub>@INWA has demonstrated superior electrochemical performance, achieving an impressive  $C_s$  of 3400 F g<sup>-1</sup> at a current density of 5 A g<sup>-1</sup>. The prepared device made with Ni(OH)<sub>2</sub>@INWA and RGO provides a remarkable specific energy of 53 Wh kg<sup>-1</sup> at a specific power of 395 W kg<sup>-1</sup>.<sup>86</sup> Co<sub>9</sub>S<sub>8</sub>@Ni(OH)<sub>2</sub> core-shell nanotube arrays, anchored on carbon fibers, have been carefully designed and fabricated for application in supercapacitors. The electrode exhibits a high  $C_s$  of 149.44 mAh g<sup>-1</sup> at 1 A g<sup>-1</sup> and sustains a  $C_s$  of 75 mAh g<sup>-1</sup> at 10 A g<sup>-1</sup>.<sup>119</sup> Additionally, a core-shell Cd(OH)<sub>2</sub>-VOOH nanorod was produced for use in solid-state supercapacitors using a two-step CBD followed by an ion exchange reaction. The prepared electrode obtained a  $C_s$  of 233.98 F g<sup>-1</sup> at 5 mV s<sup>-1</sup> with 60.5% capacitance retention over 2500 cycles and the designed device achieved a  $C_s$  of 53.62 F g<sup>-1</sup>.<sup>120</sup> Nanowires with a core-shell structure are secured on nickel foil by hydrothermally synthesizing NiCo<sub>2</sub>O<sub>4</sub> as the core and then electrodepositing  $\alpha$ -Co(OH)<sub>2</sub> as the shell. The reaction time greatly influenced the morphology of the prepared composite along with the composite electrodes

synergistic redox processes originating from both NiCo<sub>2</sub>O<sub>4</sub> and  $\alpha$ -Co(OH)<sub>2</sub> can be provided more active sites with shell material of  $\alpha$ -Co(OH)<sub>2</sub> offers open networks that facilitate electrolyte transport. Also, the integral conductivity of the composite is improved by the highly conductive NiCo<sub>2</sub>O<sub>4</sub>, which lowers the resistance between the current collector and  $\alpha$ -Co(OH)<sub>2</sub>. The nanosheet aggregation is successfully inhibited by the uniform development of  $\alpha$ -Co(OH)<sub>2</sub> on NiCo<sub>2</sub>O<sub>4</sub> nanowires. Fig. 17(a) represents the two step fabrications process of NiCo<sub>2</sub>O<sub>4</sub>@ $\alpha$ -Co(OH)<sub>2</sub>. Using nickel foam as the substrate, NiCo<sub>2</sub>O<sub>4</sub> nanowires were created using a straightforward hydrothermal process followed by the electrochemical method to coat  $\alpha$ -Co(OH)<sub>2</sub> to get unique core-shell morphology (Fig. 17(b)). CV was used to study the  $C_s$  of individual NiCo<sub>2</sub>O<sub>4</sub>,  $\alpha$ -Co(OH)<sub>2</sub> and the core-shell composite of NiCo<sub>2</sub>O<sub>4</sub>@ $\alpha$ -Co(OH)<sub>2</sub>, at 5 mV s<sup>-1</sup> (Fig. 17(c and d)).<sup>121</sup> The CoMoO<sub>4</sub>@Ni(OH)<sub>2</sub> nanotubes displayed a high  $C_s$  value of 1246 F g<sup>-1</sup> at a current density of 1 A g<sup>-1</sup>, with 86.7% capacitance retention.<sup>122</sup> The combined method of hydrothermal process and electrodeposition technique on Ti foil with ammonia; annealing was used to create the core-shell of TiN@Ni(OH)<sub>2</sub> NWAs. CV and GCD were carried out, which revealed an exceptionally high  $C_s$  of 2680 F g<sup>-1</sup> at 6 A g<sup>-1</sup> along with 54% retention of capacity at 60 A g<sup>-1</sup>.<sup>123</sup> The  $C_s$  and ED values of the most efficient supercapacitor device (CNeAg/Ni) were 888.6 F g<sup>-1</sup> and 177.3 Wh kg<sup>-1</sup>, respectively.<sup>124</sup> A simple hydrothermal approach is employed to grow ternary metal hydroxide nanorods on nickel foam, which serve as an efficient electrode for pseudocapacitors. The morphology displays a distinct core-shell architecture, featuring a Co(OH)<sub>2</sub> core containing Mn(OH)<sub>2</sub> and a shell made of Ni(OH)<sub>2</sub>. The Co(OH)<sub>2</sub>/Ni(OH)<sub>2</sub> core-shell structure containing Mn(OH)<sub>2</sub> was



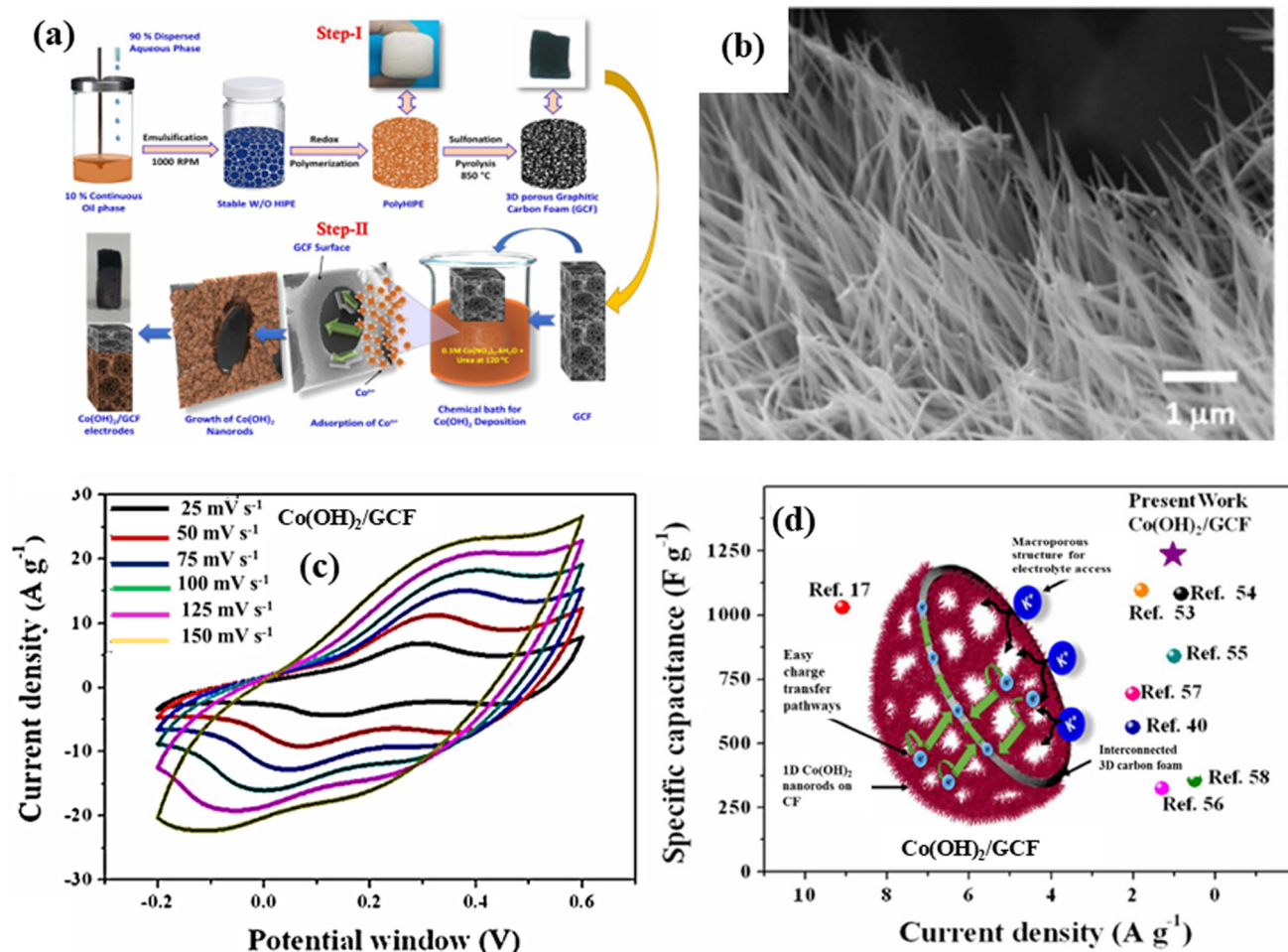


Fig. 16 (a) Synthesis method of  $\text{Co}(\text{OH})_2$ , (b) SEM image at  $1 \mu\text{m}$ , (c) CV cycle, and (d) comparison of specific capacitance with other materials. "Reprinted with permission from U. M. Patil, R. V. Ghorpade, M. S. Nam, A. C. Nalawade, S. Lee, H. Han, S. C. Jun, PolyHIPE Derived Freestanding 3D Carbon Foam for Cobalt Hydroxide Nanorods Based High Performance Supercapacitor", copyright © 2016 *Scientific Reports*.<sup>85</sup>

optimized to achieve a capacitance of  $2286 \text{ F g}^{-1}$ . The asymmetric supercapacitor cell demonstrated an exceptional ED of  $92 \text{ Wh kg}^{-1}$  at a PD of  $1.7 \text{ kW kg}^{-1}$ .<sup>125</sup> For high-performance supercapacitor applications, an extensible, economically viable, and surfactant-free method has been developed to synthesize hybrid nanostructures comprising  $\text{MnO}_2$  nanoflakes and  $\text{Ni}(\text{OH})_2$  nanowires. This  $\text{Ni}(\text{OH})_2/\text{MnO}_2$  core-shell nanowires contained 70.4 wt%  $\text{MnO}_2$  and displayed a remarkable  $C_s$  of  $355 \text{ F g}^{-1}$ , along with improved rate capability and cycling stability, achieving 97.1% retention after 3000 cycles in aqueous  $\text{Na}_2\text{SO}_4$ .<sup>126</sup>  $\text{Cu}(\text{OH})_2@/\text{Cd}(\text{OH})_2$  was synthesized using a cation exchange reaction. Electrochemical testing reveals that this type of core-shell nanowire structure exhibits a high  $C_s$  of  $374 \text{ F g}^{-1}$  in a 1 M NaOH aqueous electrolyte.<sup>127</sup> Similarly iron hydroxide@cadmium hydroxide nanostructures were produced by a cation exchange reaction, which demonstrated a  $C_s$  value of  $368 \text{ F g}^{-1}$  at a current density of  $0.5 \text{ A g}^{-1}$ .<sup>128</sup> The nanostructure of  $\text{NiCo-O}/\text{Ni}(\text{OH})_2$  electrodes has shown promising results in experiments for high-performance electrochemical energy storage devices. A comparative analysis of supercapacitor performance for core-

shell structures of  $\text{Ni}(\text{OH})_2$  that were developed on two types of nanowires  $\text{NiCo}_2\text{O}_4$  and  $\text{Co}_3\text{O}_4$  was shown.  $\text{NF}/\text{Co}_3\text{O}_4/\text{Ni}(\text{OH})_2$  exhibits a  $C_s$  of  $1330 \text{ F g}^{-1}$ . Similarly,  $\text{NF}/\text{NiCo}_2\text{O}_4/\text{Ni}(\text{OH})_2$  exhibits  $2079 \text{ F g}^{-1}$ .<sup>129</sup> The core-shell of nickel hydroxide and silver nanowire (Ag NW) was designed to form a nanocomposite electrode material for supercapacitor application; thus, the electrochemical performance was enhanced by increasing the transportation rate of oppositely charge ions. It exhibited a  $C_s$  of  $1165.2 \text{ F g}^{-1}$  at  $3 \text{ A g}^{-1}$  with 93% of residual capacitance over 3000 cycles (Fig. 18).<sup>130</sup>

### 14.3 Doped metal hydroxides

Doped metal hydroxides have been well explored as per Table 5. Generally, metal ion insertion gives rise to oxygen vacancies that lead to a change in oxidation state and charging capability of the electroactive material.<sup>131</sup> High-performance TMHs are regarded as promising materials for energy storage due to their straightforward and cost-effective synthesis, high surface area, and easily adjustable composition. Heteroatom doping is a widely used strategy to modify



Table 4 Literature review on metal hydroxide-based core-shell composites

Material	ST	Morphology	Electrolyte	Configuration	Voltage window (V)	Specific capacitance	Energy density (Wh kg <sup>-1</sup> )	Power density (W kg <sup>-1</sup> )	Retention@cycles	Method	Ref.
Ni(OH) <sub>2</sub> @nickel	Ga-In	CSNW	KOH	Three electrodes	0-0.6	3400 F g <sup>-1</sup>	53 Wh kg <sup>-1</sup>	395 W kg <sup>-1</sup>	86%@5000	ED	86
Ni(OH) <sub>2</sub> @nickel/reduced graphene oxide			6 M KOH	Two electrodes	1.6	154 F g <sup>-1</sup>			91%@10 000		
Co <sub>3</sub> S <sub>8</sub> @Ni(OH) <sub>2</sub>	CF	CSNT	KOH	Three electrodes	0-0.5	149.44 mAh g <sup>-1</sup>	31.35 Wh kg <sup>-1</sup>	252.8 W kg <sup>-1</sup>	97.3%@5000	ED	119
Co <sub>3</sub> S <sub>8</sub> @Ni(OH) <sub>2</sub> /AC				Two electrodes	0-2						
Cd(OH) <sub>2</sub> -VOOH	SS	CSNR	1 M LiClO <sub>4</sub>	Three electrodes	-0.8	233.98 F g <sup>-1</sup>	9.92 Wh kg <sup>-1</sup>	428.57 W kg <sup>-1</sup>	60.55%@2000	CBD-IER	120
Cd(OH) <sub>2</sub> -VOOH/Cd(OH) <sub>2</sub> -VOOH			PVA-LiClO <sub>4</sub>	Two-electrodes	1.5	53.62 F g <sup>-1</sup>			74.03%@1500		
NiCo <sub>2</sub> O <sub>4</sub> @Co(OH) <sub>2</sub>	CF	CSNW	2 M KOH	Three electrodes	-0.2-0.55	1298 F g <sup>-1</sup>	39.7 Wh kg <sup>-1</sup>	387.5 W kg <sup>-1</sup>	83%@5000	HT	121
NiCo <sub>2</sub> O <sub>4</sub> @Co(OH) <sub>2</sub> /AC				Two electrodes	1.55	119 F g <sup>-1</sup>					
CoMoO <sub>4</sub> @Ni(OH) <sub>2</sub>	NF	CSNT	3 M KOH	Three electrodes	0-0.5	1246 F g <sup>-1</sup>	62.5 Wh kg <sup>-1</sup>	0.776 kW kg <sup>-1</sup>	89.2%@5000	HT	122
CoMoO <sub>4</sub> @Ni(OH) <sub>2</sub> /porous carbon				Two electrodes	0-1.5	192.8 F g <sup>-1</sup>			86.7%@10 000		
TiN@Ni(OH) <sub>2</sub>	Ti foil	CSNW	2 M KOH	Three electrodes	0-0.6	2680 F g <sup>-1</sup>			54%	ED	123
Ag NWs/Ni(OH) <sub>2</sub> /CNT		CSNW	PMMA	Two electrodes	0-1.2	888.6 F g <sup>-1</sup>	177.3 Wh kg <sup>-1</sup>			TM	124
Mn(OH) <sub>2</sub> /Co(OH) <sub>2</sub> /Ni(OH) <sub>2</sub>	CF	CSNR	3 M KOH	Three electrodes	-0.2-0.5	2286 F g <sup>-1</sup>	92 Wh kg <sup>-1</sup>	1.7 kW kg <sup>-1</sup>	89%@2000	HT	125
				Two electrodes	0-2.0				91.7%@5000		
Ni(OH) <sub>2</sub> /MnO <sub>2</sub>		CSNW	1 M Na <sub>2</sub> SO <sub>4</sub>	Three electrodes	-0.2-1.0	355 F g <sup>-1</sup>				SF	126
Cu(OH) <sub>2</sub> @Cd(OH) <sub>2</sub>	SS	CSNW	1 M NaOH	Three electrodes	-0.8--0.3	374 F g <sup>-1</sup>			62%@1000	IER	127
Iron hydroxide@cadmium hydroxide	SS	CSNW	1 M Na <sub>2</sub> SO <sub>4</sub>	Three electrodes	0.3--0.9	368 F g <sup>-1</sup>			52%@5000	IER	128
NF/Co <sub>3</sub> O <sub>4</sub> /Ni(OH) <sub>2</sub>	NF	CSNW	6 M KOH	Two electrodes	1.8	1330 F g <sup>-1</sup>	44.5 Wh kg <sup>-1</sup>	86.3 W kg <sup>-1</sup>	61%@1000	HT	129
NF/NiCo <sub>2</sub> O <sub>4</sub> /Ni(OH) <sub>2</sub>	NF	CSNW	6 M KOH	Two electrodes	1.8	2079 F g <sup>-1</sup>			93%@1000	CBD	129
AgNW/Ni(OH) <sub>2</sub>	PET	CSNW	1 M KOH	Three electrodes	0.50	1165.2 F g <sup>-1</sup>			93%@3000	SC	130

Note: ST – substrate, ED – electrodeposition, HT – hydrothermal, TM – template method, SF – surfactant free, IER – ion exchange reaction, SC – spray coating, CSNW – core-shell nanowire, CSNT – core-shell nanotube, CSNR – core-shell nanorod.



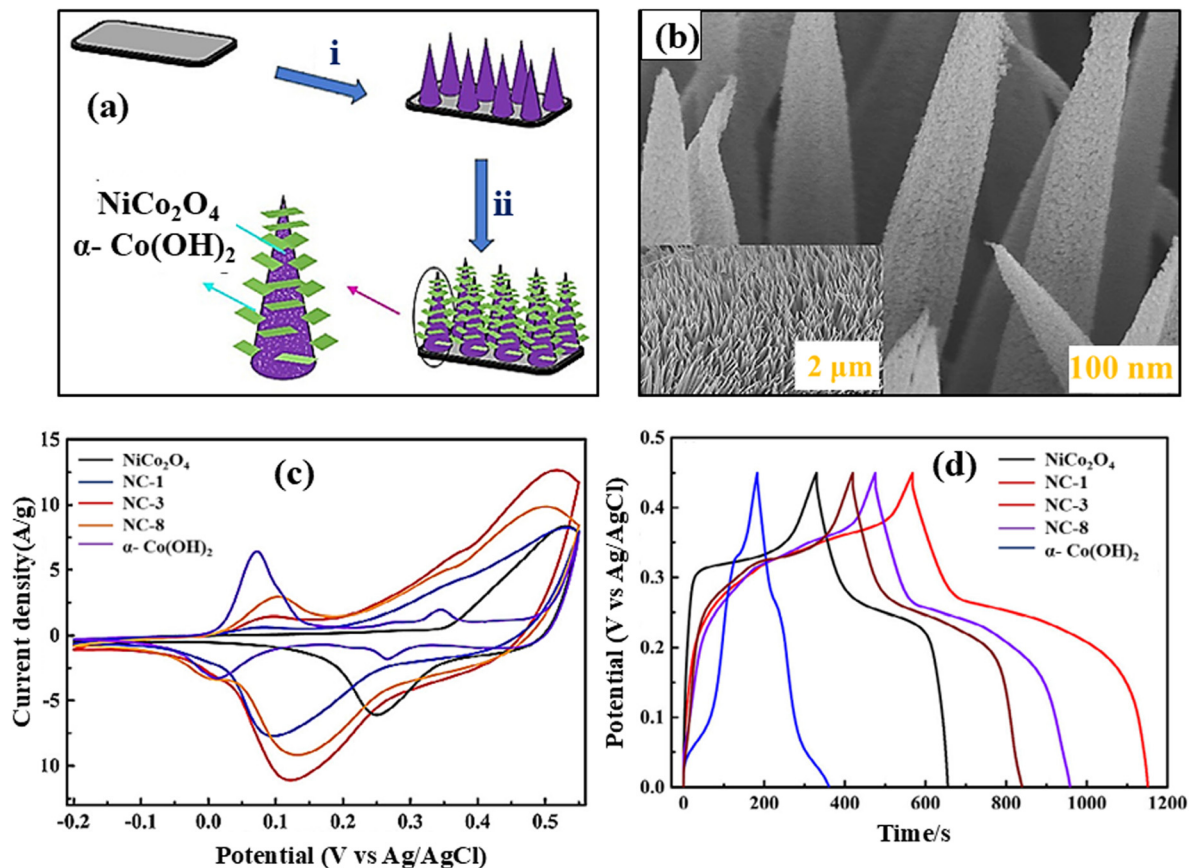


Fig. 17 (a) Fabrication process of  $\text{NiCo}_2\text{O}_4@Co(OH)_2$ , (b) SEM images at low magnification showing nanowire morphology at 100 nm (inset: showing 2  $\mu\text{m}$  scale) (c) CV cycle, and (d) variation of GCD with variation in current density. "Reprinted with permission from W. D. Wang, P. P. Zhang, S. Q. Gao, B. Q. Wang, X. C. Wang, M. Li, F. Liu, J. P. Cheng, Core-shell nanowires of  $\text{NiCo}_2\text{O}_4@Co(OH)_2$  on Ni foam with enhanced performances for supercapacitors", copyright © 2020 *J. Colloid Interface Sci.*<sup>121</sup>

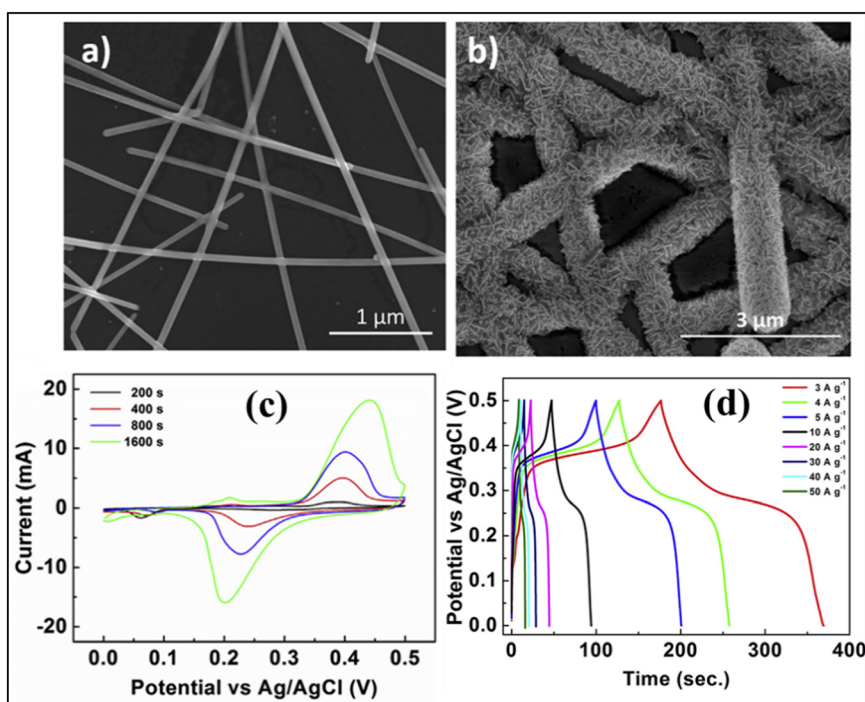


Fig. 18 (a and b) SEM images showing nanowire morphology for Ag NW/ $\text{Ni(OH)}_2$ , (c) CV cycle, and (d) GCD variation.<sup>130</sup>





**Table 5** Literature review on doping in metal hydroxides

Material	Method	ST	Morphology	Electrolyte	Configuration	Voltage window (V)	Specific capacitance	Energy density (Wh kg <sup>-1</sup> )	Power density (W kg <sup>-1</sup> )	Retention@cycles	Ref.
Cl doped carbonated Co(OH) <sub>2</sub>	HT	SS	NW	1 M KOH	Three electrodes	0–0.6	2150 F g <sup>-1</sup>	41.8 Wh kg <sup>-1</sup>	1280.7 W kg <sup>-1</sup>	94.3%@500	132
Mn doped Co(OH) <sub>2</sub>	HT	NF	NW	6 M KOH	Three electrodes	0–0.4	2800 F g <sup>-1</sup>			95%@5000	133
K <sup>+</sup> doped Mn(OH) <sub>4</sub>	HT	AC	NR	3 M Na <sub>2</sub> SO <sub>4</sub>	Three electrodes	-1–1	319 F g <sup>-1</sup>	41.38 Wh kg <sup>-1</sup>	143.37 W kg <sup>-1</sup>	107.3%@6000	134
AC/K <sup>+</sup> -Mn(OH) <sub>4</sub>					Two electrodes	2	399 F g <sup>-1</sup>				
Fe doped Sr(OH) <sub>2</sub>	SILAR	SS	Tuberosse fibre	1 M Na <sub>2</sub> SO <sub>4</sub>	Three electrodes	-1.1–0	792 F g <sup>-1</sup>			79%@5 mA cm <sup>-2</sup>	153
Cu-doped Sr(OH) <sub>2</sub>	SILAR	SS	Tuberosse fibre	1 M Na <sub>2</sub> SO <sub>4</sub>	Three electrodes	0–0.8	817 C g <sup>-1</sup>			71%@5000	154

Note: ST – substrate, SS – stainless steel, NF – nickel foam, AC – activated carbon, HT – hydrothermal, NW – nanowire, NR – nanorod, SILAR – successive ionic layer adsorption and reaction.

both the physical and chemical properties of TMHs, including their lattice and electronic structures, defects, and diffusion characteristics. This doping technique also boosts the overall performance of TMH electrode materials, improving  $C_s$  and charge–discharge rates. Recently, significant research has been focused on using heteroatom doping to develop TMHs and TMH-based composites for electrochemical applications. Research has indicated that both metal and non-metal doping of metal oxide and hydroxide electrodes can significantly improve electrochemical performance and customize material properties for a range of applications. Fig. 19(I) shows that cobalt hydroxide nanowires doped with chlorine, which are stable and well-defined, have been successfully synthesized and the test results indicate that the Co-ClNWs (NiE) electrode achieved a  $C_s$  of 2150 F g<sup>-1</sup> at a current density of 1 A g<sup>-1</sup>. It also demonstrates excellent cycling stability, maintaining 94.3% capacitance retention after 500 cycles. The asymmetric device provides a high ED of 41.8 W h kg<sup>-1</sup> at a PD of 1280.7 W kg<sup>-1</sup>.<sup>132</sup> Fig. 19(II) shows the effect of Mn ion insertion to the cobalt hydroxide nanowires through the hydrothermal approach. Initially, Co(OH)<sub>2</sub> had a  $C_s$  of 1600 F g<sup>-1</sup>; however, following Mn doping, the value rose to 2800 F g<sup>-1</sup>. This work showed that chemical doping is a simple and effective technique to improve transition metal hydroxide supercapacitor performance.<sup>133</sup> K<sup>+</sup> doped Mn(OH)<sub>4</sub> nanorods were synthesized using the hydrothermal method (Fig. 19(III)). K<sup>+</sup> ions help preserve structural stability during the GCD process while also enhancing pseudocapacitive performance. The developed K<sup>+</sup> doped Mn(OH)<sub>4</sub> symmetric electrochemical pseudocapacitors exhibit a remarkable ED of 10.11 Wh kg<sup>-1</sup> and a high-PD of 51.04 W kg<sup>-1</sup> across a voltage range of 1.0 V in an aqueous electrolyte. A total of 107.3% of the  $C_s$  value was maintained at 6000 cycles, indicating its great potential for real-world application in electrochemical supercapacitors.<sup>134</sup>

#### 14.4 Metal hydroxide nanowires – conductive polymer nanocomposites

Conducting polymers (CPs) with exceptional electrical conductivity and mechanical flexibility have drawn a lot of interest towards supercapacitor applications (Table 6). In particular, nanostructured conducting polymers have been a key area of focus, offering advantages such as increased surface area, reduced ion diffusion distances, and enhanced electrochemical properties.<sup>51</sup> Generally, CPs include polypyrrole, polyaniline, polythiophene, poly(3,4-ethylenedioxythiophene), and polyindole, and they are the subject of significant research in the field of supercapacitors. Their chemical valence state-conjugated architectures facilitate effective doping and de-doping procedures, which improve areal capacitance and  $C_s$ .<sup>135</sup> This section highlights recent progress in the development of conducting polymer–metal hydroxide composites for supercapacitors. A concise overview of different synthesis methods is also provided, covering both chemical techniques with and without the use of templates or binder additives.

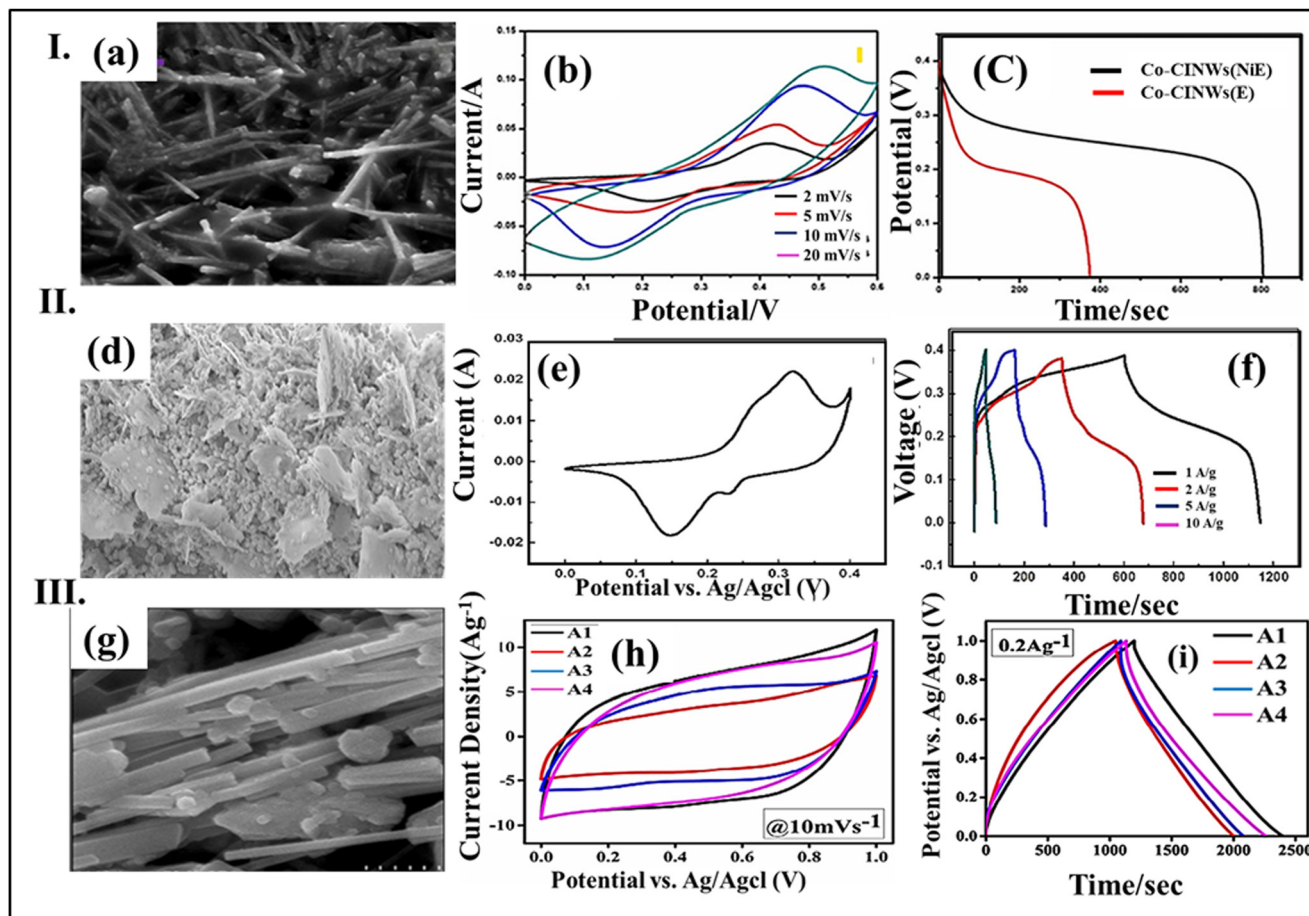


**Fig. 19** (I) Cl doped  $\text{Co}(\text{OH})_2$ . (a) FE-SEM of Cl doped  $\text{Co}(\text{OH})_2$ , (b and c) electrochemical performance showing CV and GCD profile of the three electrode system (II) Mn doped  $\text{Co}(\text{OH})_2$ . (d) Represents SEM image, (e and f) CV and GCD of the three electrode system, (III)  $\text{K}^+$  ion doped  $\text{Mn}(\text{OH})_4$ . (g) SEM image, (h and i) CV cycle with variation of scan rate and GCD profile.<sup>132–134</sup> Reprinted from Y. Zhao, S. Liu, B. Zhang, J. Zhou, W. Xie, H. Li, One-Step Synthesis of Mesoporous Chlorine-Doped Carbonated Cobalt Hydroxide Nanowires for High-Performance Supercapacitors Electrode, via Creative Commons CC BY 4.0 licence.

Several TMO based polymer composites were suggested as electrodes materials for supercapacitors. The carbon material is used to incorporate into the metal oxide or hydroxide material to improve the electrical conductivity. However, it was shown how the crucial contribution of the polymer's conductivity changed with variations in electrode potential.<sup>136</sup> A two-step anodization process in conjunction with the electrodeposition process was used to prepare polypyrrole (PPy)- $\text{Ni}(\text{OH})_2$  nanowire arrays. The obtained capacitance values were found to be  $25 \text{ F cm}^{-2}$  for the PPy electrode and  $75 \text{ F cm}^{-2}$  for the PPy- $\text{Ni}(\text{OH})_2$  array electrode respectively (Fig. 20(a–d)). However, a capacitance loss of 13% was achieved over 100 CV cycles.<sup>137</sup> Facile wet chemical synthesis was used to produce the composite of cobalt hydroxide nanowires and carbon nanotubes with polymer sponge. Cobalt hydroxide's extraordinarily high theoretical capacitance of  $3458 \text{ F g}^{-1}$  makes an important component of energy storage systems.<sup>138</sup> The addition of polyaniline increased the  $C_s$  by 48% compared to CNT-Co foam. The CNT polyaniline-cobalt hydroxide composite exhibited a  $C_s$  of  $920 \text{ F g}^{-1}$ . The increase in  $C_s$ ,

nearly doubling with the addition of polyaniline, can be attributed to the pseudocapacitance provided by polyaniline.<sup>139</sup>

#### 14.5 1D nanoform composites

Combining two or more materials to create a composite improves each material's overall qualities by increasing mechanical strength, improving the active surface area, and enabling customized functionality at the nanoscale. Fast and reversible faradaic surface reactions are used by pseudocapacitors or redox capacitors to store charge. TMOs, TMHs and conducting polymers have been researched as potential redox capacitor electrode materials. Design innovation is made possible by the ability to build composites to satisfy certain performance requirements. Additionally, because of their combined effect, hybrid composites can improve the electroactivity of each of its constituent parts, leading to better electrochemical performance than single-component materials. Multiple oxidation states are the outcome of the combined action, which raises the electrical conductivity and, consequently, the ED. Due to this symbiotic



Table 6 Review reports on conducting polymers and metal hydroxide composites

Material	Method	ST	Morphology	Electrolyte	Configuration	Voltage window (V)	Specific capacitance	Energy density (Wh kg <sup>-1</sup> )	Power density (W kg <sup>-1</sup> )	Retention@cycles	Ref.
PPy-Ni(OH) <sub>2</sub>	AAO template growth	AF	NW	1 M LiSO <sub>4</sub> + 0.19 M 1,4-DHB	Three electrodes	-1-0.5	75 F cm <sup>-2</sup>				137
Ppy/Co(OH) <sub>2</sub> /CNT	FWCS	PF	NF	2 M KOH	Three electrodes	-0.12-0.38	920 F g <sup>-1</sup>				139

Note: ST – substrate, FWCS – facile wet chemical synthesis, AF – aluminium foil, PF – polyurethane foam, DHB – dihydroxy benzene, NW – nanowire, NF – nanoflower.

effect, the electrodes exhibit enhanced functionality and efficiency for supercapacitor applications (Table 7). Babar *et al.*<sup>140</sup> synthesized a nickel hydroxide/reduced graphene oxide composite for water splitting application. Nickel hydroxide nanowires/RGO composites were synthesized through a one-step, ionic liquid-assisted hydrothermal process. In this method, the multi-functional 1-butyl-3-methylimidazolium trifluoroacetate was used as a template, co-solvent, and reactant. A very high  $C_s$  of approximately 1875 F g<sup>-1</sup> was achieved at a current density of 1 A g<sup>-1</sup> in 6 M KOH. Additionally, it retained 98.3% of its initial capacity after 1000 GCD cycles.<sup>141</sup> An ultrathin graphene oxide composite with  $\alpha$ -FeOOH nanorods has been developed using the hydrothermal process using GO and iron acetate solution. The composite prepared with 20% iron loading demonstrated the highest  $C_s$  of 127 F g<sup>-1</sup> at 10 A g<sup>-1</sup> and good CV stability of 85% capacitance retention over 2000 cycles. These properties were significantly superior to those of GO-free  $\alpha$ -FeOOH nanorods (Fig. 22).<sup>142</sup> Fig. 18 represents the composite of carbon ink and Co(OH)<sub>2</sub>. The cobalt hydroxide nanowires were utilized to create a solid-state device using PVA-KOH gel as the electrolyte. This prototype displayed an impressive areal capacitance of 6.27 mF cm<sup>-2</sup>, along with an areal ED of 0.7101  $\mu$ Wh cm<sup>-2</sup> and an areal PD of 32.7  $\mu$ W cm<sup>-2</sup>. Fig. 21(a) shows the SEM image of cobalt hydroxide with nanowire morphology, (b) atomic force microscopy was used to study the surface roughness, particle distribution and topography of the prepared electrode, (c) the CV performance of a single cell, two cell and three cells in series mode is shown. At 1.5 V of potential window, the electrode attained a maximum areal capacitance of 6.27 mF cm<sup>-2</sup> at a scan rate of 2 mV S<sup>-1</sup>. Fig. 21(d) represents capacitive retention of 82.7% through 10 000 CV cycles, indicating good cyclic stability of the device. The practical application of the device is shown in Fig. 21(e) where it was used to glow an LED (light emitting diode) using series combination of printed supercapacitors.<sup>143</sup> The cobalt manganese hydroxides were successfully synthesized in a scalable manner with rGO as the composite to serve as supercapacitive electrodes (Fig. 23). A high  $C_s$  of 784 F g<sup>-1</sup> at a current density of 0.5 A g<sup>-1</sup> was obtained, along with excellent rate capability, maintaining 84.2% of its capacitance. Furthermore, an asymmetric device was designed using CoMn-HW/rGO and activated carbon and obtained an ED of 38.3 Wh kg<sup>-1</sup> and a PD of 8000 W kg<sup>-1</sup>.<sup>144</sup>

## 15. Present challenges of 1D metal hydroxides for supercapacitor application

The detailed degradation mechanism with the stability mechanism of metal hydroxides is presented in Fig. 24.

### 15.1 Degradation

The long-term cycling stability of one-dimensional (1D) metal hydroxide-based electrodes remains a significant challenge in energy storage research. Materials such as Ni(OH)<sub>2</sub>, Co(OH)<sub>2</sub>,



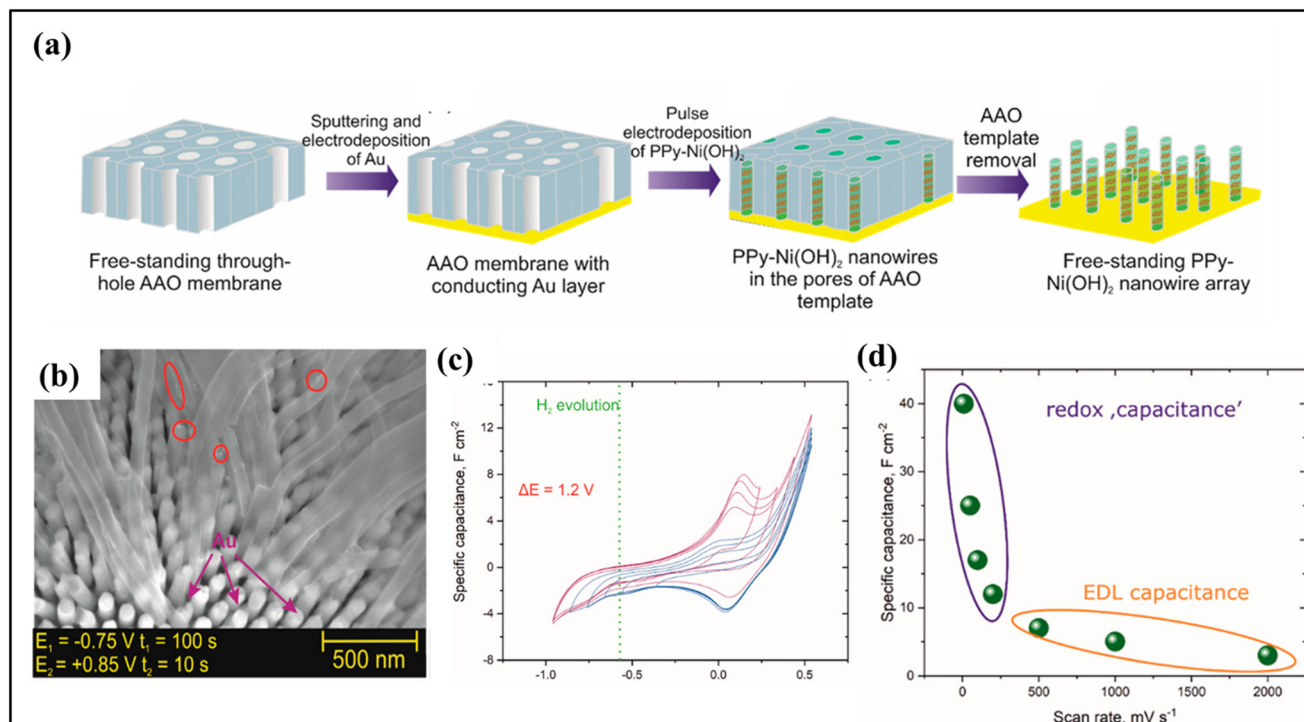


**Fig. 20** (a) Diagram illustrating the synthesis process of synthesizing free-standing nanowire array electrodes, (b) FE-SEM image, (c) CV scans, and (d) the actual capacitance of PPy-Ni(OH)<sub>2</sub>.<sup>137</sup> “Reprinted from A. Brzózka, K. Fic, J. Bogusz, A. M. Brudzisz, M. M. Marzec, M. Gajewska, G. D. Sulka, Polypyrrole-Nickel hydroxide hybrid nanowires as future materials for energy storage”, *Nanomaterials* 9 (2019), via Creative Commons CC BY 4.0 licence. © 2019 The Authors. Licensee MDPI, Basel, Switzerland.

and Mn(OH)<sub>2</sub> nanowires or nanorods offer a high surface area and short ion diffusion paths. However, their electrochemical activity is frequently accompanied by structural and chemical instability. Repeated redox transitions cause substantial volume changes, resulting in mechanical strain, cracking, and eventual collapse of the 1D nanostructures. Phase transformations from layered hydroxides to less conductive oxyhydroxides or oxides during extended operation further reduce electronic conductivity and capacity retention. Electrolyte-driven degradation, especially in alkaline systems, leads to gradual dissolution of metal cations and the formation of passivating surface layers that impede ion transport. The low intrinsic conductivity of metal hydroxides is further diminished over cycling as nanostructures detach from the current collector or lose interconnectivity, increasing charge-transfer resistance. Instability at the electrode-substrate interface, due to weak adhesion or the development of resistive interfacial layers, accelerates capacity fading.

### 15.2 Stability

Several strategies have been developed to address these issues. These include nanostructure engineering such as core-shell designs, incorporation of conductive supports like graphene, carbon nanotubes (CNTs), or MXenes, doping with stabilizing elements to suppress lattice distortion, and direct growth of 1D hydroxides on conductive scaffolds to improve adhesion. Also, polymer composites with metal hydroxides lead to an increased rate of ion and charge carrier

transport, while providing mechanical flexibility and stability over long cycles, as well as enhancing the electrical conductivity. A detailed discussion of these degradation mechanisms and corresponding mitigation strategies would strengthen the manuscript by linking the fundamental challenges of 1D hydroxide electrodes to rational design approaches that enhance cycling stability for practical energy storage applications.

### 15.3 Several approaches to mitigate degradation mechanisms

As repeated redox reactions cause volume changes in metal hydroxides, so to reduce this volume shrinkage the metal hydroxide should be grown on conducting substrates like nickel foam and carbon cloths.<sup>145</sup> Also the core-shell architecture confined the volume change that reduces the volume expansion by providing interfacial stability that improves the electrical conductivity. In order to make stable phase formation in metal hydroxides, the surface of metal hydroxide should be coated with a conducting polymer or carbon-based material. Doping with metal ions somehow reduces the phase formation in a better way. Zhao *et al.* analysed the phase-controlled growth technique of nickel hydroxide nanostructures on nickel foam for enhanced supercapacitor performance.<sup>146</sup> To reduce electrical corrosion and achieve control over potential electrolyte optimization should be carried out during supercapacitor analysis. The poor adhesion behavior of metal hydroxides can be avoided by the intermediate adhesion layer using NiO, carbon and TiO<sub>2</sub>. Synthesis of metal hydroxides using *in situ* chemical





Table 7 Literature review on metal hydroxides and composites

Material	Method	Substrate	Morphology	Electrolyte	Configuration	Voltage window (V)	Specific capacitance	Energy density (Wh kg <sup>-1</sup> )	Power density (W kg <sup>-1</sup> )	Retention@cycles	Ref.
Ni(OH) <sub>2</sub> /RGO	HT	NF	NW	KOH	Three electrodes	0–1	1875 F g <sup>-1</sup>			98.3% 1000	141
α-FeOOH/graphene	HT	NF	NR	1 M KOH	Two electrodes	-0.3–0.4	127 F g <sup>-1</sup>			85%@2000	142
Co(OH) <sub>2</sub> /carbon ink	UH	PET	NR	PVA–KOH	Three electrodes	-0.2–0.6	6.27 mF cm <sup>-2</sup>	0.7101 μW cm <sup>-2</sup>	32.7 μW cm <sup>-2</sup>	82.7%@100 000	143
CoMn/rGO	HT	NF	NW	3 mol L <sup>-1</sup>	Two electrodes	1.8	784 F g <sup>-1</sup>	38.3 Wh kg <sup>-1</sup>	8000 W kg <sup>-1</sup>	89.5%@3000	144
CoMn/rGO/AC	PP	NF	NS	KOH	Three electrodes	0–0.6	107.6 F g <sup>-1</sup>				155
rGO/Ni(OH) <sub>2</sub>				6 M KOH	Two electrodes	1.8	1866.8 F g <sup>-1</sup>	54.1 Wh kg <sup>-1</sup>	1 kW kg <sup>-1</sup>	15% @3000	155
rGO/Ni(OH) <sub>2</sub> /rGO				1 mol L <sup>-1</sup>	Three electrodes						156
MnOOH–GO	HT	NF	NW	Na <sub>2</sub> SO <sub>4</sub>			76 F g <sup>-1</sup>				

Note: NF – nickel foam, UH – urea hydrolysis, HT – hydrothermal, pp – precipitation, PET – polyethylene terephthalate, NR – nanorod, NW – nanowire, NS – nanostick.

methods like hydrothermal, co-precipitation, *etc.* can also decrease the poor surface adhesion.<sup>147</sup>

Future advancement for one-dimensional metal hydroxides not only required material design but also methodological innovation.

**a. Potential developments in research methodologies.** Several advance synthesis methods, including hydrothermal, electrodeposition and spray assisted growth techniques, have been developed to control the structure and defect.

➤ By controlling the growth through atomic layer deposition in nanolayer form, well-defined for nanostructure can be designed.

➤ The diameter range can be controlled by the seed-mediated growth approach. Solvent free methods are introduced for green synthesis.

#### b. Experimental developments

➤ Several experimental techniques are developed like *in situ* characterization to distinguish the crystal phase formation through X-ray diffraction study and redox reactions through Raman spectroscopy.

➤ High-resolution TEM analysis is used to visualize the nanoarchitecture. Several advanced interfacial characterizations like 3D tomography are also used to study the pore connectivity in thick electrodes.

#### c. Different modelling approaches

➤ A three electrode study with high mass loading was required with complete study through the two electrode system.

➤ Different theoretical modelling techniques like density function theory, multiscale modelling, ion transport and porous electrode modelling through machine learning need to be developed for defect related strategies for metal hydroxide design.

## 16. Summary, conclusions and future scopes

### 16.1 Summary

Current developments and technical advancements necessitate the use of reliable energy sources to guarantee the sustainability of the near future. Advancements in energy storage systems like batteries and capacitors have already made energy autonomy possible, which is essential for most of the current technologies. By designing the nanostructure form of metal hydroxides while maintaining the high aspect ratio of surface to volume, it is possible to enhance the charge carrier transportation to a faster rate. The porous and hollow one-dimensional structure increases the active surface area and ion accessibility. Also, maintaining the diameter of the nanostructure in the range of 10–100 nm reduces the diffusion length to a lower value that maintains mechanical strength. Rather than structural design, interface engineering like making core-shell design and composition modification by metal atom or ion doping and finally the electrolyte compatibility influences the evaluation performance of 1D hydroxide. The major challenges arise from the

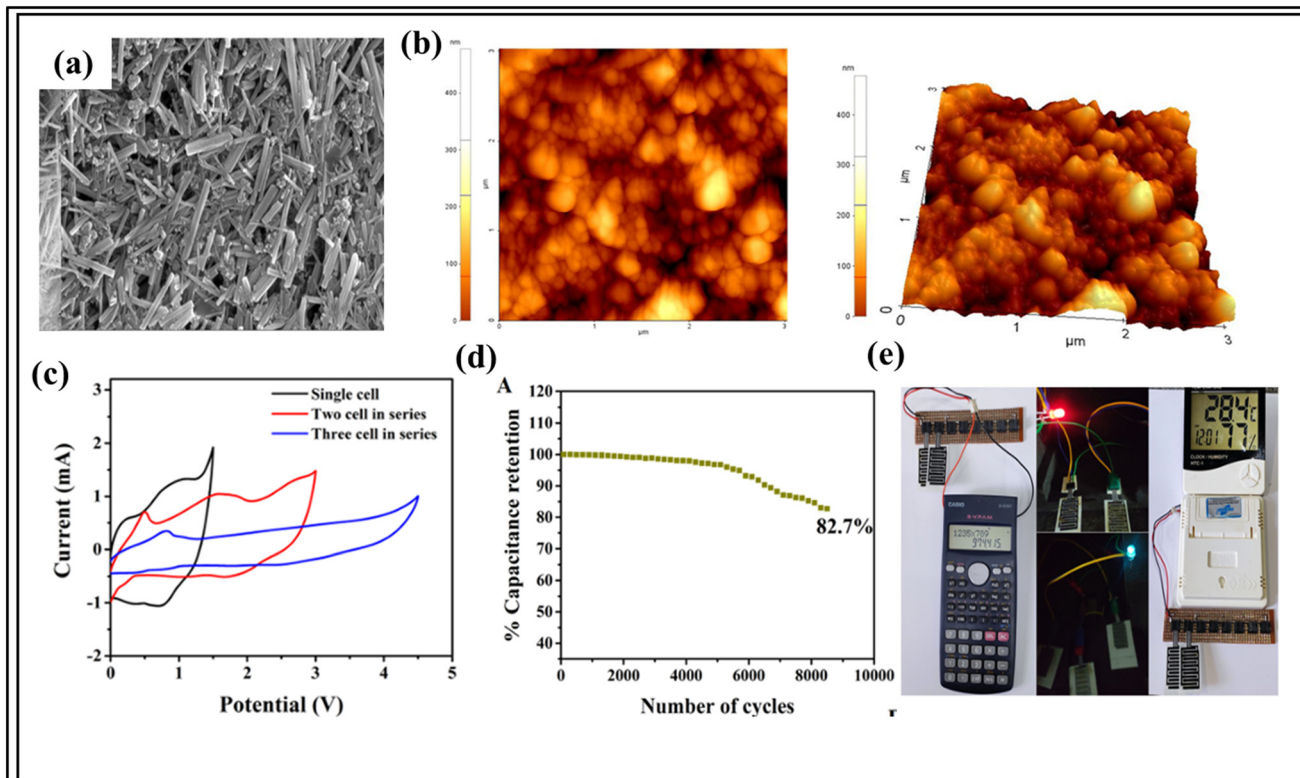


**Fig. 21** (a) FESEM images and elemental mapping of the synthesized cobalt hydroxide nanowire structures, (b) two-dimensional atomic force microscopy of the screen-printed electrode, (c) single cell's CV findings as well as those from two or three cells connected in series, (d) cyclic stability showing over 10 000 CV cycles, and (e) device used to power various electronic devices and LEDs. "Reprinted with permission from P. Navaneeth, A. Kumar, B. G. Nair, S. B. TG and P. V. Suneesh, Studies on fabrication of high-performance flexible printed supercapacitor using cobalt hydroxide nanowires", copyright © 2022 *Electrochim. Acta*.<sup>145</sup>

degradation mechanism of metal hydroxides through repeated redox transition causing mechanical strain, cracking and agglomeration caused by hydroxyl groups in the interlayer spacing of metal hydroxides and also due to dissolution of the electrode in electrolyte that limits the ion diffusion; such shrinkage of the surface area consequently leads to a reduction in electrochemical performance.

To counteract these difficulties, the enhancement of properties can be achieved by

1. Increasing the nano structural surface area and electrical conductivity.
2. Metal hydroxide undergoing several modifications like doping of metal atoms or ions in hydroxides, hydroxide-based composites, core-shell composites and polymer composites with metal hydroxide.
3. Improvements in design leads to a certain set of underlined trade-offs like lower mechanical stability and poor electrochemical performance in 1D metal hydroxides.
4. Using heterostructure design and a lower proportion of doping by inserting an ultra-thin conducting layer.
5. Adopting the core-shell heterostructure or heterojunction.
6. Depositing quantum dots on nanoforms with a dual charge storage mechanism.

## 16.2 Conclusions

In conclusion from the supercapacitor application point of view, the electrodes should have high mechanical flexibility for cyclic stability, high active surface area, and enhanced structural morphology as well as high specific capacitance, energy density and power density. As EDLCs have greater cyclic strength as compared to pseudocapacitor materials so by combining the synergistic effect between EDLCs with that of pseudocapacitor type electrodes the best possible electrode materials are formed with very high cyclic stability and specific capacitance value. The metal hydroxide provides possible microstructure morphology with a high specific surface area for supercapacitor application. Well-known literature studies were done over individual metal hydroxides like  $\text{Co}(\text{OH})_2$ ,  $\text{Cd}(\text{OH})_2$ ,  $\text{Ni}(\text{OH})_2$  and  $\text{MnOOH}$  with nanorod, nanowire and nanotube like morphology that provide greater electrochemical performance. Also to study the synergistic effect of combined electrodes the individual metal hydroxides with core-shell composite structure have been also well explored. The formation of core-shell surface architecture plays a significant role in supercapacitor application. Several reports on  $\text{Ni}(\text{OH})_2$ @nickel,  $\text{CO}_9\text{S}_8$ @ $\text{Ni}(\text{OH})_2$ , cadmium hydroxide-vanadyl hydroxide core-shell nanorods are listed in



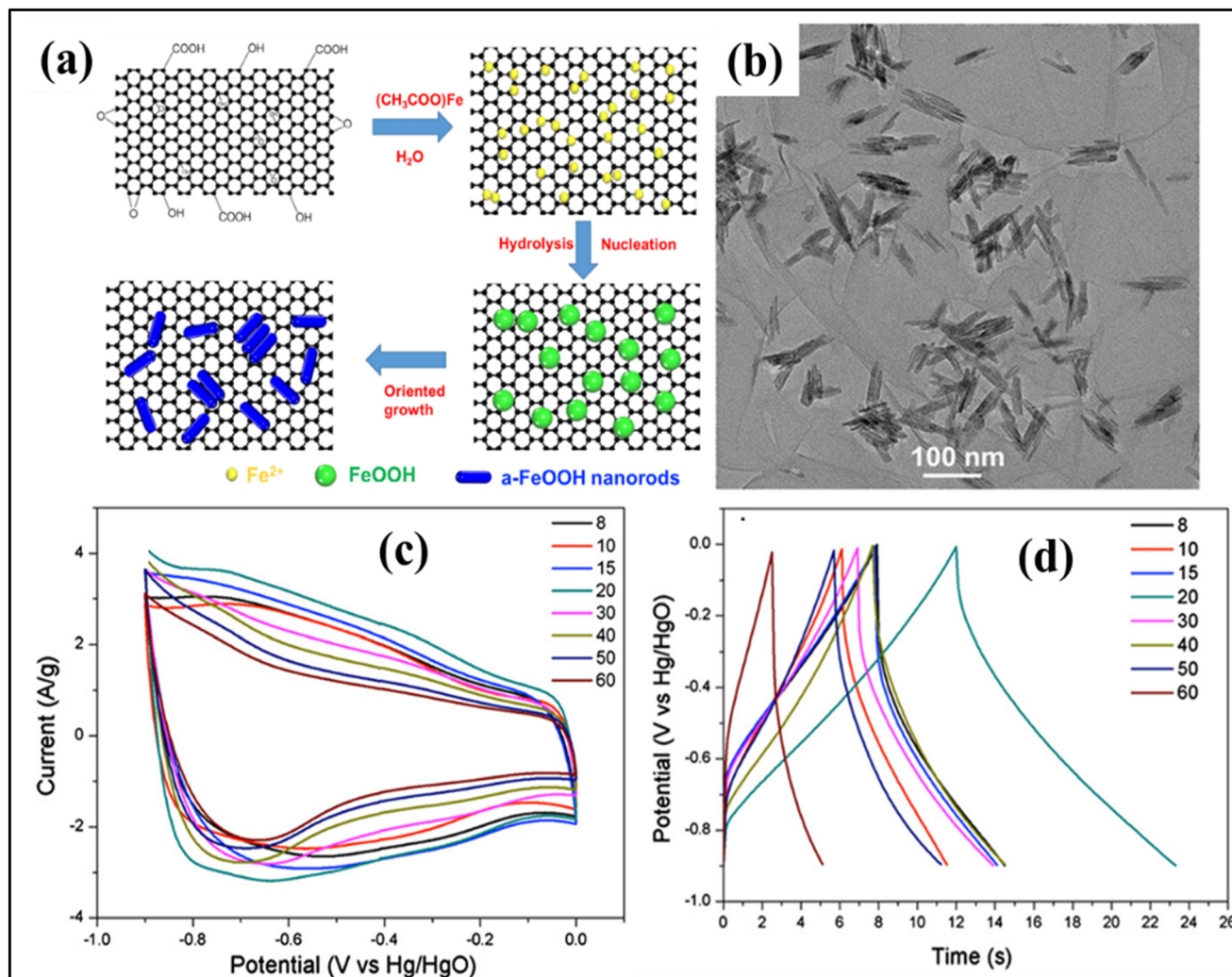


Fig. 22 (a) Synthesis mechanism of  $\alpha$ -FeOOH/GO, (b) TEM showing nanorods, (c) current variation with potential and (d) potential vs. time. Reprinted with permission from "Y. Wei, R. Ding, C. Zhang, B. Lv, Y. Wang, C. Chen, X. Wang, J. Xu, Y. Yang, Y. Li, Facile synthesis of self-assembled ultrathin  $\alpha$ -FeOOH nanorod/graphene oxide composites for supercapacitors", copyright © 2017 *J. Colloid Interface Sci.*<sup>142</sup>

tabular form along with their greater electrochemical performance. Further to improve the electrical conductivity through structural improvement by improving physical structure with increase in specific capacitance values, metal atoms were doped onto individual metal hydroxides. The doping effect of chlorine, Mn, K, Fe and Cu onto cobalt hydroxide, manganese hydroxide and strontium hydroxide is well established in the literature. Metal hydroxides with conducting polymer composites like polypyrrole (PPy)-Ni(OH)<sub>2</sub> and Ppy/Co(OH)<sub>2</sub>/CNT composites were also explored to improve cyclic strength along with the increase in specific capacitance value that was clearly explained as state of art. The 1D nanoform composites with rGO, graphene, and carbon ink achieved huge capacitance values with high cyclic strength due to the combined effect of EDLCs and the pseudocapacitor type material which increases the mechanical strength by improving the active surface area.

### 16.3 Future prospects towards scalable production

Compared to other electrode materials like metal oxides, metal chalcogenides, conducting polymers, and metal nitrides, metal hydroxide is becoming more and more popular because it is inexpensive, easy to synthesize, requires a low temperature process with wide availability and is valuable from a marketing and commercialization standpoint. But still there exist certain critical bottlenecks that limit their practical application. From the supercapacitor application point of view, high areal capacitances are required, so for this purpose a thick electrode is required. But, sometimes the dense packing of electrode blocks the electrolyte ions from the interface of the electrode thus causing poor electrical conductivity. So, to combat this issue, research mainly focused on the design of 1D structure with hierarchical multiscale porosity with vertically aligned nanowire arrays. Also, the conductivity can be increased by growing the



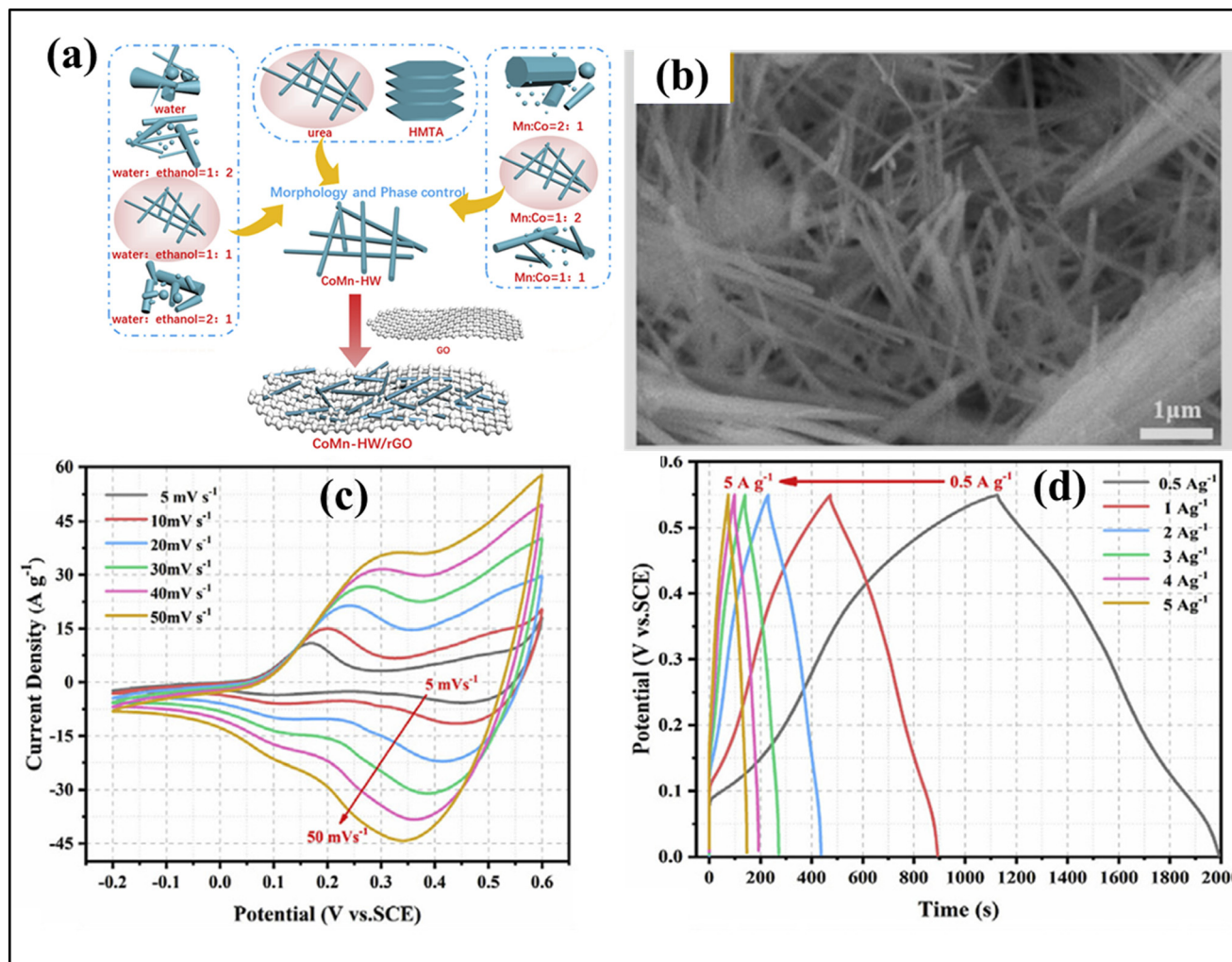


Fig. 23 (a) Synthesis procedure of the CoMn-HW/rGO composite, (b) SEM image, (c) CV, and (d) GCD analysis. Reprinted with permission from Bai, Xue, Dianxue Cao, and Hongyu Zhang. "Simultaneously morphology and phase controlled synthesis of cobalt manganese hydroxides/reduced graphene oxide for high performance supercapacitor electrodes", copyright © 2020, Ceramics International.<sup>144</sup>

metal hydroxide on a conducting substrate like nickel foam or carbon cloth, as well as hybridization with carbon nanotubes. Structural degradation during CV cycling causes volume shrinkage and finally cracking. By designing core-shell confinement architectures a flexible substrate is provided which increases the mechanical strength. Interface instability can be also

avoided by forming a chemical bonding layer by surface functionalization. High-performance hydroxides like  $\text{Co}(\text{OH})_2$ ,  $\text{Ni}(\text{OH})_2$  and novel metal hydroxides must be translated from lab research to workable energy-storage solutions through standardized device-level testing and scalable fabrication pathways.

## Conflicts of interest

There are no conflicts to declare.

## Data availability

All of the research included in this review article has already been published. The data used in this article are properly cited. No new datasets have been generated.

## Acknowledgements

All authors acknowledge Director, VNIT, Nagpur.

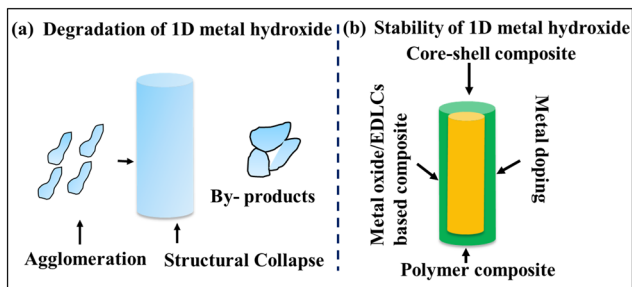
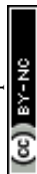


Fig. 24 (a) Degradation and (b) stability mechanism of 1D metal hydroxide.



## References

- 1 D. A. Elalfy, E. Gouda, M. F. Kotb, V. Bureš and B. E. Sedhom, Comprehensive review of energy storage systems technologies, objectives, challenges, and future trends, *Energy Strat. Rev.*, 2024, **54**, 101482, DOI: [10.1016/j.esr.2024.101482](https://doi.org/10.1016/j.esr.2024.101482).
- 2 S. A. Pervez, D. Kim, C. H. Doh, U. Farooq, H. Y. Choi and J. H. Choi, Anodic WO<sub>3</sub> mesosponge @ carbon: A novel binder-less electrode for advanced energy storage devices, *ACS Appl. Mater. Interfaces*, 2015, **7**, 7635–7643, DOI: [10.1021/acsami.5b00341](https://doi.org/10.1021/acsami.5b00341).
- 3 X. Miao, H. Wang, R. Sun, C. Wang, Z. Zhang, Z. Li and L. Yin, Interface engineering of inorganic solid-state electrolytes for high-performance lithium metal batteries, *Energy Environ. Sci.*, 2020, **13**, 3780–3822, DOI: [10.1039/d0ee01435d](https://doi.org/10.1039/d0ee01435d).
- 4 M. Z. Iqbal, M. M. Faisal, S. R. Ali, S. Farid and A. M. Afzal, Co-MOF/polyaniline-based electrode material for high performance supercapattery devices, *Electrochim. Acta*, 2020, **346**, 136039, DOI: [10.1016/j.electacta.2020.136039](https://doi.org/10.1016/j.electacta.2020.136039).
- 5 S. Kour, S. Tanwar and A. L. Sharma, A review on challenges to remedies of MnO<sub>2</sub> based transition-metal oxide, hydroxide, and layered double hydroxide composites for supercapacitor applications, *Mater. Today Commun.*, 2022, **32**, 104033, DOI: [10.1016/j.mtcomm.2022.104033](https://doi.org/10.1016/j.mtcomm.2022.104033).
- 6 F. Cheng, X. Yang, S. Zhang and W. Lu, Boosting the supercapacitor performances of activated carbon with carbon nanomaterials, *J. Power Sources*, 2020, **450**, 227678, DOI: [10.1016/j.jpowsour.2019.227678](https://doi.org/10.1016/j.jpowsour.2019.227678).
- 7 D. Lemian and F. Bode, Battery-Supercapacitor Energy Storage Systems for Electrical Vehicles: A Review, *Energies*, 2022, **15**, 5683, DOI: [10.3390/en15155683](https://doi.org/10.3390/en15155683).
- 8 K. Kowsuki, R. Nirmala, Y. H. Ra and R. Navamathavan, Recent advances in cerium oxide-based nanocomposites in synthesis, characterization, and energy storage applications: A comprehensive review, *Results Chem.*, 2023, **5**, 100877, DOI: [10.1016/j.rechem.2023.100877](https://doi.org/10.1016/j.rechem.2023.100877).
- 9 S. S. Shah, M. A. Aziz, T. Ogawa, L. Zada, M. A. Marwat, S. M. Abdullah, A. J. Khan, M. Usman, I. Khan, Z. Said and M. Oyama, Revolutionary NiCo layered double hydroxide electrodes: Advances, challenges, and future prospects for high-performance supercapacitors, *Mater. Sci. Eng., R*, 2025, **166**, 101041, DOI: [10.1016/j.mser.2025.101041](https://doi.org/10.1016/j.mser.2025.101041).
- 10 J. S. Ananna, M. T. U. Rahman, P. Saha, S. S. Shah, B. J. Kim, M. A. Aziz and A. J. S. Ahammad, Supercapacitors beyond energy storage: multi-functional devices for sensing, actuation, and smart systems, *Sustainable Mater. Technol.*, 2026, **47**, e01840, DOI: [10.1016/j.susmat.2025.e01840](https://doi.org/10.1016/j.susmat.2025.e01840).
- 11 B. R. Sankapal and C. D. Lokhande, Effect of annealing on chemically deposited Bi<sub>2</sub>Se<sub>3</sub>-Sb<sub>2</sub>Se<sub>3</sub> composite thin films, *Mater. Chem. Phys.*, 2002, **74**, 126–133.
- 12 S. Majumder, P. K. Baviskar and B. R. Sankapal, Light-induced electrochemical performance of 3D- CdS nanonet-work: Effect of annealing, *Electrochim. Acta*, 2016, **222**, 100–107, DOI: [10.1016/j.electacta.2016.10.147](https://doi.org/10.1016/j.electacta.2016.10.147).
- 13 S. S. Karade and B. R. Sankapal, Room temperature PEDOT: PSS encapsulated MWCNTs thin film for electrochemical supercapacitor, *J. Electroanal. Chem.*, 2016, **771**, 80–86, DOI: [10.1016/j.jelechem.2016.04.012](https://doi.org/10.1016/j.jelechem.2016.04.012).
- 14 A. Agarwal, S. Majumder and B. R. Sankapal, Carbon Nanotube-Functionalized Surface-Assisted Growth of Cobalt Phosphate Nanodots: A Highly Stable and Bendable All-Solid-State Symmetric Supercapacitor, *Energy Fuels*, 2022, **36**, 5953–5964, DOI: [10.1021/acs.energyfuels.2c00600](https://doi.org/10.1021/acs.energyfuels.2c00600).
- 15 S. Panda, K. Deshmukh, S. K. Khadheer Pasha, J. Theerthagiri, S. Manickam and M. Y. Choi, MXene based emerging materials for supercapacitor applications: Recent advances, challenges, and future perspectives, *Coord. Chem. Rev.*, 2022, **462**, 214518, DOI: [10.1016/j.ccr.2022.214518](https://doi.org/10.1016/j.ccr.2022.214518).
- 16 S. S. Shah, M. Das, T. Ogawa, A. Ali, L. Zada, S. Ullah, Z. Said, M. Usman, A. Younis, M. A. Aziz and M. Oyama, Synergistic Strategies for High-Energy Carbon Supercapacitors: A Comprehensive Review of Nanostructure, Doping, Composite, and Electrolyte Engineering, *Batteries Supercaps*, 2025, e202500564, DOI: [10.1002/batt.202500564](https://doi.org/10.1002/batt.202500564).
- 17 R. Shakil, M. N. Shaikh, S. S. Shah, A. H. Reaz, C. K. Roy, A. N. Chowdhury and M. A. Aziz, Development of a Novel Bio-based Redox Electrolyte using Pivalic Acid and Ascorbic Acid for the Activated Carbon-based Supercapacitor Fabrication, *Asian J. Org. Chem.*, 2021, **10**, 2220–2230, DOI: [10.1002/ajoc.202100314](https://doi.org/10.1002/ajoc.202100314).
- 18 M. M. Hasan, T. Islam, S. S. Shah, A. Awal, M. A. Aziz and A. J. S. Ahammad, Recent Advances in Carbon and Metal Based Supramolecular Technology for Supercapacitor Applications, *Chem. Rec.*, 2022, **22**(7), e202200041, DOI: [10.1002/tcr.202200041](https://doi.org/10.1002/tcr.202200041).
- 19 F. Niaz, S. S. Shah, K. Hayat, M. A. Aziz, G. Liu, Y. Iqbal and M. Oyama, Utilizing rubber plant leaf petioles derived activated carbon for high-performance supercapacitor electrodes, *Ind. Crops Prod.*, 2024, **219**, 119161, DOI: [10.1016/j.indcrop.2024.119161](https://doi.org/10.1016/j.indcrop.2024.119161).
- 20 S. S. Shah, Biomass-Derived Carbon Materials for Advanced Metal-Ion Hybrid Supercapacitors: A Step Towards More Sustainable Energy, *Batteries*, 2024, **10**, 168, DOI: [10.3390/batteries10050168](https://doi.org/10.3390/batteries10050168).
- 21 T. Ahmad, S. S. Murtaza, S. Shah, A. A. Khan, N. Khan, M. Ullah and M. A. A. Oyama, Preparation and electrochemical performance of Convolvulus arvensis-derived activated carbon for symmetric supercapacitors, *Mater. Sci. Eng., B*, 2023, **292**, 116430, DOI: [10.1016/j.mseb.2023.116430](https://doi.org/10.1016/j.mseb.2023.116430).
- 22 S. M. Abu Nayem, A. Ahmad, S. Shaheen Shah, A. Saeed Alzahrani, A. J. Saleh Ahammad and M. A. Aziz, High Performance and Long-cycle Life Rechargeable Aluminum Ion Battery: Recent Progress, Perspectives and Challenges, *Chem. Rec.*, 2022, **22**(12), e202200181, DOI: [10.1002/tcr.202200181](https://doi.org/10.1002/tcr.202200181).
- 23 A. J. Khan, S. S. Shah, S. Khan, A. Mateen, B. Iqbal, M. Naseem, L. He, Y. Zhang, Y. Che, Y. Tang, M. Xu, L. Gao and G. Zhao, 2D metal borides (MBenes): Synthesis methods for energy storage applications, *Chem. Eng. J.*, 2024, **497**, 154429, DOI: [10.1016/j.cej.2024.154429](https://doi.org/10.1016/j.cej.2024.154429).



- 24 M. M. Faisal, S. R. Ali, S. S. Shah, M. W. Iqbal, S. Pushpan, M. A. Aziz, N. Pineda Aguilar, M. M. Alcalá Rodríguez, S. L. Loredó and K. C. Sanal, Redox-active anomalous electrochemical performance of mesoporous nickel manganese sulfide nanomaterial as an anode material for supercapattery devices, *Ceram. Int.*, 2022, **48**, 28565–28577, DOI: [10.1016/j.ceramint.2022.06.170](https://doi.org/10.1016/j.ceramint.2022.06.170).
- 25 M. Pei, M. Cui, J. Y. Kim, Y. Jung and S. Kim, Electrodeposition of NiMn-layered double hydroxide on NiCo metal-organic frameworks and their electrochemical characteristics for supercapacitor electrodes, *Electrochim. Acta*, 2025, **537**, 146866, DOI: [10.1016/j.electacta.2025.146866](https://doi.org/10.1016/j.electacta.2025.146866).
- 26 R. Palm, A. M. Baena-Moncada and J. M. Gonçalves, From medium- to high-entropy hydroxides for hybrid supercapacitors: a review, *J. Mater. Chem. A*, 2024, **12**, 29402–29431, DOI: [10.1039/d4ta05625f](https://doi.org/10.1039/d4ta05625f).
- 27 S. Naeem, A. V. Patil, A. V. Shaikh, U. P. Shinde, D. Husain, M. T. Alam, M. Sharma, K. Tewari, S. Ahmad, A. A. Shah, S. A. Ali and A. Ahmad, A Review of Cobalt-Based Metal Hydroxide Electrode for Applications in Supercapacitors, *Adv. Mater. Sci. Eng.*, 2023, **2023**, 1–15, DOI: [10.1155/2023/1133559](https://doi.org/10.1155/2023/1133559).
- 28 M. Chakraborty, H. R. Inta, A. Roy, H. V. S. R. M. Koppiseti, S. Ghosh, N. Bhandary, D. Roy, S. Debnath and V. Mahalingam, Electrochemical etching mediated enhanced supercapacitor performance of a binder-free Ni/Co/Mo carbonate hydroxide electrode material, *Sustainable Energy Fuels*, 2025, **9**, 4337–4351, DOI: [10.1039/d5se00627a](https://doi.org/10.1039/d5se00627a).
- 29 T. T. Mishra, M. Chakraborty, J. N. Behera and D. Roy, Comprehensive Review on Bimetallic (Ni and Co)-Chalcogenides and Phosphides with Three-Dimensional Architecture for Hybrid Supercapacitor Application, *Energy Fuels*, 2024, **38**, 9186–9217, DOI: [10.1021/acs.energyfuels.4c00382](https://doi.org/10.1021/acs.energyfuels.4c00382).
- 30 P. Muthu, S. Rajagopal, D. Saju, V. Kesavan, A. Dellus, L. Sadhasivam and N. Chandrasekaran, Review of Transition Metal Chalcogenides and Halides as Electrode Materials for Thermal Batteries and Secondary Energy Storage Systems, *ACS Omega*, 2024, **9**(7), 7357–7374, DOI: [10.1021/acsomega.3c08809](https://doi.org/10.1021/acsomega.3c08809).
- 31 T. K. Shivasharma, N. Upadhyay, T. B. Deshmukh and B. R. Sankapal, Exploring Vacuum-Assisted Thin Films toward Supercapacitor Applications: Present Status and Future Prospects, *ACS Omega*, 2023, **8**, 37685–37719, DOI: [10.1021/acsomega.3c05285](https://doi.org/10.1021/acsomega.3c05285).
- 32 C. Xiong, M. Li, S. Nie, W. Dang, W. Zhao, L. Dai and Y. Ni, Non-carbonized porous lignin-free wood as an effective scaffold to fabricate lignin-free Wood@Polyaniline supercapacitor material for renewable energy storage application, *J. Power Sources*, 2020, **471**, 228448, DOI: [10.1016/j.jpowsour.2020.228448](https://doi.org/10.1016/j.jpowsour.2020.228448).
- 33 *Handbook of Nanocomposite Supercapacitor Materials IV*, ed. K. K. Kar, Springer International Publishing, Cham, 2023, DOI: [10.1007/978-3-031-23701-0](https://doi.org/10.1007/978-3-031-23701-0).
- 34 L. Phor, A. Kumar and S. Chahal, Electrode materials for supercapacitors: A comprehensive review of advancements and performance, *J. Energy Storage*, 2024, **84**, 110698, DOI: [10.1016/j.est.2024.110698](https://doi.org/10.1016/j.est.2024.110698).
- 35 D. Muthu, R. K. Dharman, S. E. Muthu and T. H. Oh, Recent developments in metal-organic framework-derived transition metal oxide@carbon nanostructure and carbon nanostructure for supercapacitor applications, *J. Energy Storage*, 2025, **119**, 116365, DOI: [10.1016/j.est.2025.116365](https://doi.org/10.1016/j.est.2025.116365).
- 36 P. Gaikwad, N. Tiwari, R. Kamat, S. M. Mane and S. B. Kulkarni, A comprehensive review on the progress of transition metal oxides materials as a supercapacitor electrode, *Mater. Sci. Eng., B*, 2024, **307**, 117544, DOI: [10.1016/j.mseb.2024.117544](https://doi.org/10.1016/j.mseb.2024.117544).
- 37 S. Sharma and P. Chand, Supercapacitor and electrochemical techniques: A brief review, *Results Chem.*, 2023, **5**, 100885, DOI: [10.1016/j.rechem.2023.100885](https://doi.org/10.1016/j.rechem.2023.100885).
- 38 A. R. Mashtizadeh, S. K. Asl, H. Aghajani, S. M. Masoudpanah and M. Wojnicki, Carbon Nanomaterials for Electrochemical Hydrogen Storage: Mechanisms and Advancements, *Inorganics*, 2025, **13**, 125, DOI: [10.3390/inorganics13040125](https://doi.org/10.3390/inorganics13040125).
- 39 S. Jayakumar, P. C. Santhosh, M. M. Mohideen and A. V. Radhamani, A comprehensive review of metal oxides (RuO<sub>2</sub>, Co<sub>3</sub>O<sub>4</sub>, MnO<sub>2</sub> and NiO) for supercapacitor applications and global market trends, *J. Alloys Compd.*, 2024, **976**, 173170, DOI: [10.1016/j.jallcom.2023.173170](https://doi.org/10.1016/j.jallcom.2023.173170).
- 40 Y. Liu, S. P. Jiang and Z. Shao, Intercalation pseudocapacitance in electrochemical energy storage: recent advances in fundamental understanding and materials development, *Mater. Today Adv.*, 2020, **7**, 100072, DOI: [10.1016/j.mtadv.2020.100072](https://doi.org/10.1016/j.mtadv.2020.100072).
- 41 Z. Lu, Z. Chang, W. Zhu and X. Sun, Beta-phased Ni(OH)<sub>2</sub> nanowall film with reversible capacitance higher than theoretical Faradic capacitance, *Chem. Commun.*, 2011, **47**, 9651–9653, DOI: [10.1039/c1cc13796d](https://doi.org/10.1039/c1cc13796d).
- 42 J. Xie, X. Sun, N. Zhang, K. Xu, M. Zhou and Y. Xie, Layer-by-layer B-Ni(OH)<sub>2</sub>/graphene nanohybrids for ultraflexible all-solid-state thin-film supercapacitors with high electrochemical performance, *Nano Energy*, 2013, **2**, 65–74, DOI: [10.1016/j.nanoen.2012.07.016](https://doi.org/10.1016/j.nanoen.2012.07.016).
- 43 A. Muzaffar, M. B. Ahamed, K. Deshmukh and J. Thirumalai, A review on recent advances in hybrid supercapacitors: Design, fabrication and applications, *Renewable Sustainable Energy Rev.*, 2019, **101**, 123–145, DOI: [10.1016/j.rser.2018.10.026](https://doi.org/10.1016/j.rser.2018.10.026).
- 44 Q. Wang, Y. F. Nie, Z. H. Xiao, X. Y. Chen and Z. J. Zhang, Simply incorporating an efficient redox additive into KOH electrolyte for largely improving electrochemical performances, *J. Electroanal. Chem.*, 2016, **770**, 62–72, DOI: [10.1016/j.jelechem.2016.03.037](https://doi.org/10.1016/j.jelechem.2016.03.037).
- 45 N. W. Duffy, W. Balasing and A. G. Pandolfo, The nickel-carbon asymmetric supercapacitor-Performance, energy density and electrode mass ratios, *Electrochim. Acta*, 2008, **54**, 535–539, DOI: [10.1016/j.electacta.2008.07.047](https://doi.org/10.1016/j.electacta.2008.07.047).
- 46 A. Afif, S. M. Rahman, A. Tasfiah Azad, J. Zaini, M. A. Islam and A. K. Azad, Advanced materials and technologies for hybrid supercapacitors for energy storage – A review,



- J. Energy Storage*, 2019, **25**, 100852, DOI: [10.1016/j.est.2019.100852](https://doi.org/10.1016/j.est.2019.100852).
- 47 S. S. Raut, J. A. Dhobale and B. R. Sankapal, SILAR deposited Bi<sub>2</sub>S<sub>3</sub> thin film towards electrochemical supercapacitor, *Phys. E*, 2017, **87**, 209–212, DOI: [10.1016/j.physe.2016.09.019](https://doi.org/10.1016/j.physe.2016.09.019).
- 48 M. Thosare, T. B. Deshmukh, R. N. Bulakhe, J. M. Kim and B. R. Sankapal, Graphitic carbon nitride: A comprehensive review towards supercapacitive energy storage applications, *J. Energy Storage*, 2025, **130**, 117338, DOI: [10.1016/j.est.2025.117338](https://doi.org/10.1016/j.est.2025.117338).
- 49 B. Pandit and B. R. Sankapal, Cerium Selenide Nanoparticle/Multiwalled Carbon Nanotube Composite Electrodes for Solid-State Symmetric Supercapacitors, *ACS Appl. Nano Mater.*, 2022, **5**, 3007–3017, DOI: [10.1021/acsanm.2c00374](https://doi.org/10.1021/acsanm.2c00374).
- 50 S. S. Raut, B. R. Sankapal, M. S. A. Hossain, S. Pradhan, R. R. Salunkhe and Y. Yamauchi, Zinc Ferrite Anchored Multiwalled Carbon Nanotubes for High-Performance Supercapacitor Applications, *Eur. J. Inorg. Chem.*, 2018, **2018**, 137–142, DOI: [10.1002/ejic.201700836](https://doi.org/10.1002/ejic.201700836).
- 51 A. Agarwal, R. Tolani and B. R. Sankapal, Conducting Polymers–Metal Chalcogenides Hybrid Composite: Current Trends and Future Prospects Toward Supercapacitor Applications, *Energy Technol.*, 2024, **12**(8), 2400133, DOI: [10.1002/ente.202400133](https://doi.org/10.1002/ente.202400133).
- 52 J. Khan, A. Ahmed and A. A. Al-Kahtani, Enhanced supercapacitor performance using EG@COF: a layered porous composite, *RSC Adv.*, 2025, **15**, 11441–11450, DOI: [10.1039/d5ra01653c](https://doi.org/10.1039/d5ra01653c).
- 53 A. Agarwal, C. Varshney, B. L. Kumar, A. C. Mendhe, T. B. Deshmukh and B. R. Sankapal, Synthesis of spongy Mn nanoparticles by electroless reduction for solid-state flexible supercapacitor application, *J. Alloys Compd.*, 2022, **922**, 166238, DOI: [10.1016/j.jallcom.2022.166238](https://doi.org/10.1016/j.jallcom.2022.166238).
- 54 Y. Liu, R. Wang and X. Yan, Synergistic effect between ultra-small nickel hydroxide nanoparticles and reduced graphene oxide sheets for the application in high-performance asymmetric supercapacitor, *Sci. Rep.*, 2015, **5**, 11095, DOI: [10.1038/srep11095](https://doi.org/10.1038/srep11095).
- 55 K. Chen, X. Chen and D. Xue, Hydrothermal route to crystallization of FeOOH nanorods via FeCl<sub>3</sub>·6H<sub>2</sub>O: effect of Fe<sup>3+</sup> concentration on pseudocapacitance of iron-based materials, *CrystEngComm*, 2015, **17**, 1906–1910, DOI: [10.1039/C4CE02504K](https://doi.org/10.1039/C4CE02504K).
- 56 J. Feng, X. Sun, C. Wu, L. Peng, C. Lin, S. Hu, J. Yang and Y. Xie, Metallic few-layered VS<sub>2</sub> ultrathin nanosheets: High two-dimensional conductivity for in-plane supercapacitors, *J. Am. Chem. Soc.*, 2011, **133**, 17832–17838, DOI: [10.1021/ja207176c](https://doi.org/10.1021/ja207176c).
- 57 R. Sahu, T. K. Shivasharma, M. C. Rath, S. J. Keny and B. R. Sankapal, Photochemically synthesized tin oxide nanoparticles: Electrode to device grade solid-state supercapacitor, *J. Energy Storage*, 2024, **101**, 113957, DOI: [10.1016/j.est.2024.113957](https://doi.org/10.1016/j.est.2024.113957).
- 58 M. Girirajan, A. K. Bojarajan, I. N. Pulidindi, K. N. Hui and S. Sangaraju, An insight into the nanoarchitecture of electrode materials on the performance of supercapacitors, *Coord. Chem. Rev.*, 2024, **518**, 216080, DOI: [10.1016/j.ccr.2024.216080](https://doi.org/10.1016/j.ccr.2024.216080).
- 59 A. A. Adul-Rasool, D. M. Athair, H. K. Zaidan, A. M. Rheima, Z. T. Al-Sharif, S. H. Mohammed and E. Kianfar, 0,1,2,3D nanostructures, types of bulk nanostructured materials, and drug nanocrystals: An overview, *Cancer Treat. Res. Commun.*, 2024, **40**, 100834, DOI: [10.1016/j.ctarc.2024.100834](https://doi.org/10.1016/j.ctarc.2024.100834).
- 60 G. Zhang, X. Xiao, B. Li, P. Gu, H. Xue and H. Pang, Transition metal oxides with one-dimensional/one-dimensional-analogue nanostructures for advanced supercapacitors, *J. Mater. Chem. A*, 2017, **5**, 8155–8186, DOI: [10.1039/c7ta02454a](https://doi.org/10.1039/c7ta02454a).
- 61 G. Ma and X. Wang, Synthesis and applications of one-dimensional porous nanowire arrays: A review, *Nano*, 2015, **10**, 1530001, DOI: [10.1142/S1793292015300017](https://doi.org/10.1142/S1793292015300017).
- 62 K. Okada, One-dimensional metal hydroxide nanomaterials with macroscopically controlled orientation and aggregation: Fascinating surface hydroxyl groups on anisotropic structures for functionalities, *J. Ceram. Soc. Jpn.*, 2020, **128**, 627–634, DOI: [10.2109/jcersj2.20105](https://doi.org/10.2109/jcersj2.20105).
- 63 S. Jahangiri and N. J. Mosey, Surface Functionalities Derived from 1-Dimensional Metal Hydroxide Nanomaterials, *Phys. Chem. Chem. Phys.*, 2017, **19**, 1963–1974, DOI: [10.24729/00000130](https://doi.org/10.24729/00000130).
- 64 B. R. Sankapal and A. Agarwal, *Simple Chemical Methods for Thin Film Deposition*, Springer Nature Singapore, Singapore, 1st edn, 2023, DOI: [10.1007/978-981-99-0961-2](https://doi.org/10.1007/978-981-99-0961-2).
- 65 K. R. Kumbhar, R. S. Redekar and N. L. Tarwal, Investigating the effect of the electrolyte variation on the supercapacitor performance of hydrothermally synthesized cobalt-manganese layered double hydroxide nanospikes, *J. Energy Storage*, 2026, **146**, 119854, DOI: [10.1016/j.est.2025.119854](https://doi.org/10.1016/j.est.2025.119854).
- 66 M. Manikkoth, M. G. Akhil, V. Manoj and T. P. D. Rajan, Towards sustainable Al–air batteries: Electrolyte engineering using water-in-salt chemistry for improved performance, *J. Energy Storage*, 2026, **143**, 119544, DOI: [10.1016/j.est.2025.119544](https://doi.org/10.1016/j.est.2025.119544).
- 67 T. Nguyen and M. de F. Montemor, Metal Oxide and Hydroxide-Based Aqueous Supercapacitors: From Charge Storage Mechanisms and Functional Electrode Engineering to Need-Tailored Devices, *Adv. Sci.*, 2019, **6**(9), 1801797, DOI: [10.1002/advs.201801797](https://doi.org/10.1002/advs.201801797).
- 68 M. Moradi, A. Afkhami, T. Madrakian, H. R. Moazami and A. Tirandaz, Partial hydrothermal sulfidation of electrosynthesized Co–Mn layered-double-hydroxide as an active material for supercapacitor applications, *J. Power Sources*, 2025, **629**, 235993, DOI: [10.1016/j.jpowsour.2024.235993](https://doi.org/10.1016/j.jpowsour.2024.235993).
- 69 C. Jing, B. Dong and Y. Zhang, Chemical Modifications of Layered Double Hydroxides in the Supercapacitor, *Energy Environ. Mater.*, 2020, **3**, 346–379, DOI: [10.1002/eem2.12116](https://doi.org/10.1002/eem2.12116).
- 70 H. Zhang, M. Usman Tahir, X. Yan, X. Liu, X. Su and L. Zhang, Ni–Al layered double hydroxide with regulated interlayer spacing as electrode for aqueous asymmetric supercapacitor, *Chem. Eng. J.*, 2019, **368**, 905–913, DOI: [10.1016/j.cej.2019.03.041](https://doi.org/10.1016/j.cej.2019.03.041).



- 71 H. Chen, L. Hu, M. Chen, Y. Yan and L. Wu, Nickel-cobalt layered double hydroxide nanosheets for high-performance supercapacitor electrode materials, *Adv. Funct. Mater.*, 2014, **24**, 934–942, DOI: [10.1002/adfm.201301747](https://doi.org/10.1002/adfm.201301747).
- 72 E. Torabi, A. Kazemi, M. Tamtaji, F. Manteghi, S. Rohani and W. A. Goddard, Sacrificial MOF-derived MnNi hydroxide for high energy storage supercapacitor electrodes via DFT-based quantum capacitance study, *Heliyon*, 2025, **11**, e41261, DOI: [10.1016/j.heliyon.2024.e41261](https://doi.org/10.1016/j.heliyon.2024.e41261).
- 73 M. Aghazadeh and H. Foratirad, Electrochemical grown Ni, Zn-MOF and its derived hydroxide as battery-type electrodes for supercapacitors, *Synth. Met.*, 2022, **285**, 117009, DOI: [10.1016/j.synthmet.2022.117009](https://doi.org/10.1016/j.synthmet.2022.117009).
- 74 J. P. Cheng, J. Zhang and F. Liu, Recent development of metal hydroxides as electrode material of electrochemical capacitors, *RSC Adv.*, 2014, **4**, 38893–38917, DOI: [10.1039/c4ra06738j](https://doi.org/10.1039/c4ra06738j).
- 75 S. Li, C. L. Guenther, M. S. Kelley and D. A. Dixon, Molecular structures, acid-base properties, and formation of group 6 transition metal hydroxides, *J. Phys. Chem. C*, 2011, **115**, 8072–8103, DOI: [10.1021/jp111031x](https://doi.org/10.1021/jp111031x).
- 76 A. R. Mule, B. Ramulu, S. J. Arbaz, A. Kurakula and J. S. Yu, Ag-integrated mixed metallic Co-Fe-Ni-Mn hydroxide composite as advanced electrode for high-performance hybrid supercapacitors, *J. Energy Chem.*, 2024, **88**, 579–591, DOI: [10.1016/j.jechem.2023.09.041](https://doi.org/10.1016/j.jechem.2023.09.041).
- 77 F. He, N. Yang, K. Li, X. Wang, S. Cong, L. Zhang, S. Xiong and A. Zhou, Hydrothermal synthesis of Ni-based metal organic frameworks/graphene oxide composites as supercapacitor electrode materials, *J. Mater. Res.*, 2020, **35**, 1439–1450, DOI: [10.1557/jmr.2020.93](https://doi.org/10.1557/jmr.2020.93).
- 78 R. S. Mane, B. R. Sankapal and C. D. Lokhande, *Thin Solid Films*, 1999, **353**, 29–32.
- 79 R. S. Mane, B. R. Sankapal and C. D. Lokhande, Studies on chemically deposited nanocrystalline Bi<sub>2</sub>S<sub>3</sub> thin films, *Mater. Res. Bull.*, 2000, **35**(4), 587–601.
- 80 P. R. Nikam, P. K. Baviskar, J. V. Sali, K. V. Gurav, J. H. Kim and B. R. Sankapal, SILAR coated Bi<sub>2</sub>S<sub>3</sub> nanoparticles on vertically aligned ZnO nanorods: Synthesis and characterizations, *Ceram. Int.*, 2015, **41**, 10394–10399, DOI: [10.1016/j.ceramint.2015.03.239](https://doi.org/10.1016/j.ceramint.2015.03.239).
- 81 B. Pandit, L. K. Bommineedi and B. R. Sankapal, Electrochemical engineering approach of high performance solid-state flexible supercapacitor device based on chemically synthesized VS<sub>2</sub> nanoregime structure, *J. Energy Chem.*, 2019, **31**, 79–88, DOI: [10.1016/j.jechem.2018.05.011](https://doi.org/10.1016/j.jechem.2018.05.011).
- 82 A. C. Mendhe, S. Majumder, N. Nair and B. R. Sankapal, Core-shell cadmium sulphide @ silver sulphide nanowires surface architecture: Design towards photoelectrochemical solar cells, *J. Colloid Interface Sci.*, 2021, **587**, 715–726, DOI: [10.1016/j.jcis.2020.11.031](https://doi.org/10.1016/j.jcis.2020.11.031).
- 83 S. Majumder, P. K. Baviskar and B. R. Sankapal, Light-induced electrochemical performance of 3D- CdS nanonet-work: Effect of annealing, *Electrochim. Acta*, 2016, **222**, 100–107, DOI: [10.1016/j.electacta.2016.10.147](https://doi.org/10.1016/j.electacta.2016.10.147).
- 84 N. B. Sonawane, K. V. Gurav, R. R. Ahire, J. H. Kim and B. R. Sankapal, CdS nanowires with PbS nanoparticles surface coating as room temperature liquefied petroleum gas sensor, *Sens. Actuators, A*, 2014, **216**, 78–83, DOI: [10.1016/j.sna.2014.05.012](https://doi.org/10.1016/j.sna.2014.05.012).
- 85 U. M. Patil, R. V. Ghorpade, M. S. Nam, A. C. Nalawade, S. Lee, H. Han and S. C. Jun, PolyHIPE Derived Freestanding 3D Carbon Foam for Cobalt Hydroxide Nanorods Based High Performance Supercapacitor, *Sci. Rep.*, 2016, **6**, 35490, DOI: [10.1038/srep35490](https://doi.org/10.1038/srep35490).
- 86 W. Ge, A. Encinas, M. F. Ruiz and S. Song, Construction of amorphous Ni(OH)<sub>2</sub>@nickel nanowire with interconnected structure as advanced core-shell electrodes for asymmetric supercapacitors, *J. Energy Storage*, 2020, **31**, 101607, DOI: [10.1016/j.est.2020.101607](https://doi.org/10.1016/j.est.2020.101607).
- 87 L. Lai, R. Li, S. Su, L. Zhang, Y. Cui, N. Guo, W. Shi and X. Zhu, Controllable synthesis of reduced graphene oxide/nickel hydroxide composites with different morphologies for high performance supercapacitors, *J. Alloys Compd.*, 2020, **820**, 153120, DOI: [10.1016/j.jallcom.2019.153120](https://doi.org/10.1016/j.jallcom.2019.153120).
- 88 S. Faraji and F. N. Ani, Microwave-assisted synthesis of metal oxide/hydroxide composite electrodes for high power supercapacitors - A review, *J. Power Sources*, 2014, **263**, 338–360, DOI: [10.1016/j.jpowsour.2014.03.144](https://doi.org/10.1016/j.jpowsour.2014.03.144).
- 89 A. K. Mondal, D. Su, S. Chen, J. Zhang, A. Ung and G. Wang, Microwave-assisted synthesis of spherical β-Ni(OH)<sub>2</sub> superstructures for electrochemical capacitors with excellent cycling stability, *Chem. Phys. Lett.*, 2014, **610–611**, 115–120, DOI: [10.1016/j.cplett.2014.07.025](https://doi.org/10.1016/j.cplett.2014.07.025).
- 90 R. Qu, S. Tang, X. Qin, J. Yuan, Y. Deng, L. Wu, J. Li and Z. Wei, Expanded graphite supported Ni(OH)<sub>2</sub> composites for high performance supercapacitors, *J. Alloys Compd.*, 2017, **728**, 222–230, DOI: [10.1016/j.jallcom.2017.08.270](https://doi.org/10.1016/j.jallcom.2017.08.270).
- 91 F. Zhou, Q. Liu, J. Gu, W. Zhang and D. Zhang, Microwave-assisted anchoring of flowerlike Co(OH)<sub>2</sub> nanosheets on activated carbon to prepare hybrid electrodes for high-rate electrochemical capacitors, *Electrochim. Acta*, 2015, **170**, 328–336, DOI: [10.1016/j.electacta.2015.04.146](https://doi.org/10.1016/j.electacta.2015.04.146).
- 92 X. Lu, C. Wang, F. Favier and N. Pinna, Electrospun Nanomaterials for Supercapacitor Electrodes: Designed Architectures and Electrochemical Performance, *Adv. Energy Mater.*, 2017, **7**(2), 1601301, DOI: [10.1002/aenm.201601301](https://doi.org/10.1002/aenm.201601301).
- 93 H. Qu, S. Wei and Z. Guo, Coaxial electrospun nanostructures and their applications, *J. Mater. Chem. A*, 2013, **1**, 11513–11528, DOI: [10.1039/c3ta12390a](https://doi.org/10.1039/c3ta12390a).
- 94 H. Chen, N. Wang, J. Di, Y. Zhao, Y. Song and L. Jiang, Nanowire-in-microtube structured core/shell fibers via multifluidic coaxial electrospinning, *Langmuir*, 2010, **26**, 11291–11296, DOI: [10.1021/la100611f](https://doi.org/10.1021/la100611f).
- 95 E. Erdemutu, C. Bai and L. Ding, Electrospun Ni-Ni(OH)<sub>2</sub>/Carbon Nanofibers as Flexible Binder-Free Supercapacitor Electrode with Enhanced Specific Capacitance, *J. Electron. Mater.*, 2020, **49**, 7211–7218, DOI: [10.1007/s11664-020-08458-3](https://doi.org/10.1007/s11664-020-08458-3).
- 96 C. C. Lai and C. T. Lo, Effect of Temperature on Morphology and Electrochemical Capacitive Properties of Electrospun Carbon Nanofibers and Nickel Hydroxide Composites, *Electrochim. Acta*, 2015, **174**, 806–814, DOI: [10.1016/j.electacta.2015.06.077](https://doi.org/10.1016/j.electacta.2015.06.077).



- 97 Z. Tai, J. Lang, X. Yan and Q. Xue, Mutually Enhanced Capacitances in Carbon Nanofiber/Cobalt Hydroxide Composite Paper for Supercapacitor, *J. Electrochem. Soc.*, 2012, **159**, A485–A491, DOI: [10.1149/2.110204jes](https://doi.org/10.1149/2.110204jes).
- 98 A. Abas, H. Sheng, Y. Ma, X. Zhang, Y. Wei, Q. Su, W. Lan and E. Xie, PEDOT:PSS coated CuO nanowire arrays grown on Cu foam for high-performance supercapacitor electrodes, *J. Mater. Sci.: Mater. Electron.*, 2019, **30**, 10953–10960, DOI: [10.1007/s10854-019-01469-9](https://doi.org/10.1007/s10854-019-01469-9).
- 99 J. Zhao, L. Yang, H. Li, T. Huang, H. Cheng, A. Meng, Y. Lin, P. Wu, X. Yuan and Z. Li, Ni<sub>3</sub>Se<sub>2</sub> nanosheets in-situ grown on 3D NiSe nanowire arrays with enhanced electrochemical performances for supercapacitor and efficient oxygen evolution, *Mater. Charact.*, 2021, **172**, 110819, DOI: [10.1016/j.matchar.2020.110819](https://doi.org/10.1016/j.matchar.2020.110819).
- 100 S. Hwang, T. Hwang, H. Kong, S. Lee and J. Yeo, Novel fabrication method of hierarchical planar micro-supercapacitor via laser-induced localized growth of manganese dioxide nanowire arrays, *Appl. Surf. Sci.*, 2021, **552**, 149382, DOI: [10.1016/j.apsusc.2021.149382](https://doi.org/10.1016/j.apsusc.2021.149382).
- 101 W. Guo, Y. Li, Y. Tang, S. Chen, Z. Liu, L. Wang, Y. Zhao and F. Gao, TiO<sub>2</sub> Nanowire Arrays on Titanium Substrate as a Novel Binder-free Negative Electrode for Asymmetric Supercapacitor, *Electrochim. Acta*, 2017, **229**, 197–207, DOI: [10.1016/j.electacta.2017.01.135](https://doi.org/10.1016/j.electacta.2017.01.135).
- 102 D. Zhu, Y. Wang, G. Yuan and H. Xia, High-performance supercapacitor electrodes based on hierarchical Ti@MnO<sub>2</sub> nanowire arrays, *Chem. Commun.*, 2014, **50**, 2876–2878, DOI: [10.1039/c3cc49800j](https://doi.org/10.1039/c3cc49800j).
- 103 N. Nair and B. R. Sankapal, Nested CdS@HgS core-shell nanowires as supercapacitive Faradaic electrode through simple solution chemistry, *Nano-Struct. Nano-Objects*, 2017, **10**, 159–166, DOI: [10.1016/j.nanoso.2017.05.004](https://doi.org/10.1016/j.nanoso.2017.05.004).
- 104 N. Nair and B. R. Sankapal, Cationic-exchange approach for conversion of two-dimensional CdS to two-dimensional Ag<sub>2</sub>S nanowires with an intermediate core-shell nanostructure towards supercapacitor application, *New J. Chem.*, 2016, **40**, 10144–10152, DOI: [10.1039/c6nj02411d](https://doi.org/10.1039/c6nj02411d).
- 105 M. Manikandan, K. Subramani, M. Sathish and S. Dhanuskodi, Hydrothermal synthesis of cobalt telluride nanorods for a high-performance hybrid asymmetric supercapacitor, *RSC Adv.*, 2020, **10**, 13632–13641, DOI: [10.1039/c9ra08692g](https://doi.org/10.1039/c9ra08692g).
- 106 M. Hussain, A. W. Alrowaily, B. M. Alotaibi, H. A. Alyousef, N. Al-Harbi, A. Dahshan, K. Ahmad, M. J. Khan and A. M. A. Henaish, Effect of silver (Ag) on manganese telluride (MnTe) for the enhancement of electrochemical properties toward supercapacitor application, *Int. J. Hydrogen Energy*, 2024, **71**, 422–432, DOI: [10.1016/j.ijhydene.2024.05.274](https://doi.org/10.1016/j.ijhydene.2024.05.274).
- 107 L. Peng, L. Lv, H. Wan, Y. Ruan, X. Ji, J. Liu, L. Miao, C. Wang and J. Jiang, Understanding the electrochemical activation behavior of Co(OH)<sub>2</sub> nanotubes during the ion-exchange process, *Mater. Today Energy*, 2017, **4**, 122–131, DOI: [10.1016/j.mtener.2017.04.004](https://doi.org/10.1016/j.mtener.2017.04.004).
- 108 Q. Gui, J. Jiang, Y. Li and J. Liu, One-pot growth of Co(OH)<sub>2</sub> nanowire bundle arrays on in situ functionalized carbon cloth for robust flexible supercapacitor electrodes, *Dalton Trans.*, 2018, **47**, 15416–15423, DOI: [10.1039/c8dt03439g](https://doi.org/10.1039/c8dt03439g).
- 109 J. Huang, T. Liu, X. Liu, L. Du, D. Cao, J. Yin and G. Wang, Electrochemical capacitive studies of cadmium hydroxide nanowires grown on nickel foam, *J. Electroanal. Chem.*, 2013, **696**, 15–19, DOI: [10.1016/j.jelechem.2013.03.006](https://doi.org/10.1016/j.jelechem.2013.03.006).
- 110 A. A. Mancharkar, M. R. Bodke, D. B. Malavekar, R. N. Bulakhe, J. M. Kim, J. H. Kim and H. M. Pathan, Cadmium Hydroxide Nanowires for High Performance Supercapacitor by Chemical Bath Deposition, *ES Energy Environ.*, 2024, **23**(2), 1048, DOI: [10.30919/esee1048](https://doi.org/10.30919/esee1048).
- 111 S. Patil, S. Raut, R. Gore and B. Sankapal, One-dimensional cadmium hydroxide nanowires towards electrochemical supercapacitor, *New J. Chem.*, 2015, **39**, 9124–9131, DOI: [10.1039/c5nj02022k](https://doi.org/10.1039/c5nj02022k).
- 112 M. J. Deng, C. Z. Song, C. C. Wang, Y. C. Tseng, J. M. Chen and K. T. Lu, Low cost facile synthesis of large-area cobalt hydroxide nanorods with remarkable pseudocapacitance, *ACS Appl. Mater. Interfaces*, 2015, **7**, 9147–9156, DOI: [10.1021/acsami.5b01163](https://doi.org/10.1021/acsami.5b01163).
- 113 Y. Tang, Y. Liu, S. Yu, S. Mu, S. Xiao, Y. Zhao and F. Gao, Morphology controlled synthesis of monodisperse cobalt hydroxide for supercapacitor with high performance and long cycle life, *J. Power Sources*, 2014, **256**, 160–169, DOI: [10.1016/j.jpowsour.2014.01.064](https://doi.org/10.1016/j.jpowsour.2014.01.064).
- 114 Z. Liu, Y. Xing, S. Fang and X. Qu, Facile synthesis of  $\gamma$ -MnOOH nanotubes and their application in electrochemical capacitors, *J. Mater. Sci.: Mater. Electron.*, 2015, **26**, 5975–5979, DOI: [10.1007/s10854-015-3172-3](https://doi.org/10.1007/s10854-015-3172-3).
- 115 Y. X. Wang, Z. A. Hu and H. Y. Wu, Preparation and electrochemical performance of alpha-nickel hydroxide nanowire, *Mater. Chem. Phys.*, 2011, **126**, 580–583, DOI: [10.1016/j.matchemphys.2011.01.022](https://doi.org/10.1016/j.matchemphys.2011.01.022).
- 116 P. Xu, K. Ye, M. Du, J. Liu, K. Cheng, J. Yin, G. Wang and D. Cao, One-step synthesis of copper compounds on copper foil and their supercapacitive performance, *RSC Adv.*, 2015, **5**, 36656–36664, DOI: [10.1039/c5ra04889c](https://doi.org/10.1039/c5ra04889c).
- 117 K. C. Ho and L. Y. Lin, A review of electrode materials based on core-shell nanostructures for electrochemical supercapacitors, *J. Mater. Chem. A*, 2019, **7**, 3516–3530, DOI: [10.1039/c8ta11599k](https://doi.org/10.1039/c8ta11599k).
- 118 H. Mi, X. Zhang, S. An, X. Ye and S. Yang, Microwave-assisted synthesis and electrochemical capacitance of polyaniline/multi-wall carbon nanotubes composite, *Electrochem. Commun.*, 2007, **9**, 2859–2862, DOI: [10.1016/j.elecom.2007.10.013](https://doi.org/10.1016/j.elecom.2007.10.013).
- 119 F. Zhu, M. Yan, Y. Liu, H. Shen, Y. Lei and W. Shi, Hexagonal prism-like hierarchical Co<sub>9</sub>S<sub>8</sub>@Ni(OH)<sub>2</sub> core-shell nanotubes on carbon fibers for high-performance asymmetric supercapacitors, *J. Mater. Chem. A*, 2017, **5**, 22782–22789, DOI: [10.1039/c7ta07160d](https://doi.org/10.1039/c7ta07160d).
- 120 S. Rout, V. Soni, R. Sahu and B. R. Sankapal, Cadmium hydroxide-vanadyl hydroxide core-shell nanorods: Electrode formation to design prototype device grade solid-state supercapacitor, *J. Alloys Compd.*, 2025, **1033**, 181322, DOI: [10.1016/j.jallcom.2025.181322](https://doi.org/10.1016/j.jallcom.2025.181322).



- 121 W. D. Wang, P. P. Zhang, S. Q. Gao, B. Q. Wang, X. C. Wang, M. Li, F. Liu and J. P. Cheng, Core-shell nanowires of NiCo<sub>2</sub>O<sub>4</sub>@ $\alpha$ -Co(OH)<sub>2</sub> on Ni foam with enhanced performances for supercapacitors, *J. Colloid Interface Sci.*, 2020, **579**, 71–81, DOI: [10.1016/j.jcis.2020.06.048](https://doi.org/10.1016/j.jcis.2020.06.048).
- 122 X. Wang, F. Rong, F. Huang, P. He, Y. Yang, J. Tang and R. Que, Facile synthesis of hierarchical CoMoO<sub>4</sub>@Ni(OH)<sub>2</sub> core-shell nanotubes for bifunctional supercapacitors and oxygen electrocatalysts, *J. Alloys Compd.*, 2019, **789**, 684–692, DOI: [10.1016/j.jallcom.2019.03.077](https://doi.org/10.1016/j.jallcom.2019.03.077).
- 123 H. Yi, X. Chen, H. Wang and X. Wang, Hierarchical TiN@Ni(OH)<sub>2</sub> core/shell nanowire arrays for supercapacitor application, *Electrochim. Acta*, 2014, **116**, 372–378, DOI: [10.1016/j.electacta.2013.11.083](https://doi.org/10.1016/j.electacta.2013.11.083).
- 124 R. Perez-Gonzalez, E. Araujo, W. Ge, S. Cherepanov, A. Zakhidov, V. Rodriguez-Gonzalez, A. Encinas and J. Oliva, Carbon nanotube anodes decorated with Ag NWs/Ni(OH)<sub>2</sub> NWs for efficient semitransparent flexible solid-state supercapacitors, *Electrochim. Acta*, 2020, **354**, 136684, DOI: [10.1016/j.electacta.2020.136684](https://doi.org/10.1016/j.electacta.2020.136684).
- 125 F. N. I. Sari, K. C. Lin and J. M. Ting, Mn(OH)<sub>2</sub>-containing Co(OH)<sub>2</sub>/Ni(OH)<sub>2</sub> Core-shelled structure for ultrahigh energy density asymmetric supercapacitor, *Appl. Surf. Sci.*, 2022, **576**, 151805, DOI: [10.1016/j.apsusc.2021.151805](https://doi.org/10.1016/j.apsusc.2021.151805).
- 126 H. Jiang, C. Li, T. Sun and J. Ma, High-performance supercapacitor material based on Ni(OH)<sub>2</sub> nanowire-MnO<sub>2</sub> nanoflakes core-shell nanostructures, *Chem. Commun.*, 2012, **48**, 2606–2608, DOI: [10.1039/c2cc18079k](https://doi.org/10.1039/c2cc18079k).
- 127 S. L. Patil, S. S. Raut and B. R. Sankapal, Cu(OH)<sub>2</sub>@Cd(OH)<sub>2</sub> core-shell nanostructure: Synthesis to supercapacitor application, *Thin Solid Films*, 2019, **692**, 137584, DOI: [10.1016/j.tsf.2019.137584](https://doi.org/10.1016/j.tsf.2019.137584).
- 128 S. Patil, S. Raut, B. Pandit, S. N. Pandey, S. A. Pande and B. Sankapal, Web-analogues one-dimensional iron hydroxide@cadmium hydroxide nanostructure: electrochemical supercapacitor, *J. Mater. Sci.: Mater. Electron.*, 2021, **32**, 22472–22480, DOI: [10.1007/s10854-021-06733-5](https://doi.org/10.1007/s10854-021-06733-5).
- 129 X. Yin, C. Tang, L. Zhang, Z. G. Yu and H. Gong, Chemical insights into the roles of nanowire cores on the growth and supercapacitor performances of Ni-Co-O/Ni(OH)<sub>2</sub> core/shell electrodes, *Sci. Rep.*, 2016, **6**, 21566, DOI: [10.1038/srep21566](https://doi.org/10.1038/srep21566).
- 130 R. Yuksel, S. Coskun, Y. E. Kalay and H. E. Unalan, Flexible, silver nanowire network nickel hydroxide core-shell electrodes for supercapacitors, *J. Power Sources*, 2016, **328**, 167–173, DOI: [10.1016/j.jpowsour.2016.08.008](https://doi.org/10.1016/j.jpowsour.2016.08.008).
- 131 T. Kang, P. Nakhavivej, K. J. Wang, Y. Chen, Y. G. Chung and H. S. Park, Anion storing, oxygen vacancy incorporated perovskite oxide composites for high-performance aqueous dual ion hybrid supercapacitors, *J. Energy Chem.*, 2024, **94**, 646–655, DOI: [10.1016/j.jechem.2024.02.032](https://doi.org/10.1016/j.jechem.2024.02.032).
- 132 Y. Zhao, S. Liu, B. Zhang, J. Zhou, W. Xie and H. Li, One-Step Synthesis of Mesoporous Chlorine-Doped Carbonated Cobalt Hydroxide Nanowires for High-Performance Supercapacitors Electrode, *Nanoscale Res. Lett.*, 2018, **13**, 415, DOI: [10.1186/s11671-018-2791-z](https://doi.org/10.1186/s11671-018-2791-z).
- 133 H. Liu, K. H. Ho, Y. Hu, Q. Ke, L. Mao, Y. Zhang and J. Wang, Doping cobalt hydroxide nanowires for better supercapacitor performance, *Acta Mater.*, 2015, **84**, 20–28, DOI: [10.1016/j.actamat.2014.09.055](https://doi.org/10.1016/j.actamat.2014.09.055).
- 134 A. R. Selvaraj, H. J. Kim, K. Senthil and K. Prabakar, Cation intercalated one-dimensional manganese hydroxide nanorods and hierarchical mesoporous activated carbon nanosheets with ultrahigh capacitance retention asymmetric supercapacitors, *J. Colloid Interface Sci.*, 2020, **566**, 485–494, DOI: [10.1016/j.jcis.2020.01.117](https://doi.org/10.1016/j.jcis.2020.01.117).
- 135 B. Maria Mahimai, E. Li, J. Pang, J. Zhang and J. Zhang, Interface engineering in conducting polymers-based supercapacitor, *J. Energy Storage*, 2024, **96**, 112598, DOI: [10.1016/j.est.2024.112598](https://doi.org/10.1016/j.est.2024.112598).
- 136 L. Fu, Q. Qu, R. Holze, V. V. Kondratiev and Y. Wu, Composites of metal oxides and intrinsically conducting polymers as supercapacitor electrode materials: the best of both worlds?, *J. Mater. Chem. A*, 2019, **7**, 14937–14970, DOI: [10.1039/c8ta10587a](https://doi.org/10.1039/c8ta10587a).
- 137 A. Brzózka, K. Fic, J. Bogusz, A. M. Brudzisz, M. M. Marzec, M. Gajewska and G. D. Sulka, Polypyrrole–Nickel hydroxide hybrid nanowires as future materials for energy storage, *Nanomaterials*, 2019, **9**, 307, DOI: [10.3390/nano9020307](https://doi.org/10.3390/nano9020307).
- 138 Q. Cheng, J. Tang, N. Shinya and L. C. Qin, Co(OH)<sub>2</sub> nanosheet-decorated graphene-CNT composite for supercapacitors of high energy density, *Sci. Technol. Adv. Mater.*, 2014, **15**, 014206, DOI: [10.1088/1468-6996/15/1/014206](https://doi.org/10.1088/1468-6996/15/1/014206).
- 139 H. S. Syed, I. K. Muhammad, S. Rida, N. Rozeen and A. Ashraf, Polyaniline enhanced supercapacitance of cobalt hydroxide nanowires/carbon nanotube containing polymer sponge layered composite, in *Key Eng. Mater.*, Trans Tech Publications Ltd, 2018, pp. 175–180, DOI: [10.4028/www.scientific.net/KEM.778.175](https://doi.org/10.4028/www.scientific.net/KEM.778.175).
- 140 P. T. Babar, B. S. Pawar, A. T. A. Ahmed, S. Sekar, S. Lee, B. R. Sankapal, H. Im, J. H. Kim and S. M. Pawar, Synthesis of nickel hydroxide/reduced graphene oxide composite thin films for water splitting application, *Int. J. Energy Res.*, 2020, **44**, 10908–10916, DOI: [10.1002/er.5627](https://doi.org/10.1002/er.5627).
- 141 W. Liu, C. Ju, D. Jiang, L. Xu, H. Mao and K. Wang, Ionic liquid-assisted grown of beta-nickel hydroxide nanowires on reduced graphene oxide for high-performance supercapacitors, *Electrochim. Acta*, 2014, **143**, 135–142, DOI: [10.1016/j.electacta.2014.08.010](https://doi.org/10.1016/j.electacta.2014.08.010).
- 142 Y. Wei, R. Ding, C. Zhang, B. Lv, Y. Wang, C. Chen, X. Wang, J. Xu, Y. Yang and Y. Li, Facile synthesis of self-assembled ultrathin  $\alpha$ -FeOOH nanorod/graphene oxide composites for supercapacitors, *J. Colloid Interface Sci.*, 2017, **504**, 593–602, DOI: [10.1016/j.jcis.2017.05.112](https://doi.org/10.1016/j.jcis.2017.05.112).
- 143 P. Navaneeth, A. Kumar, B. G. Nair, S. B. TG and P. V. Suneesh, Studies on fabrication of high-performance flexible printed supercapacitor using cobalt hydroxide nanowires, *Electrochim. Acta*, 2022, **430**, 141096, DOI: [10.1016/j.electacta.2022.141096](https://doi.org/10.1016/j.electacta.2022.141096).
- 144 X. Bai, D. Cao and H. Zhang, Simultaneously morphology and phase controlled synthesis of cobalt manganese hydroxides/reduced graphene oxide for high performance



- supercapacitor electrodes, *Ceram. Int.*, 2020, **46**, 19135–19145, DOI: [10.1016/j.ceramint.2020.04.249](https://doi.org/10.1016/j.ceramint.2020.04.249).
- 145 R. M. Obodo, N. M. Shinde, U. K. Chime, S. Ezugwu, A. C. Nwanya, I. Ahmad, M. Maaza, P. M. Ejikeme and F. I. Ezema, Recent advances in metal oxide/hydroxide on three-dimensional nickel foam substrate for high performance pseudocapacitive electrodes, *Curr. Opin. Electrochem.*, 2020, **21**, 242–249, DOI: [10.1016/j.coelec.2020.02.022](https://doi.org/10.1016/j.coelec.2020.02.022).
- 146 L. Zhao, S. Lei, Q. Tu, L. Rao, W. Zen, Y. Xiao and B. Cheng, Phase-controlled growth of nickel hydroxide nanostructures on nickel foam for enhanced supercapacitor performance, *J. Energy Storage*, 2021, **43**, 103171, DOI: [10.1016/j.est.2021.103171](https://doi.org/10.1016/j.est.2021.103171).
- 147 J. Wei, C. Zhang, X. Yang, J. Jia and Z. Qin, Synthesis of CoO-anchored nickel-cobalt layered hydroxide nanowire arrays via low-cobalt hydrothermal method for high-performance supercapacitors, *J. Alloys Compd.*, 2025, **1021**, 179517, DOI: [10.1016/j.jallcom.2025.179517](https://doi.org/10.1016/j.jallcom.2025.179517).
- 148 M. Islam, M. S. Hossain, B. Adak, M. M. Rahman, K. kubra Moni, A. S. M. Nur, H. Hong, H. Younes and S. Mukhopadhyay, Recent advancements in carbon-based composite materials as electrodes for high-performance supercapacitors, *J. Energy Storage*, 2025, **107**, 114838, DOI: [10.1016/j.est.2024.114838](https://doi.org/10.1016/j.est.2024.114838).
- 149 J. Jiang, J. Liu, R. Ding, J. Zhu, Y. Li, A. Hu, X. Li and X. Huang, Large-Scale Uniform  $\alpha$ -Co(OH)<sub>2</sub> Long Nanowire Arrays Grown on Graphite as Pseudocapacitor Electrodes, *ACS Appl. Mater. Interfaces*, 2011, **3**, 99–103, DOI: [10.1021/am1009887](https://doi.org/10.1021/am1009887).
- 150 Y. Chen, Z. Zhang, Z. Sui, Z. Liu, J. Zhou and X. Zhou, Ni(OH)<sub>2</sub> nanowires/graphite foam composite as an advanced supercapacitor electrode with improved cycle performance, *Int. J. Hydrogen Energy*, 2016, **41**, 12136–12145, DOI: [10.1016/j.ijhydene.2016.05.104](https://doi.org/10.1016/j.ijhydene.2016.05.104).
- 151 X. Dong, Z. Guo, Y. Song, M. Hou, J. Wang, Y. Wang and Y. Xia, Flexible and wire-shaped micro-supercapacitor based on Ni(OH)<sub>2</sub>-nanowire and ordered mesoporous carbon electrodes, *Adv. Funct. Mater.*, 2014, **24**, 3405–3412, DOI: [10.1002/adfm.201304001](https://doi.org/10.1002/adfm.201304001).
- 152 Kavyashree, S. S. Raut, B. R. Sankapal and S. N. Pandey, Tuberosity surface architecture of Sr(OH)<sub>2</sub> film as supercapacitive electrode, *Electrochim. Acta*, 2017, **258**, 34–42, DOI: [10.1016/j.electacta.2017.10.093](https://doi.org/10.1016/j.electacta.2017.10.093).
- 153 Kavyashree, S. Parveen, S. S. Raut, M. K. Tiwari, B. R. Sankapal and S. N. Pandey, Flexible iron-doped Sr(OH)<sub>2</sub> fibre wrapped tuberosity for high-performance supercapacitor electrode, *J. Alloys Compd.*, 2019, **781**, 831–841, DOI: [10.1016/j.jallcom.2018.12.023](https://doi.org/10.1016/j.jallcom.2018.12.023).
- 154 Kavyashree, S. S. Raut, S. Parveen, B. R. Sankapal and S. N. Pandey, Influence of Cu on the Performance of Tuberosity Architecture of Strontium Hydroxide Thin Film as a Supercapacitor Electrode, *ChemElectroChem*, 2018, **5**, 4021–4028, DOI: [10.1002/celec.201801023](https://doi.org/10.1002/celec.201801023).
- 155 L. Lai, R. Li, S. Su, L. Zhang, Y. Cui, N. Guo, W. Shi and X. Zhu, Controllable synthesis of reduced graphene oxide/nickel hydroxide composites with different morphologies for high performance supercapacitors, *J. Alloys Compd.*, 2020, **820**, 153120, DOI: [10.1016/j.jallcom.2019.153120](https://doi.org/10.1016/j.jallcom.2019.153120).
- 156 L. Wang and D. L. Wang, Preparation and electrochemical characterization of MnOOH nanowire-graphene oxide, *Electrochim. Acta*, 2011, **56**, 5010–5015, DOI: [10.1016/j.electacta.2011.03.105](https://doi.org/10.1016/j.electacta.2011.03.105).

